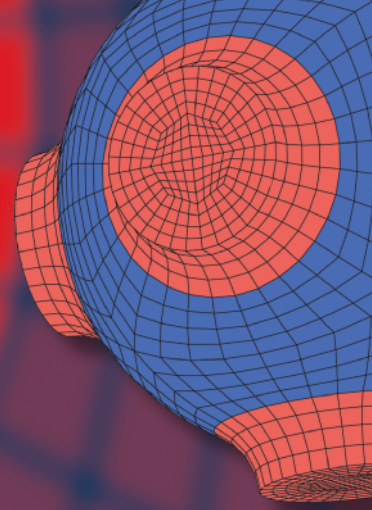J. M. P. Q. Delgado
A. G. Barbosa de Lima
Laura H. Carvalho

Moisture Transport in Polymer Composite Materials

Computational Modelling and Experiments

Advanced Structured Materials

Volume 160

Series Editors

Andreas Öchsner, Faculty of Mechanical Engineering, Esslingen University of Applied Sciences, Esslingen, Germany

Lucas F. M. da Silva, Department of Mechanical Engineering, Faculty of Engineering, University of Porto, Porto, Portugal

Holm Altenbach , Faculty of Mechanical Engineering, Otto von Guericke University Magdeburg, Magdeburg, Sachsen-Anhalt, Germany

Common engineering materials reach in many applications their limits and new developments are required to fulfil increasing demands on engineering materials. The performance of materials can be increased by combining different materials to achieve better properties than a single constituent or by shaping the material or constituents in a specific structure. The interaction between material and structure may arise on different length scales, such as micro-, meso- or macroscale, and offers possible applications in quite diverse fields.

This book series addresses the fundamental relationship between materials and their structure on the overall properties (e.g. mechanical, thermal, chemical or magnetic etc.) and applications.

The topics of *Advanced Structured Materials* include but are not limited to

- classical fibre-reinforced composites (e.g. glass, carbon or Aramid reinforced plastics)
- metal matrix composites (MMCs)
- micro porous composites
- micro channel materials
- multilayered materials
- cellular materials (e.g., metallic or polymer foams, sponges, hollow sphere structures)
- porous materials
- truss structures
- nanocomposite materials
- biomaterials
- nanoporous metals
- concrete
- coated materials
- smart materials

Advanced Structured Materials is indexed in Google Scholar and Scopus.

More information about this series at https://link.springer.com/bookseries/8611

J. M. P. Q. Delgado · A. G. Barbosa de Lima ·
Laura H. Carvalho

Moisture Transport in Polymer Composite Materials

Computational Modelling and Experiments

J. M. P. Q. Delgado
CONSTRUCT-LFC
Department of Civil Engineering
Faculty of Engineering
University of Porto
Porto, Portugal

A. G. Barbosa de Lima
Department of Mechanical Engineering
Federal University of Campina Grande
Campina Grande, Paraíba, Brazil

Laura H. Carvalho
Department of Mechanical Engineering
Federal University of Campina Grande
Campina Grande, Paraíba, Brazil

Preface

Professionals from chemical, materials, mechanical and manufacturing engineering, as well as from other scientific areas are responsible for the great advance in new materials, particularly in the field of polymer composites.

Nowadays, the development of new and advanced fiber-reinforced polymer composites has allowed the manufacture of innovative products with high quality from the technological and mechanical points of view. These products are manufactured by the automotive, marine, aerospace, and sports products industries. A significant amount of research on polymer composites deals with thermoset vegetable fiber-reinforced systems manufactured by hand lay-up. In fact, these materials have gained preference because they offer some advantages such as easy processing and manufacturing in products of different shapes, quality and good mechanical properties of the manufactured products and high potential for diverse industrial and technological applications, especially those associated with socio-economic and environmental benefits. However, raw materials from renewable sources, such as vegetable fibers, present some disadvantages when used as reinforcement in polymers, due to their strong hydrophilic nature and weak interfacial adhesion with most polymer matrices, which are responsible for reducing the mechanical properties of polymer composites.

The strong tendency of vegetable fiber-reinforced polymer composites to absorb water plays an important role to address studies related to the water absorption process in these materials. Several specialized journals report experimental data on this topic and most of them analyze the results by simple modeling. Unfortunately, this issue is hardly discussed in textbooks, which leads to a gap and the need for new academic books aimed at this issue, especially on topics related to non-traditional vegetable fibers and advanced mathematical modeling. Therefore, this book is intended to provide valuable information about the water absorption process in vegetable fiber-reinforced thermoset polymer composites with emphasis in experiments, modeling and simulation. In this document, emerging topics related to theory, engineering applications, advanced mathematical modeling (anomalous diffusion) and experiments on the water absorption process in polymer composites are presented and discussed.

For many years, we have the enormous pleasure of working with various talented researchers including our current and former students (undergraduate, graduate and post-graduate levels), in the themes "fiber-reinforced polymer composite and their related topics". This book documents our research progress in this field. The book has six chapters about water absorption process in composite materials, particularly of vegetable fiber-reinforced polymer composites.

Chapter 1 provides an introduction on fiber-reinforced polymer composites and the motivation to study the water absorption process in these materials.

Chapter 2 deals with the water absorption process in vegetable fiber-reinforced polymer composite materials. The main issues, including foundations, advantages and problems associated with the use of vegetable fiber-polymer composites, especially those provoked by weak adhesion and exposure to hot and humid environments are described.

Chapter 3 presents the experimental techniques developed by our research group related to water absorption in vegetable fiber-reinforced polymer composites. Herein, important information related to fiber morphology, composite manufacturing, moisture absorption, and mechanical characterization tests in polymer composites reinforced by caroá, macambira and sisal fibers are detailed.

Chapter 4 presents a comprehensive and rigorous analysis about pure diffusion through fibrous porous media (Fick's second law), with particular emphasis to the process of water absorption in vegetable fiber-reinforced polymer composites. In this chapter different approaches (analytical, numerical and by CFD) and their limitations for the correctly describing the water absorption process in vegetable fiber-reinforced polymer composites are given. Herein, a homogeneous and three-dimensional mathematical modeling that includes different effects of some process parameters (sample thickness and water bath temperature) in the moisture migration behavior inside the material is presented, with especial emphasis to polyester composites reinforced by caroá, macambira and sisal fibers.

Chapter 5 presents a rigorous theoretical approach to the anomalous diffusion through porous fibrous media (Langmuir-type model), its advantages and limitations. An advanced macroscopic mathematical modeling that considers the existence of water molecules in the free and entrapped states inside the material, during the process of water absorption is proposed. In this chapter, we perform different approaches (analytical and numerical) for the correct prediction of the process of water absorption in vegetable fiber-reinforced polymers. Here, we report applications on caroá fiber-reinforced polyester composites and other arbitrary cases, including the effect of water layer thickness at the surface of the composite on the overall water pick-up.

In Chap. 6, we present conclusions on the different chapter contents and the main results present in them. The idea is to help professionals, engineers, industrials and academics involved in this advanced and interdisciplinary field.

Porto, Portugal   J. M. P. Q. Delgado
Campina Grande, Brazil   A. G. Barbosa de Lima
Campina Grande, Brazil   Laura H. Carvalho

Acknowledgements

Contents

Chapter 1
Introduction

This chapter provides several information about polymer composites with emphasis on vegetable fiber-reinforced polymer composite materials, as well the motivation to study the water absorption process in these materials. Herein, we present and discuss different topics such as definition, classification, constituents, technological characteristics, manufacturing techniques, performance and applications of polymer composites.

1.1 Motivation

Both academy and industry have given special attention to understand and predict the properties of composite materials as these materials have a wide range of applications in different sectors such as: boats, ships, automotive and aircraft components, submersibles, offshore structures and prostheses. Fiber reinforced polymer composite materials have been preferred to designing structural materials when compared to conventional materials (metals and ceramics), especialy that originated from vegetable fiber as reinforcement. The reasons for replacing syntetic fibers in polymer composites are the good set of mechanical properties (strength and stiffness) displayed by vegetable fibers, their availability, low cost, low density as well as other characteristics.

The mechanical properties of composite materials strongly depend on good adhesion between fiber and polymer matrix, which in turn, strongly depend on the manufacturing techniques employed to make them and on the operational and environmental conditions during use. One of these conditions is moisture absorption, especially at high temperatures.

Despite of its importance, few books offer detailed information about the water absorption process in vegetable-fiber reinforced polymer composites including experiments, mathematical models and their analytical and numerical solutions.

Mathematical modeling and numerical computation are processes to obtain solutions for physical problems of academic and/or industrial interest and these include differential equations of mass and energy conservations. In these areas, books dedicated to this theme are rather scarce and limited to providing an understanding on this issue only under rectilinear infiltration using Fick´s second law of diffusion. However, is some situations, polymer composites display an anomalous behavior during the water absorprion process. In these cases, Fickian diffusion fails, particularly in the final stages of the process. Information addressed to the physical problems associated with the water uptake in polymer composite materials involve partial to non-Fickian moisture absorption. This information is almost null when dealing with polymer composites reinforced by vegetable fibers in 3D-geometry.

This comprehensive book aims to respond to the large growing interest associated with Fickian and non-Fickian moisture absorption processes in polymer composites, especially that involving advanced mathematical treatment of the governing equations, experiments and numerical computation. It is the first book entirely dedicated to this important subject.

The key challenge of this book is to document different information related to fiber-reinforced polymer composites ranging from basic material and manufacturing to advanced mathematical modeling of water migration in fibrous media, their effect, and applications, in a unique volume. This book contains information about Fickian and non-Fickian diffusion of water inside vegetable-fiber reinforced polymer composites, a subject not yet treated and discussed together.

The goal is to provide an in-depth analysis of the key issues including rigorous and coupled engineering models, theoretical and experimental results, and general fundamentals about water absorption in polymer composites reinforced by vegetable fiber. Thus, this book will assist professionals, curious readers, undergraduate and graduate students, as well as applied mathematicians, engineers and scientists to better understand advanced topics associated with fiber-reinforced polymer composites especially those related to the moisture absorption process.

Further, the authors sincerely believe that this book becomes an excellent reference source for professionals already cited and a start point for encouraging different people to study both polymer composite materials and the effect of water absorption in these materials.

1.2 Composite Materials: Fundamentals

Composites are multiphase materials consisting of one or more discontinuous phases (reinforcing filler), embedded in a continuous phase (matrix) [1–7]. Based in this definition, it is a new material obtained by combination of two or more materials insoluble in each other, with specific properties not found in either material alone.

Composites can be classified according to the type of matrix, the type, geometry and shape of the reinforcement used. In general, inorganic materials are used as reinforcement in organic matrices. Thus, composite materials can be classified

as fiber-reinforced composites (fibrous composites) and particle-reinforced composites (particulate composites). Sometimes metallic wires and ribbons are used as reinforcement in composites.

Composite materials can also be classified according to the chemical and physical nature of the matrix which can be: ceramic, metallic or polymeric. Ceramic materials are inorganic in nature, have high resistance to heat and are fragile. Metallic materials, in general, present high ductility and excellent thermal and electrical conductivities. The great limitation in the use of metallic materials as reinforcement in composites is their high density and manufacturing costs. On the other hand, polymeric materials stand out for their low density, easy conformation and high electrical resistivity [8, 9].

Composites properties are strongly dependent on the properties of their constituents (matrix and reinforcement). In general, reinforcing materials are harder and stronger than the matrix. Thus, these materials are added to the matrix in order to increase some of its properties so as to achieve the best properties for a given application.

The shape, size, distribution, content and filler (reinforcement) orientation as well as the matrix/filler interfacial bonding strongly affect the initial and long term properties (hydro, thermal, electrical and mechanical) of the composites whose performance can also be affected by environmental exposure resulting in volumetric variations (swelling). Thus, it is very important to know these materials (matrix and reinforcement) in detail.

Depending on the nature and geometry of the reinforcement, the following classification applies:

(a) Nature: These materials must be hard to promote increase in hardness and abrasion resistance; rupture resistant to provide high tensile, flexural and shear strength; rigid to increase elastic modulus; flexible to increase impact resistance, and heat resistant to increase thermal stability of the composite.
(b) Geometric characteristics: These materials can be particulate, fibrous, and laminates.

Further, fiber reirforcements (long or short), globular particles and platelets can be incorporated into ductile or brittle matrices at random or in oriented laminates, generating composites with different structures and properties [8–14].

The reinforcing material can be a synthetic fiber (glass, carbon, aramid, etc.) or a natural fiber (sisal, ramie, jute, cotton, kenaf, pineapple, etc.) or particles (clay, mica, tungsten carbide, titanium carbide, etc.). Mineral fillers as reinforcements, often can be incorporated into matrix in order to reduce costs, especially when associated to ultra high strength fibers. Figure 1.1 illustrates a scheme for the classification and types of composite materials.

The matrix is responsible for the external appearance of the composite and the protection of the reinforcement against chemical and physical attacks. The fillers may be well dispersed of agglomerated in the composite matrix. However, when subjected to stresses, the matrix must deform sufficiently in order to adequately distribute and transfer stresses to the reinforcing material. The proper choice of matrix and reinforcement to be used in a structural application is defined based on the strain that
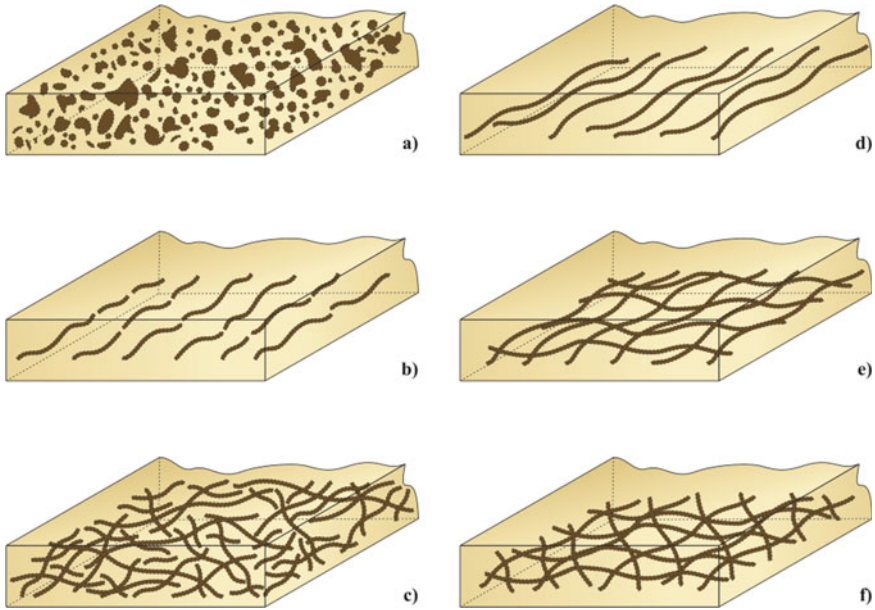
Fig. 1.1 Classification and types of composite materials. **a** Dispersed particle-reinforced, **b** Discontinuous fiber-reinforced (aligned), **c** Discontinuous fiber-reinforced (randomly oriented), **d** Continuous fiber-reinforced (aligned), **e** Continuous fiber-reinforced (aligned 0°–90° fiber orientation angle), and **f** Continuous fiber-reinforced (multidirectional fiber orientation angle)

the composite will receive during use. Mechanically speaking, matrix deformation must be compatible with the maximum deformation of the reinforcement [15–17].

Polymer composites can be defined as multi-phase materials formed by reinforcing fillers embedded in a polymer matrix.

Polymer matrices are classified as thermosets (epoxy, polyester, phenolic, silicone, polyimide, etc.) or thermoplastics (polyethylene, polystyrene, nylons, polycarbonate, polyether-ether ketone, polyphenylene sulfide, etc.). These matrices are most widely used due to their moderate cost, easy processing, good chemical resistance, and low density [1].

The use of conventional and engineering thermoplastics, as polymer matrices has been restricted to medium performance composites. The limited thermal stability of thermoplastics at high temperatures restricts their use for specific applications. However, the incorporation of reinforcements with specific characteristics in thermoplastic matrices has allowed applications of the polymer composite in temperatures up to 150 °C [15].

Epoxy resins, despite having excellent mechanical properties, are penalized by high costs and low resistance to weathering. Curing of these resins is much more complex than that of polyester resins. In the case of phenolic resins, their main disadvantage to the polyester and epoxy resins is that during their curing,

water is formed as a by-product. Therefore, its application in composites is more complex, since the removal of produced moisture becomes an important factor during manufacturing [16].

Polyester resins are used in composites due to their low cost and satisfactory mechanical properties. After cured, these materials present good electrical properties, corrosion resistance and chemical attacks. Curing of the polyester resin is an exothermic process and requires an organic peroxide based curing system as the catalyst [16, 17]. Furthermore, polyester resins have ester groups as fundamental elements in their molecular chains, resulting from the condensation reaction of a diol with a diacid. Thus, depending on the type of acid used in the process, the polyester can be either saturated (thermoplastic) or unsaturated (thermoset) [17].

In general, fiber-reinforced polymer composite manufacturing techniques are classified as open mold and closed mold processes. The first allows for multi-directional orientation of the fibers relative to the mold or mandrel, except for pultrusion, where fibers are oriented in the direction parallel to the laminated surface. These processes include hand lay-up, spray up [18–22], filament winding [20, 21, 23], and pultrusion [20, 23, 24]. Closed mold process, in turn, produce fiber orientation in the direction parallel to the mold surface, includes compression molding and transfer molding [23, 25, 26].

Hand lay-up is the oldest and simplest manual production process; however, it also is the slowest. It can be adapted for the production of large structures, although it is more interesting for small productions [18].

Hand lay-up continues to be one of the most important manufacturing processes for small batch production of fiber reinforced composites, although increasing stringency of emission regulations has forced many manufacturers to explore the use of closed mold alternatives. Hand lay-up is carried out at room temperature using catalyzed liquid resins. The resin is poured in the mold containing the reinforcement. The matrix starts to cure in the mold, through an exothermic chemical reaction between the catalyst and the resin, solidifies and a fiber reinforced composite is obtained without the need of external heating. The method begins with the preparation of the mold where the reinforcing fiber layers will be stacked; usually a release agent is used on the mold, in order to facilitate demolding after curing. The impregnation process is performed manually with the help of rollers or brushes by pressing the resing and fiber layers to eliminate air bubbles and excess resin. Layers of fabric, mats, oriented or random fibers are stacked and impregnated with resin one by one in an open mold. After stacking all layers, an upper molding plate may be applied to allow for a better finish on both outer surfaces of the composite. Despite the steady progress to replace the manual layout with an automated process, it still persists as the method by which at least half of the entire advanced composite aerospace structures are made [19, 20, 27].

Hand lay-up continues to be used because it is extremely flexible to allow a wide variety of shapes of the desired composite [21]. Although it presents some disadvantages such as the quality of the final product depends on the ability of the worker, has low productivity and releases volatiles during manufacturing. Furthermore, as

production volumes increase and economic factors become very important for decision making, manual placement gradually must be replaced or modified by the use of new automated technologies.

Nowadays, synthetic fiber-reinforced polymer composite materials are used in different sectors such as: aerospace, maritime, automotive, biomedical and transportation in specific applications as well as in high-tech sporting equipment [1–8, 12]. Already, vegetable fiber-reinforced polymer composites are used in the several construction sectors such as: automotive, building, transportation, consumer goods, sports equipment, design equipment, etc. [28–36].

Despite of the attractiveness, depending on the type of polymer composites, these materials are strongly affected when exposed to the adverse operating conditions such as electromagnetic and thermal radiation, galvanic corrosion (metals as reinforcement), oxygen at high temperatures (thermo-acted oxidative reactions), and water in the liquid and vapor (including moist air) phases. Therefore, innovative researches related to polymer composite degradation are strongly recommended, and with it, new challenges should arise.

References

1. Agarval, B., Broutman, L.J., Chandrashekha, K.: Analysis and Performance of Fiber Composites. John Wiley & Sons Inc., New Jersey (2006)
2. Brydson, J.A.: Plastics Materials, 7th edn. Butterworth-Heinemann, London (1999)
3. Crawford, R.J.: Plastics Engineering, 3rd edn. Butterworth-Heinemann, Oxford (1999)
4. Hull, D., Clyne, T.W.: An Introduction to Composite Materials, Cambridge Solid State Science Series, 2nd edn. Cambridge (1996)
5. Callister, W.D., Jr., Rethwisch, D.G.: Fundamental of Materials Science and Engineering: An Integrated Approach, 3rd edn. Jonh Wiley & Son Inc., USA (2008)
6. Peters, S.T.: Handbook of Composites. Chapman & Hall Cambridge University Press, England (1998)
7. Richardson, H.: Polymer Engineering Composites. Applied Science Publishers, London (1997)
8. Callister, W.D., Jr.: Materials Science and Engineering an Introduction. John Wiley & Sons Inc., New York (2007)
9. Shackelford, J.F.: Materials Science For Engineers, six Peason Prentice Hall, New Jersey (2005)
10. Flinn, R., Trojan, P.: Engineering Materials And Their Applications. Houghton Mifflin Company, Boston (1981)
11. Laranjeira, E.: Properties of Composites Polyester/Jute. Influence of the Addition of Nanoparticulate Mineral Charge and Antichama System. Thesis in Process Engineering. Federal University of Campina Grande (2004). Brazil, p 159 (In Portuguese)
12. Mitchell, B.S.: An Introduction to Materials Engineering and Science. John Wiley & Sons, Inc., New Jersey (2004)
13. Cavalcanti, W.S.: Composites Polyester/vegetable woven-glass: mechanical characterization and simulation of water sorption. Thesis in Process Engineering. Federal University of Campina Grande (2006). Brazil, p 122 (In Portuguese)
14. Kaw, A.K.: Mechanics Composite Materials, 2nd edn. Taylor & Francis Group Llc, New York (2006)
15. Hage Jr., E.: Polymeric Composites and Blends. Instituto Latino Americano e IBM, Campinas (1989) (In Portuguese)

16. Cheremisinoff, N.P.: Advanced Polymer Processing Operations. Noyes Publications, New Jersey (1998)
17. Goodman, S.H.: Handbook of Thermoset Plastics. Noyes Publications, New Jersey (1998)
18. Bunsell, A.R., Renard, J.: Fundamentals of Fibre Reinforced Composite Materials. Institute of Physics (IOP), UK (2005)
19. Astrom, B.T.: Manufacturing of Polymer Composites. CRC Press (1997)
20. Moura, M.F.S.F., Morais, A.B., Magalhães, A.G.: Composite Materials-Materials. Manufacturing and Mechanical Behavior. Publindústria, Porto (2010).(In Portuguese)
21. Gutowski, T.G.: Advanced Composites Manufacturing. Wiley, John & Sons, Cambrigde (1997)
22. Mazumdar, S.K.: Composites Manufacturing. Materials, Product and Process Engineering. Taylor & Francis, New York (2002)
23. Mallick, P.K.: Fiber-Reinforced Composites: Materials. Manufacturing and Design. CRC Press, New York (2007)
24. Huber, T., Graupner, N., Müssig, J.: Natural Fibre Composite Processing: A technical Overview. In: Mussig, J. (ed.) Industrial applications of natural fibres: structure, properties and technical applications, pp. 407–422. John Wiley & Sons (2010)
25. Ashby, M.F.: Materials and Design: Art and Science of Material Selection in Product Design. Elsevier, Rio de Janeiro (2011).(In Portuguese)
26. Ho, M.P., Wang, H., Lee, J.H., Ho, C.K., Lau, K.T., Leng, J., Hui, D.: Critical factors on manufacturing processes of natural fibre composites. Compos. B. Eng. **43**, 3549–3562 (2012)
27. Castro, B.F.M. : Study and Mechanical Characterization of Composites Reinforced with Natural Fibers, Master Dissertation in Mechanical Engineering, Porto (2013) (In Portuguese)
28. Dhakal, H.N., Zhang, Z.: The use of hemp as reinforcements in composites. In: Faruk, O., Sain, M. (Eds.) Biofiber Reinforcement in Composites Materials. Elsevier Ltda. , Amsterdam, Chapter 3, pp. 86–103 (2015)
29. Du, Y., Yan, N., Kortschot, M.T.: The Use Of Ramie Fibers as Reinforcements in Composites. In: Faruk, O., Sain, M. (Eds.) Biofiber Reinforcement in Composites Materials. Elsevier Ltda. , Amsterdam, Chapter 4, pp. 104–137 (2015)
30. Li, Y.; Shen, Y.O.: The Use of Sisal And Henequen Fibers as Reinforcements in Composites. In: Faruk, O., Sain, M. (Eds.) Biofiber Reinforcement in Composites Materials. Elsevier Ltda., Amsterdam, Chapter 6, pp. 165–210 (2015)
31. Leão, A.L., Cherian, B.M., Narine, S., Souza, S.F., Sain, M., Thomas, S.: The use of pineapple leaf fibers (palts) as reinforcements in composites. In: Faruk, O., Sain, M. (Eds.) Biofiber Reinforcement in Composites Materials. Elsevier Ltda. , Amsterdam, Chapter 7, pp. 211–235 (2015)
32. Mamun, A.A., Heim, H.P., Faruk, O., Bledzki, A.K.: The use of banana and abaca fibers as reinforcements in composites. In: Faruk, O., Sain, M. (Eds.) Biofiber Reinforcement in Composites Materials. Elsevier Ltda., Amsterdam, Chapter 8, pp. 236–272 (2015)
33. Kucak, D., Mistik, S.I.: The use of palm leaf fibers as reinforcements in composites. In: Faruk, O., Sain, M. (Eds.) Biofiber Reinforcement in Composites Materials. Elsevier Ltda., Amsterdam, Chapter 9, pp. 273–281 (2015)
34. Khalil, H.P.S.A., Alwani, M.S., Islam, M.N., Suhaily, S.S., Dungani, R., H'ng, Y.M.: The use of bamboo fibers as reinforcements in composites. In: Faruk, O., Sain, M. (Eds.) Biofiber Reinforcement in Composites Materials. Elsevier Ltda., Amsterdam, Chapter 16, pp. 488–524 (2015)
35. Shanks, R.A.: Isolation and application of cellulosic fibres in composites. In: Faruk, O., Sain, M. (Eds.) Biofiber Reinforcement In Composites Materials. Elsevier Ltda., Amsterdam, Chapter 18, pp.553–570 (2015)
36. Souza, S.F., Ferreira, M., Sain, M., Ferreira, M.Z., Pupo, H.F., Cherian, B.M., Leão, A.L.: The use of curaua fibers as reinforcements in composites. In: Faruk, O., Sain, M. (Eds.) Biofiber Reinforcement In Composites Materials. Elsevier Ltda., Amsterdam, Chapter 22, pp. 700–720 (2015)

Chapter 2
Fundamentals

This chapter focuses on the water diffusion process in composites materials. Special attention is given to vegetable fiber reinforced polymer composites. Herein, the main issues related to this important topic such as foundations, advantages and problems associated with the use of vegetable fibers as reinforcement in polymer composites are discussed, especially that caused by weak adhesion and exposure to the hot and humid environments, are presented and discussed.

2.1 Natural Fiber-Reinforced Polymer Composites

Currently, environmental issues are increasingly assuming a prominent role in our society, including conditioning technological development. In materials engineering, this role evidences the greater importance attributed to renewable and biodegradable materials whose manufacture involves low energy consumption. In this context, the evolution of different technologies has allowed the use of reinforced plastics with several productive, economic and ecological advantages.

More recently, environmental concerns as well as very stringent regulations and standards, have prompted the industries to research and use more eco-friendly and/or sustainable processing methods or products. In order to achieve this goal, available manufacturing processes are being modified or adapted to comply with these regulations, alternative technologies are developed and improved or else renewable biomaterials and biofibers are being used to generate eco-friendly composite materials. Broadly defined, biocomposites are composite materials made from natural/bio fibers; the polymer matrix may be petroleum based or naturally derived (biopolymer), and the former may be biodegradable or not. Biocomposites derived from plant fibers and biopolymers are likely to be more eco-friendly and such composites are termed green composites. While synthetic matrix/plant fiber composites are not as

ecofriendly, they are still more environmental friendly than an all-synthetic material. Natural fibers, both of animal and plant (lignocellulosic) origin, meet these requirements.

Vegetable fibers are biodegradable, sustainable and renewable, carbon dioxide neutral and have a positive environmental impact, as they are nontoxic and nonabrasive to mixing and molding equipment, leading to significant production cost reductions. Their major constituents are cellulose, hemicellulose, lignin, pectin, waxes and water-soluble substances.

Plant fibers are a choice material for biocomposite production due to their worldwide availability, economical production, safer handling and working conditions compared to synthetic reinforcements, good set of mechanical properties, low cost per volume, low density and high relative strength and stiffness, which results in composites with specific strength and stiffness comparable to that of glass reinforced ones.

Strong arguments for encouraging the use of these materials include ecological, technological and economic advantages presented by vegetables fibers as well as social concerns since from an economical point of view, they generally originate from poor regions [1].

The main disadvantages presented by vegetable fibers for polymer composite applications are related to their high moisture sorption (hydrofilicity), relatively low processing temperatures (≤ 200 °C (although it is possible to use higher temperatures for short periods), low resistance to microorganisms and poor fiber/polymer adhesion to most polymer matrices. All these factors ends up by compromising the composite´s immediate and long-term mechanical performance [2]. Therefore, despite their attractiveness, natural fiber-reinforced polymer matrix composites are very sensitive to influences from external environmental agents such as water (in the liquid or vapor phases), humid air, temperature, radiation (X-rays, β and γ rays, ultraviolet rays), chemical agents or any combination between them [3–5]. They are also very sensitive to internal factors such as fiber volume fraction and orientation, for example. The different factors cited above justify the significant amount of effort and research on understanding vegetable fiber-reinforced polymer composites degradation under adverse operating conditions. These actions also contemplate many others types of polymer composites, such as those reinforced by metallic fillers.

One of the most important factors in composite materials, manufactured by one or more continuous phases, is the region of interactions between the reinforcement and the matrix. It encompasses two sub-regions: the interface and the interphase. The interface is the boundary of contact (contact surface) between composite components (reinforcement and matrix) and has null thickness. In contrast, the interphase is a volumetric region where matrix and reirforcement are mixed and the chemical, physical and mechanical properties changes continuously from those of the matrix to reirforcement. Thus, its thickness is not null. The interphase is generated by the interdiffusion of atoms and molecules of the matrix across the interface, to inside the reinforcement. This phenomenon is more intense in situations involving polymer

Fig. 2.1 A schematic illustration identifying the interface and interphase regions inside a polymer composite
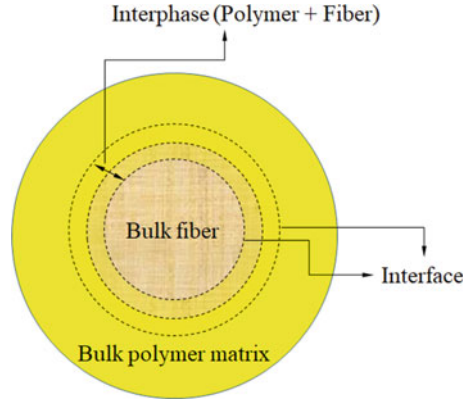
matrices in the liquid state and vegetable fiber as reinforcement. Based on these definitions, two contact inferfaces constitute the interphase. Figure 2.1 illustrates the physical representations of the interface and interphase inside a fiber-reinforced polymer composite.

The final properties of the composites depend fundamentally on how the individual components interact with each other, that is, they depend on the interface and interphase regions between the discontinuous and continuous phases. These regions are mainly responsibles to transfer the mechanical load from the matrix to the reinforcement. Inadequate adhesion between the phases involved in the interface may lead to premature failures, compromising the performance of the composite. Therefore, in addition to the individual properties of each component of the composite, the interface should be as suitable as possible to optimize the combination of the properties involved [6–13]. The adhesion between reinforcement and matrix characterize the physical and mechanical behavior of a composite.

In polymer composites, the failure should occur in the matrix. In practice, the adhesion between the constituentes isn´t perfect and the process of rupture is generated at the interface. Therefore, in most cases, failure of reinforced polymers occurs by shearing in the interfacial region. The failure occurs due to the weakness of the atomic or intermolecular bonds between the surface of the matrix and the surface of the reinforcement in the composite. The following types of failures can be cited: matrix cracking, local deterioration, delamination, fiber debonding, and pull-out.

One of the factors that favor interfacial interaction is the contraction undergone by the polymer matrix during its curing (crosslinking and solidification). In order for a better stress distribution to occur on the reinforcement surface during matrix contraction, a perfect wetting of the reinforcement by the resin is necessary [9].

2.2 Water Absorption in Natural Fiber-Reinforced Polymer Composites

Despite their strongly hydrophobic characteristic, polymers can absorb water when immersed in aqueous media or exposed to moisture. The intensity of this phenomenon is dependent on factors such as: polymer polarity, hydrogen bonding ability, crystallinity (thermoplastic polymers), degree of crosslinking (thermoset polymers) and manufacturing process. Thus, moisture in any form is deleterious to polymer composites, especially to those reinforced by natural fibers, which are highly hydrophilic materials.

There are two modes of moisture absorption in vegetable fiber reinfroced polymer composites: (a) hydrogen bonds between the polymer and the hydrophilic groups of the filler and (b) through surface microcracks which are responsible for water transport and deposition inside the material [14].

The water absorbed by polymers consists of both free water and bound water [15]. The free water are water molecules with the ability to move independently through the void spaces, while bound water are water molecules that are attached to polar groups of the polymers [16].

Moisture diffusion in polymeric composites is governed by three different mechanisms. The first involves the diffusion of water molecules within micro gaps between polymer chains. The second involves moisture transfer through gaps and faults at the interface between fiber and matrix. This is a result of poor wetting and impregnation during the manufacturing process. The third involves the transport of water molecules through micro cracks in the matrix originated during manufacture [17–19].

When natural fiber-reinforced polymer composites are exposed to moisture, free water penetrates and binds with hydrophilic groups of the fiber, establishing intermolecular hydrogen bonds with the fiber and reducing interfacial adhesion between fiber and matrix. This leads to swelling of the cellulose fibers, which promotes an increase in the stress at the interfacial regions resulting in its embrittlement and thus, leading to formation of micro cracks inside the matrix around the swollen fibers [20–22]. This promotes capillarity and transport of moisture via micro cracks, causing deterioration of the fibers, which eventually lead to the definitive debonding between fibers and matrix. After long time periods, biological activities such as fungal growths eventually degrade the natural fibers [15, 16] compromising the mechanical performance of the composite. Thus, water absorption is one of the limiting factors that reduce the applicability, physical and mechanical properties of the composite [23]. Figure 2.2 illustrates the moisture types (Free water and bound water) and the effect of water migration on the fiber—matrix interface.

Considering that these materials may be exposed to moisture or even submerged in water during their use, water absorption studies are of great academic interest, especially when heated environments are involved [17, 24].

Vegetable fibers are hydrophilic and fiber moisture not only acts as plasticizer but makes polymer impregnation more difficult, causing weak adhesion on the polymer matrix-fiber interface, which leads to internal stresses, void formation and premature failure of the fiber-polymer system [25–27].
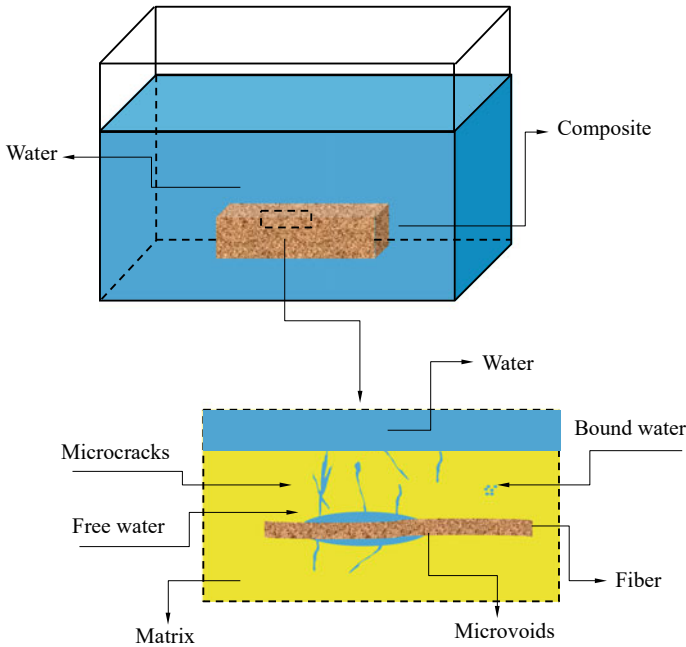
Fig. 2.2 Water migration mechanisms in vegetable fiber-reinforced polymer composite

This weak interfacial adhesion is associated with low polarity and low chemical affinity between the matrix and the fiber, which causes the formation of voids at the interface, initiation of faults and interfacial degradation that compromise the mechanical performance of the composites.

Effectively, vegetable fiber-reinforced polymer composites display lower mechanical properties than synthetic fiber-reinforced composites. However, as previously exposed, water sorption adversely affects the mechanical performance and physical integrity of natural fiber-reinforced polymer composite; so, the differences in mechanical properties between the natural and syntetic fiber-reinforced polymer composites can be even greater. Thus, knowing the effect of moisture on the composite properties is crucial for outdoor applications. The incompatibilities between natural fiber reinforced composites and water may be diminished by surface modification (chemical treatment) of the fiber or the matrix. In general it is the fiber, not the matrix, that is treated [28].

Several studies show that the mechanical properties of vegetable fiber reinforced composites significantly improve at high fiber content [29–31]. However, when fibrous polymer composites absorb moisture effects such as swelling, plasticizing, dissolving, leaching and/or hydrolyzing, result in discoloration, embrittlement, lower resistance to heat and weathering, and lower mechanical properties.

Due to their importance, several works on the water sorption kinetics of vegetable fiber reinforced polymer composites are reported in the literature [32–50]. In general,

the amount of water absorbed by a sample varies as a function of its composition, dimensions, void fraction (available free volume), temperature, surface area, surface protection, and exposure time. In this context, the effects of moisture and temperature of composites on several performance parameters, such as tensile and shear strengths, elastic moduli, fatigue behavior, creep, rupture stress, response to dynamic impact, and electrical parameters (electrical resistance and dielectric constant, for example), have been regularly investigated [3].

References

1. Silva, R.V.: Composite polyurethane resin derived from castor oil and vegetable fibers. Thesis in Science and Materials Engineering. Federal University of São Paulo (2003). São Carlos, Brazil, 157f. (In Portuguese)
2. John, M.J., Thomas, S.: Biofibres and biocomposites. Carbohydr. Polym. **71**(3), 343–364 (2008)
3. Agarval, B., Broutman, L.J., Chandrashekha, K.: Analysis and Performance of Fiber Composites. John Wiley & Sons Inc., New Jersey (2006)
4. Callister, W.D., Jr.: Materials Science and Engineering an Introduction. John Wiley & Sons Inc., New York (2007)
5. Thwe, M.M., Liao, K.: Effects of environmental aging on the mechanical properties of bamboo-glass fiber reinforced polymer matrix hybrid composites. Compos. Part A Appl. Sci. Manuf. **33**, 43–52 (2002)
6. Callister Jr., W.D.: Materials Science and Engineering an Introduction, six.ed. John Wiley & Sons Inc., USA (2003)
7. Shackelford, J.F.: Materials Science For Engineers, six Peason Prentice Hall, New Jersey (2005)
8. Mitchell, B.S.: An Introduction to Materials Engineering and Science. John Wiley & Sons Inc., New Jersey (2004)
9. Cavalcanti, W.S.: Composites Polyester/vegetable woven-glass: mechanical characterization and simulation of water sorption. Thesis in Process Engineering. Federal University of Campina Grande (2006). Brazil, p 122 (In Portuguese)
10. Kaw, A.K.: Mechanics Composite Materials, 2nd edn. Taylor & Francis Group Llc, New York (2006)
11. Hull, D., Clyne, T.W.: An Introduction to Composite Materials, Cambridge Solid State Science Series, second ed. Cambridge (1996)
12. Hage Jr., E.: Compósitos e Blendas Poliméricas, Instituto Latino Americano e IBM, Campinas (1989)
13. Nóbrega, M.M.S.: Mechanical Properties of Polyester Composites Reinforced by Jute/Glass Hybrid Fabrics. Master Dissertation in Chemical Engineering, University Federal of Paraíba (2000). Campina Grande, Paraíba, Brazil (In Portuguese)
14. Sreekala, M.S., Kumaran, M.G., Thomas, S.: Water sorption in oil palm fiber reinforced phenol formaldeyde composites. Compos. Part A Appl. Sci. Manuf. **33**, 763–777 (2002)
15. Chen, H., Miao, M., Ding, X.: Influence of moisture absorption on the interfacial strength of bamboo/vinyl ester composites.Compos. Part A Appl Sci Manuf **40**(12), 2013–2019 (2009)
16. Azwa, Z.N., Yousif, B.F., Manalo, A.C., Karunasena, W.: A review on the degradability of polymeric composites based on natural fibres. Mater. Des. **47**, 424–442 (2013)
17. Espert, A., Vilaplana, F., Karlsson, S.: Comparison of water absorption in natural cellulosic fiber from wood and one-year crops in polypropylene composites and its influence on their mechanical properties. Compos. A Appl. Sci. Manuf. **35**(11), 1267–1276 (2004)
18. Lin, Q., Zhou, X., Dai, G.: Effect of hydrothermal environment on moisture absorption and mechanical properties of wood flour-filled polypropylene composites. J. Appl. Polym. Sci. **85**(14), 2824–2832 (2002)

19. Comyn, J.: Polymer Permeability. Elsevier, London, England, 383 (1985)
20. Li, Y., Mai, Y.W., Ye, L.: Sisal fibre and its composites: a review of recent developments. Compos. Sci. Technol. **60**(11), 2037–2055 (2000)
21. Wambua, P., Ivens, J., Verpoest, I.: Natural fibres: can they replace glass in fibre reinforced plastics? Compos. Sci. Technol. **63**(9), 1259–1264 (2003)
22. Aziz, S.H., Ansell, M.P., Clarke, S.J., Panteny, S.R.: Modified polyester resins for natural fibre composites. Compos. Sci. Technol. **65**(3–4), 525–535 (2005)
23. Hodzic, A., Shanks, R.: Natural fibre composites-materials, processes and properties. Ed. Woodhead Publishing Limited, Philadelphia, USA (2014)
24. Pothan, L., Thomas, S.: Effect of hybridization and chemical modification on the water-absorption behaviour of banana fiber-reinforced polyester composites. J. Appl. Polym. Sci. **91**(6), 3856–3865 (2004)
25. Carvalho, L.H., Canedo, E.L., Neto, S.F., Lima, A.G.B.: Moisture transport process in vegetable fiber composites: theory and analysis for technological applications. In: Delgado, J.M.P.Q. (ed.) Industrial and Technological Applications of Transport in Porous Materials, pp. 37–62. Berlin Heidelberg, Springer (2013)
26. Kim, J.-K., Mai, Y.-W.: Engineered Interfaces in Fiber Reinforced Composites. Elsevier, Amsterdam (1998)
27. Bunsell, A.R., Renard, J.: Fundamentals of Fibre Reinforced Composite Materials. IOP Publishing Ltda, Bristol (2005)
28. Li, X., Tabil, L.G., Panigrahi, S.: Chemical treatments of natural fiber for use in natural fiber-reinforced composites: a review. J. Polym. Environ. **15**, 25–33 (2007)
29. Joseph, P.V., Rabello, M.S., Mattoso, L.H.C., Joseph, K., Thomas, S.: Environmental effects on the degradation behaviour of sisal fibre reinforced polypropylene composites Compos. Sci. Technol. **62**, 1357–1372 (2002)
30. Wessler, K., Fogagnolo, C., Everling, M., Bernardo, H.P., Sobral, J.C., Balzer, P. S., Araujo, M.I.S.: Obtenção e caracterização de compósitos de resina poliéster e fibras de bananeira. In: Congresso de Ciência dos Materiais do Mercosul SULMAT 2004, Joinvile, Brazil, 1–6 (2004)
31. Carvalho, L.H., Ladchumananandasivam, R., Alexandre, M.E.O., Cavalcanti, W.S.: Propriedades de compósitos poliéster/fibra da folha do abacaxi. In: Congresso em Ciência dos Materiais do Mercosul. SULMAT 2004, Joinvile, Brazil, 1–6 (2004)
32. Kucak, D., Mistik, S.I.: The use of palm leaf fibers as reinforcements in composites. In: Faruk, O., Sain, M. (Eds.) Biofiber reinforcement in composites materials. Elsevier Ltda. , Amsterdam, Chapter 9, pp. 273–281
33. Rouison, D., Couturier, M., Sain, M., Macmillan, B., Balcom, B.J.: Water absorption of hemp fiber/unsaturated polyester composites. Polym. Compos. **26**(4), 509–524 (2005)
34. Dhakal, H.N., Zhang, Z.: The use of hemp as reinforcements in composites. In: Faruk, O., Sain, M. (Eds.) Biofiber Reinforcement In Composites Materials. Elsevier Ltda., Amsterdam, Chapter 3, pp. 86–103 (2007)
35. Dhakal, H.N., Zhang, Z.Y., Richardson M.O.W.: Effect of water absorption on the mechanical properties of hemp fibre reinforced unsaturated polyester composites. Compos. Sci. Technol. **67**(7–8), 1674–1683 (2007)
36. Bismarck, A., Askargorta, I.A., Springer, J., Lampke, T., Wielage, B., Stamboulis, A.: Surface characterization of flax, hemp and cellulose fibres; surface properties and the water uptake behaviour. Polym. Compos. **23**(5), 872–894 (2002)
37. Paiva, J.M.F., Frollini, E.: Phenolic thermofix matrix in reinforced composites with sugarcane bagasse fibers. Polímeros. **2**, 78–87 (1999)
38. Sanchez, E.M., Cavani, C.S., Leal, C.V., Sanchez, C.G.: Composites of unsaturated polyester resin with sugarcane bagasse: influence of fiber treatment on properties. Polymer **20**(3), 194–200 (2010)
39. Du, Y., Yan, N., Kortschot, M.T.: The use of ramie fibers as reinforcements in composites. In: Faruk, O., Sain, M. (Eds.) Biofiber Reinforcement in Composites Materials. Elsevier Ltda., Amsterdam, Chapter 4, pp. 104–137 (2015)

40. Leão, A.L., Cherian, B.M., Narine, S., Souza, S.F., Sain, M., Thomas, S.: The use of pineapple leaf fibers (palts) as reinforcements in composites. In: Faruk, O., Sain, M. (Eds.) Biofiber Reinforcement in Composites Materials. Elsevier Ltda., Amsterdam, Chapter 7, pp. 211–235 (2015)
41. Jayamol, G., Bhagawan, S.S., Thomas, S.: Effects of environment on the properties of low-density polyethylene composites reinforced with pineapple-leaf fibre. Compos. Sci. Technol. **58**(9), 1471–1485 (1998)
42. Khalil, H.P.S.A., Alwani, M.S., Islam, M.N., Suhaily, S.S., Dungani, R., H'ng, Y.M.: The use of bamboo fibers as reinforcements in composites. In: Faruk, O., Sain, M. (Eds.) Biofiber Reinforcement in Composites Materials. Elsevier Ltda., Amsterdam, Chapter 16, pp. 488–524 (2015)
43. Liu, W., Qiu, R., Li, K.: Effects of fiber extraction, morphology, and surface modification on the mechanical properties and water absorption of bamboo fibers-unsaturated polyester composites. Polym. Compos. **37**(5), 1612–1619 (2016)
44. Souza, S.F., Ferreira, M., Sain, M., Ferreira, M.Z., Pupo, H.F., Cherian, B.M., Leão, A.L.: The use of curaua fibers as reinforcements in composites. In: Faruk, O., Sain, M. (Eds.) Biofiber Reinforcement In Composites Materials. Elsevier Ltda., Amsterdam, Chapter 22, pp. 700–720 (2015)
45. Mamun, A.A., Heim, H.P., Faruk, O., Bledzki, A.K.: The use of banana and abaca fibers as reinforcements in composites. In: Faruk, O., Sain, M. (Eds.) Biofiber Reinforcement In Composites Materials. Elsevier Ltda., Amsterdam, Chapter 8, pp. 236–272 (2015)
46. Haneefa, A., Bindu, P., Arvind, I., Thomas, S.: Studies on tensile and flexural properties of short banana/glass hybrid fiber reinforced polystyrene composites. J. Compos. Mater. **42**(15), 1471–1489 (2008)
47. Kiran, C.U., Reddy, G.R., Dabade, B.M., Rajesham, S.: Tensile properties of sun hemp, banana and sisal fiber reinforced with polyester composites. J. Reinf. Plast. Compos. **26**(10), 1043–1050 (2007)
48. Badia, J.D., Kittikorn, T., Strömberg, E., Santonja-Blasco, L., Martínez-Felipe, A., Ribes-Greus, A., Ek, M., Karlsson, S.: Water absorption and hydrothermal performance of PHBV/sisal biocomposites. Polym. Degrad. Stab **108**, 166–174 (2014)
49. Chow, C.P.L., Xing, X.S., Li, R.K.Y.: Moisture absorption studies of sisal fibre reinforced polypropylene composites Compos. Sci. Technol. **67**, 306–313 (2007)
50. Li, Y., Shen, Y.O.: The use of sisal and henequen fibers as reinforcements in composites. In: Faruk, O., Sain, M. (Eds.) Biofiber Reinforcement in Composites Materials. Elsevier Ltda., Amsterdam, Chapter 6, pp. 165–210 (2015)

Chapter 3
Experimental Analysis

This chapter provides experimental information on water absorption in unsaturated porous media, with particular reference to vegetable fiber-reinforced polymer composites. Herein, important information related to fiber morphology, manufacturing, moisture absorption, and mechanical caracterization tests in polymer composites reinforced by caroá, macambira and sisal fibers are presented in detail. Results of the fiber morphology, moisture gain kinetics, for different sample thickness and process temperature, and mechanical properties (tensile strength, elastic modulus, impact resistance and elongation) are shown and analyzed.

3.1 Background

In physical problems involving moisture absorption or desorption in composites, it is very important to determine the moisture content at any instant of the process. In general, mass transfer rate from or to the body depends on different factors such as temperature, filler content, initial moisture content, and nature and orientation of the reinforcement. Further, hydric, thermal and mechanical events (in a micro scale analysis) occurring in short fiber reinforced composites are very different from those verified for long fiber reinforced composites [1].

All of the factors mentioned above affect mechanical performance and properties and limit the field of application of vegetable reinforced polymer composites [2–9] and new researches in this area are required. Several of the papers reported in the literature are directed to the problem of moisture absorption by composites reinforced by plant fibers and their influence on the properties of the material such as those by Marcovich et al. [10], Thwe and Liao [11], Mulinari [12], Sreekala et al. [13], Espert et al. [14], Angrizani et al. [15], Fernandes [16], Vieira [17], Jayamol et al. [18], Cavalcanti et al. [19], Santos [20], Sanchez et al. [21], Tita et al. [22], Rao et al. [23],

Sensarzadeh and Amiri [24], Idriss et al. [25], Soni and Soni [26], Srihari et al. [27], Pavlidou and Papaspyrides [28], Pegoretti and Penati [29], Kumosa et el. [30], and many others.

As a complement to the theme discussed in this book, and due to the importance of accurately describing the water sorption phenomena in vegetable fiber-reinforced polymer composites, experimental studies about water sorption by unsaturated polyester composites reinforced with short fibers of macambira (*Bromelia Laciniosa*), caroá (*Neoglaziovia Variegata*), and sisal (*Agave sisalana*) fibers are presented here.

3.2 Experimental Setup

Nóbrega [8] and Nóbrega et al. [31] conducted several experiments on the water absorption of caroá fiber-reinforced unsaturated polyester composites. Similarly Cruz et al. [32] conducted experiments with macambira fiber-reinforced unsaturated polyester composites, while Santos [20] conducted sorption experiments with sisal fiber-reinforced unsaturated polyester composites.

Macambira fibers (Fig. 3.1) are extracted from the macambira plant, which belongs to the family Bromeliaceae. The plant used in the study, was obtained from the Cariri region of the State of Paraíba State in Brazil and its chemical composition was determined to be: α-cellulose (58.72%), hemicellulose (19.37%), lignin (12.62%), moisture (8.94%), and others [33].

Caroá fibers (Fig. 3.2) are extracted from the caroá plant, which also belongs to the family Bromeliaceae. The plant employed in the study reported here was obtained at a farm in the town of Pocinhos in the State of Paraíba State in Brazil. Caroá leaves provide long fibers, of great resistance and durability. The chemical composition of the caroá fiber is as follows: cellulose (35.5%), hemicellulose (17.9%) and lignin (30.1%) and others [8, 34].

(a)   (b)

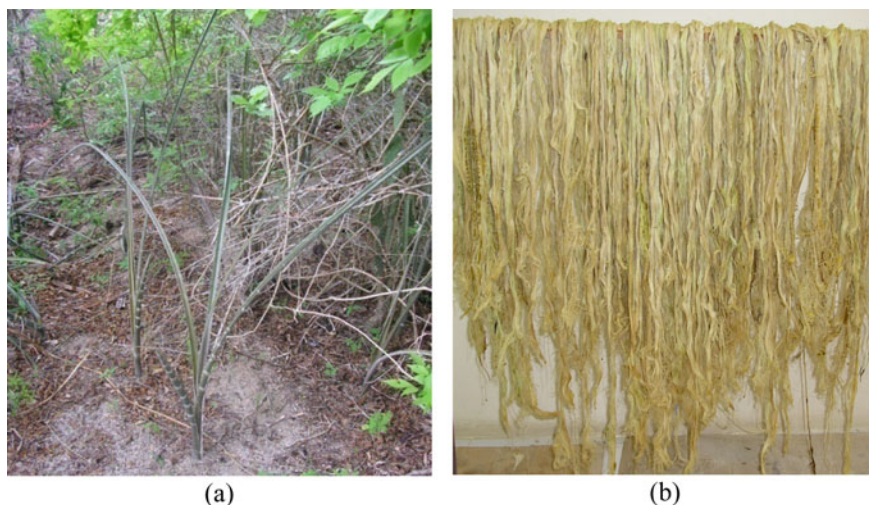**Fig. 3.1** Macambira (Bromelia Laciniosa). **a** Plant and **b** fibers

Fig. 3.2 Caroá (Neoglaziovia Variegata). **a** Plant and **b** fibers

Sisal fibers (Fig. 3.3) are extracted from the Sisal plant which belongs to the family Agavaceae. The plant obtained in the study reported here came from a farm in the town of Pocinhos in the State of Paraíba in Brazil. Sisal leaves provide long fibers, of great resistance and durability. The chemical composition of the sisal fiber is as follows: cellulose (65.8%), hemicellulose (12.0%) and lignin (9.9%) and others [6, 20, 34].

The fibers of caroá and macambira were washed with running water, allowed to air dry at room temperature for at least 72 h before being combed and cut up to 5 cm.
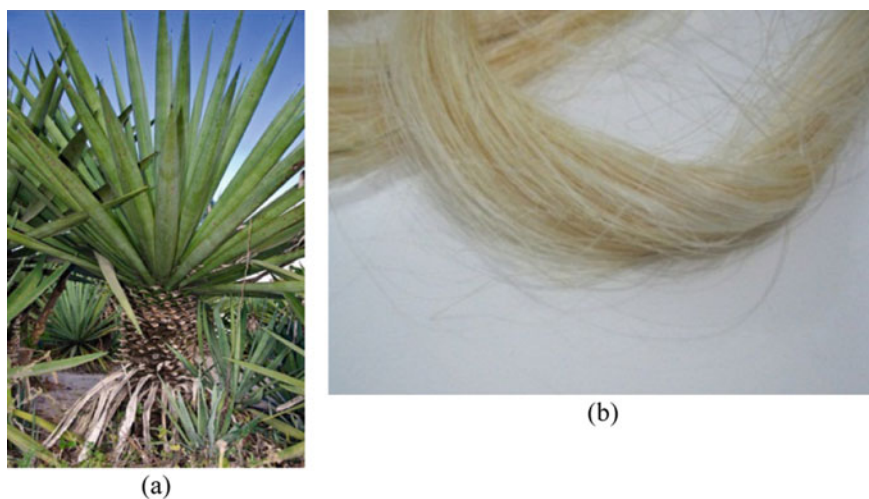

Fig. 3.3 Sisal (Agave sisalana). **a** Plant and **b** fibers

The sisal fibers were dried in an air circulation oven operating at 60 °C until constant weight and subsequently heated at 105 °C for 24 h, in order to obtain the dry fiber. The dried sisal fibers were cut in 35 mm lengths prior to use. Unsaturated polyester cured with 1% MEK (methyl ethyl ketone) was used as the matrix.

Composites with varying fiber contents were compression molded. Since the thermal degradation of natural fibers and thermoset or thermoplastic polymers occurs at upper temperature limits, composite samples were made at low temperature. A fiber mat was produced by randomly distributing a pre-determined amount of fibers in steel molds (220 × 180 × 3 mm and 220 × 180 × 6 mm) and compressed with 2 ton for 5 min at room temperature. The mats thus produced were removed from the mold for further use as reinforcement. An appropriate quantity of polyester resin was mixed with the catalyst and a small amount was poured onto the mold. The fiber mats were placed in the steel mold, impregnated with more resin and the mold was closed (8 ton).

The system was allowed to cure under pressure for 4 h at room temperature before the composite plate was removed from the mold. The caroá and macabira reinforced composite plates obtained were post-cured in an air circulating oven operating at 50 °C for 48 h (Fig. 3.4), while sisal composite plates were post-cured in an air circulating oven operating at 60 °C for 48 h.
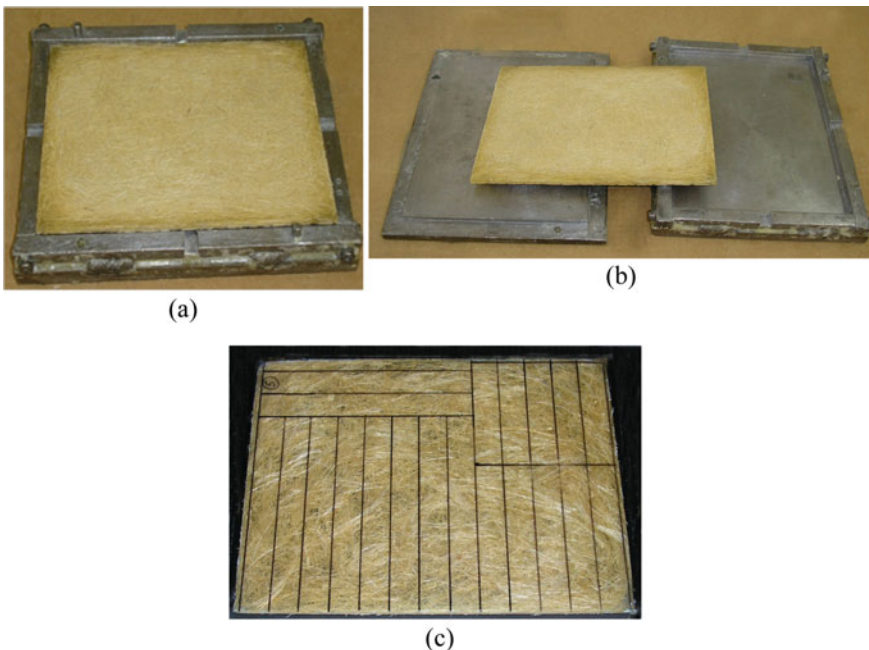

Fig. 3.4 Manufacturing of caroá fiber-reinforced polymer composite by hand lay up technique. **a** Fiber mat in the mold, **b** Demolding, and **c** cut samples

Tests for mechanical properties were conducted according to ASTM standards D-3039 and D-256 for tensile and impact tests (Fig. 3.5a–b), respectively. Composites samples of 20×20 mm were cut-off from the plates, and their edges were sealed with resin prior to the water absorption tests (to avoid water transport by capillarity) and dried in an air-circulating oven at 105 °C to constant weight or dry mass (Fig. 3.5c).

The water absorption experiments were carried out according to the following procedure. Firstly, the pre-dried composites samples were fully immersed in water baths (Fig. 3.6) kept at 25, 50 and 70 °C. At regular time intervals, the samples were removed from the water bath; pat-dried with a paper tissue to remove surface water
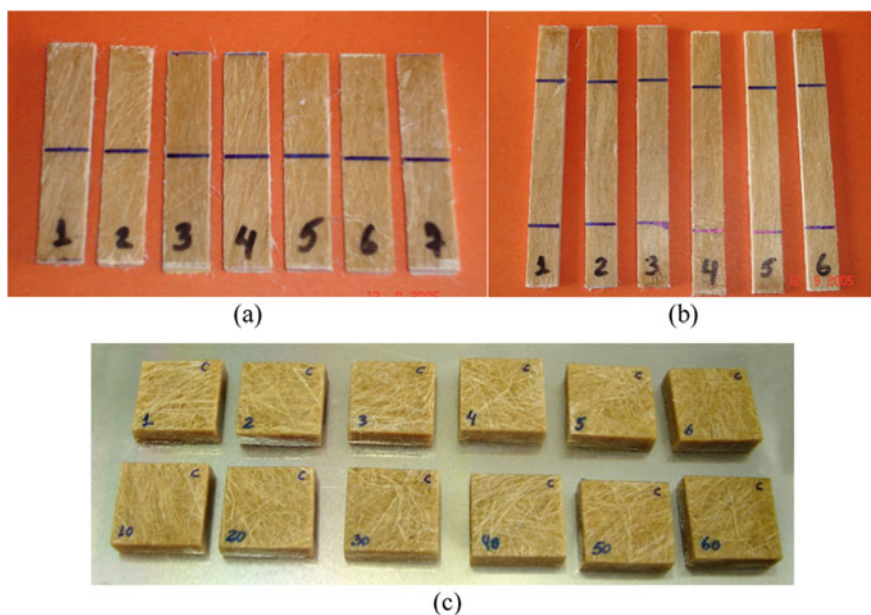

Fig. 3.5 Caroá fiber-reinforced polymer composite samples used at different test. **a** Impact, **b** Tensile and **c** Water sorption

Fig. 3.6 **a** Caroá and macambira composite specimens and **b** Macambira and caroá composites samples in water bath

and immediately weighted in a digital scale (uncertainty ±0.001 g). The samples were re-immersed in the water bath and the procedure repeated so that the water sorption process continued until equilibrium was reached. Each measurement took less than 1 min, so water evaporation at the surface was deemed insignificant.

The results of absorbed moisture were reported as mass of absorbed water per unit of dry composites mass. Thus, moisture content was computed as follows:

$$\bar{M}(t) = \frac{m_t - m_0}{m_0} \times 100\% \tag{3.1}$$

where m_0 and m_t represent the dry mass of the composites samples (t = 0) and the wet mass at any specific time t, respectively.

Saturation (equilibrium) condition was assumed when the daily weight gain of the composite samples was less than 0.1%. We notice that complete immersion of composite samples in water bath constitutes the most severe physical situation; exposure to humid air results in lower equilibrium moisture content.

3.3 Experimental Results Analysis

3.3.1 Morphology Characterization of the Fibers

The microstructure of vegetable fibers is complex, and dependent on each kind of the fiber. In this research some single caroá, macambira and sisal fiber samples (untreated) were analyzed by scanning electron microscopy (SEM), in order to characterize their morphology. Figures 3.7, 3.8 and 3.9 present micrographs (transversal section) of macambira, caroá and sisal fibers in the natural state, respectively.

Analysis of these figures shows that the arrangement is similar to other natural fibers, with a spongy aspect and thin, compacted cellular arrangement (regular fiblilar arrangement). In some places is verified the presence of small amout of organic material at the fiber surface, probably a residue left when the fibers were extracted from the leaves of the each plant.

Images obtained from SEM also showed rougher surfaces and many void spaces, which implies that macambira, caroá ans sisal fibers could be adequate to be used as reinforcement in composite materials; this surface condition allows good adhesion between fibers and polymer matrix. However, it is important to state that, after treatment or mechanical characterization, the fibers achieve some degradation, and impurities existing at the surface are minimized. Furthermore, since cellulose is the major constituent with a crystalline structure, it is the main contributor towards the mechanical properties.

From the viewpoint of water absorption, cellulose fibers are difficult to dissolve because of their high crystallinity, but, they tend to retain liquids in the interfibrilar space [35].
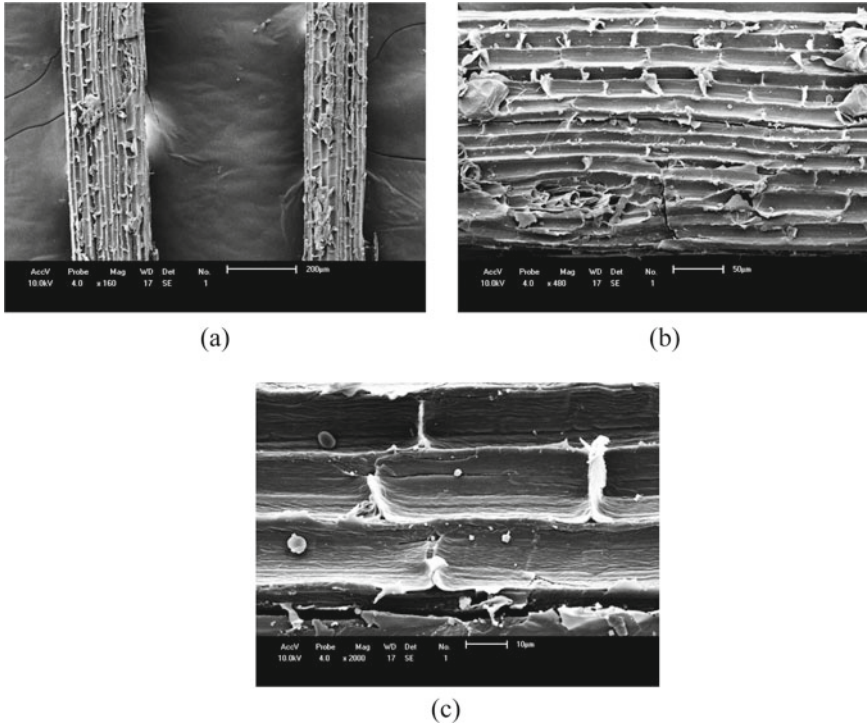
(a)   (b)

(c)

Fig. 3.7 SEM micrographs for untreated macambira fiber: **a** 160×, **b** 480× and **b** 2000×

3.3.2 Water Absorption Kinetics

Water sorption curves of unsaturated polyester/macambira composites, unsaturated polyester/caroá composites and unsaturated polyester/sisal composites are illustrated in Figs. 3.10 and 3.11. Results are reported for different dimensions of the samples (3 mm and 6 mm thickness) and water bath temperatures (25, 50 and 70 °C) as function of exposure (immersion) time. Upon analyzing of these figures it can be seen that the general shape of the curves is similar to those of others natural fiber-reinforced polymer matrix composites.

For all investigated composites the moisture content increases monotonically with water immersion time until it reaches a maximum value, the so-called equilibrium moisture content (saturation or hygroscopic condition). This behavior strongly indicates that the vegetable fibers were uniformly distributed in the matrix, as reported in the literature [2]. Figures 3.10, 3.11 and 3.12 also show that water sorption for all composites increase with the area/volume ratio and temperature (Table 3.1). Sample size effect was more pronounced at the lower temperature.

Table 3.1 summarizes the saturation data for all tested composites and for neat polyester. The data indicates that water absorption for the composites is higher than
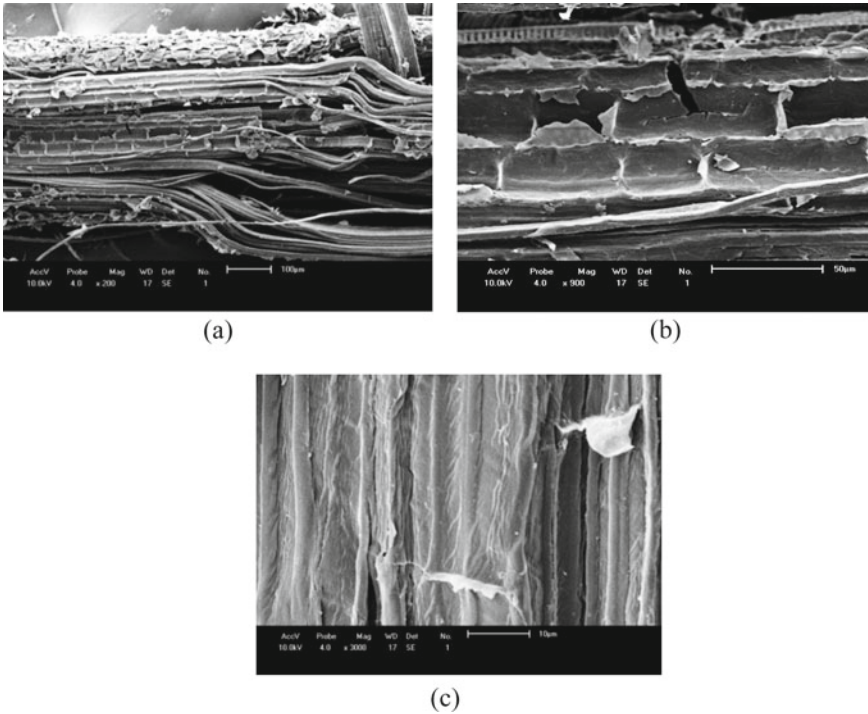
Fig. 3.8 SEM micrographs for untreated caroá fiber: **a** 200×, **b** 900× and **b** 3000×

for the matrix. Neat polyester shows a very low percentage of absorbed water. While the water sorption at the equilibrium condition for the unsaturated polyester is about 1%, for the composites it ranged from 14.04 to 18.09%. It was verified that the weight gain of pure polyester was almost insignificant, indicating minimal degradation. These results are consistent with studies reported in the literature for similar systems [2, 8, 10, 13, 36]. Some authors attribute the increase in the water sorption by polymer composites reinforced with vegetable fiber not only to the hydrophilic nature and the permeability of this type of reinforcement but also to the sample surface area exposed to water. Capillarity effects and the interfacial area between fiber and matrix may also contribute to water pick-up by these composites.

Results indicate that the water uptake of the composite sample immersed in a water bath at 70 °C was faster than under the other (25 and 50 °C) experimental conditions. This behavior is attributed to the increased water mobility within the solid at higher temperature. It is believed that higher water temperatures lead to thermal dilation of the composites and to increased composite porosity, which would, in turn, cause a faster moisture migration. Temperature activates the water diffusion process inside the sample, and sorption rate increases with the increases in temperature (thermo-activation).
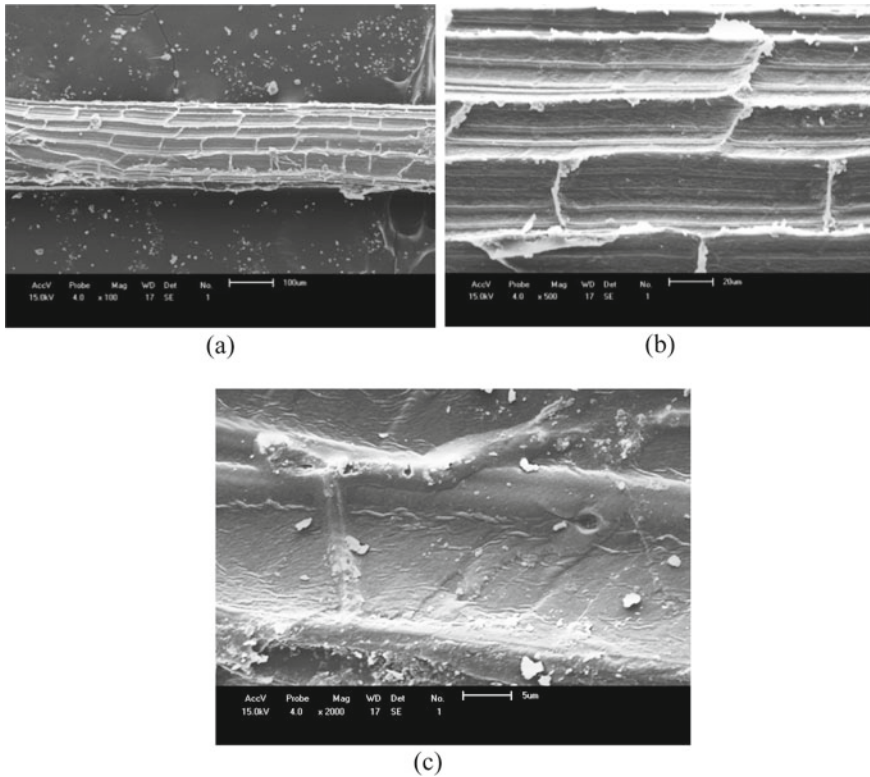
Fig. 3.9 SEM micrographs for untreated sisal fiber: **a** 100×, **b** 500× and **b** 2000×

These results are consistent with those reported in similar systems for unsaturated polyester/caroá composites [8, 31], unsaturated polyester/jute composites [36] and unsaturated polypropylene/sisal composites [35]. Other aspects were not analyzed, such as fiber size and orientation (events that occur in long fiber reinforced composites are different those observed in short fiber reinforced composites) [1], and water migration by capillarity into micro cracks inside the solid, mainly in the fiber-matrix interface where adhesion plays an important role. Reading reported works on these topics is strongly recommended.

3.3.3 Mechanical Properties

As already mentioned in the previous sections, the mechanical performance of the composites depends on the properties of both reinforcement and matrix, and the adhesion between them after manufacturing. Figure 3.13 show the results of tensile strength of the caroá fiber-reinforced polymer composites (in dry condition) as a
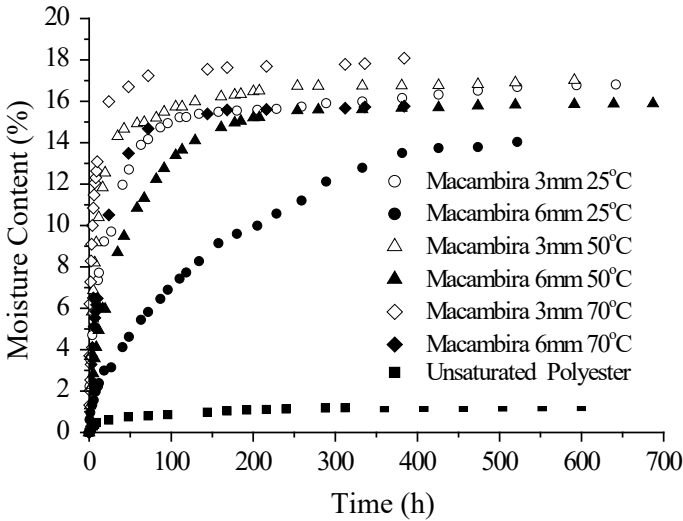
Fig. 3.10 Water sorption kinetics of macambira fiber-reinforced unsaturated polyester composites (30% w/w fiber content)
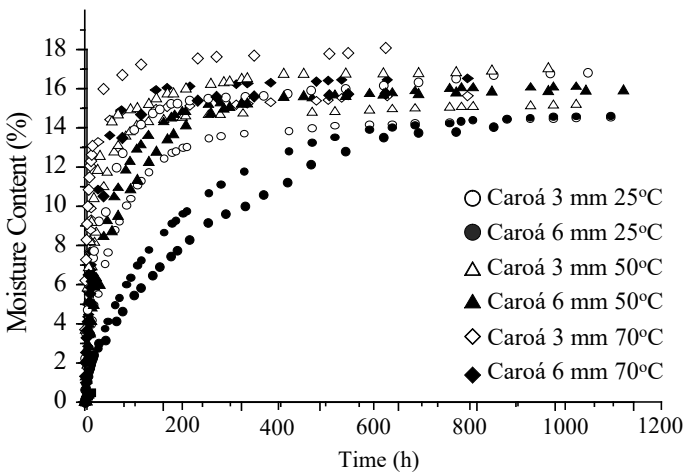
Fig. 3.11 Water sorption kinetics of caroá fiber-reinforced unsaturated polyester composites (30% w/w fiber content)

function of fiber content. Analysis of this figure, shows that the tensile strength of the composite is lower than that of the matrix for loadings up to 25% by weight for caroá fibers. This behavior can be attributed to inefficient loading, so the fibers act as defects (stress concentrators) and effectively weaken the matrix, resulting in a composite with lower mechanical strength. At low fiber content, the matrix is not sufficiently fixed
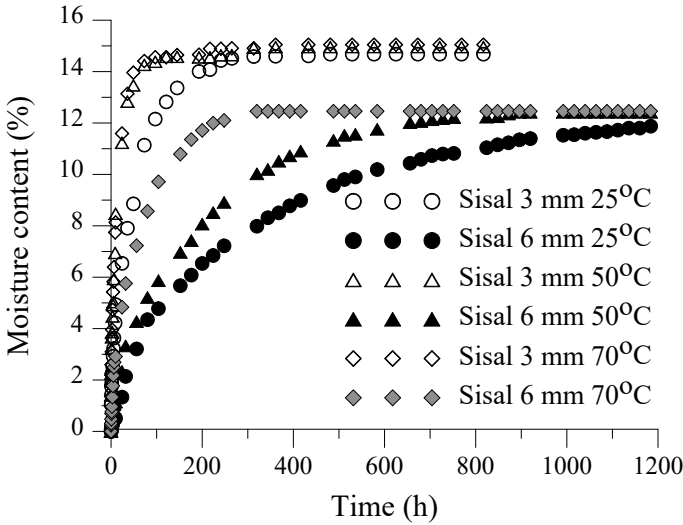
Fig. 3.12 Water sorption kinetics of sisal fiber-reinforced unsaturated polyester composites (46.6% w/w fiber content)

(poor adhesion) and high deformations imposed on it lead to a break of the matrix-fiber bond. As the loading increases, stresses are more uniformly distributed and the composite's strength increases. Obviously this behavior is dependent on the critical volume of the fiber into the matrix.

At loadings above 40% by weight, the tensile strength of the composites decreases with a further increase in fiber content. This behavior associated with fiber agglomeration and poor impregnation, which leads to an increase in their effective diameter, a decrease in their aspect ratio and to void formation.

Figure 3.14 illustrates the effect of the fiber content on the elastic modulus of the caroá fiber-reinforced polymer composite composites (in dry condition). The results show that fiber incorporation increases the stiffness of the composite. This behavior was expected, since the strength and Young´s modulus of the fibers used are higher than the matrix. In addition, fiber addition minimizes the movement of polymer chains resulting in an increase in the elasticity modulus of the composite with fiber content.

Figure 3.15 displays the impact resistance of the caroá fiber-reinforced polymer composite as a function of fiber content (in dry condition). Upon analyzing this figure, it can verified that impact strength increases with fiber content at all loading levels for the type of fiber tested. Based on the results, we state that the caroá fiber is able to diverge crack propagation and delay breakage, thus increasing impact strength. It is worth noticing that impact properties are not as dependent on fiber/matrix adhesion as the tensile strength and, in fact, this mechanical property often is improved for physical situations with looser interfaces.

Table 3.1 Moisture content and geometric data for the water sorption in vegetable fiber reinforced composites (30% w/w fiber contents)

Sample	Thickness (mm)	T_W (°C)	t (h)	M_t (%) (d. b.) ($t \to \infty$)	Area/Volume (mm^2/mm^3) (t = 0)
Polyester matrix	3.00	25	600	1.26	866.67
Macambira composite	3.00	25	642	16.81	866.67
	6.00	25	594	14.04	533.33
	3.00	50	687	17.02	866.67
	6.00	50	687	15.89	533.33
	3.00	70	384	18.09	866.67
	6.00	70	648	16.18	533.33
Caroá composite	3.00	25	1100	14.49	866.67
	6.00	25	1623	14.81	533.33
	3.00	50	1022	15.16	866.67
	6.00	50	1022	16.08	533.33
	3.00	70	796	15.61	866.67
	6.00	70	796	16.52	533.33
Sisal composite	3.00	25	817	14.68	533.33
	6.00	25	1328	12.27	866.67
	3.00	50	817	14.96	533.33
	6.00	50	848	12.42	866.67
	3.00	70	817	15.05	533.33
	6.00	70	848	12.46	866.67

Figure 3.16 shows the elongation at break of the caroá fiber-reinforced polyester composite as function of fiber content (in dry condition). It can be observed that elongation at break increases with fiber incorporation the incorporation of fiber increases the properties of elongation at fiber contents above 23%. This behavior is attributed to the greater stiffness of the fiber, thus, increasing the stiffness of the composite.

Since moisture absorption affects the mechanical performance of fiber-reinforced polymer composites, results of the mechanical tests of sisal fiber-reinforced polymer composites are shown in Figs. 3.17, 3.18, 3.19 and 3.20, as reported by Santos [20] and Santos et al. [37]. These results were obtained with 3 and 6 mm thick samples. Saturation conditions at different water bath temperatures are cited in Table 3.1.

Analysis of these figures indicate that tensile strength, impact strength, Young's modulus and elongation at break of the composites decrease with the increasing water bath temperature. This behavior can probably be associated with the fact that an increase in water bath temperature provokes deterioration and dilation of the samples and, thus, increasing moisture rate and facilitating water migration to inside the composite and, thus leading to a decrease in mechanical properties. The effect of sample thickness also is evident.
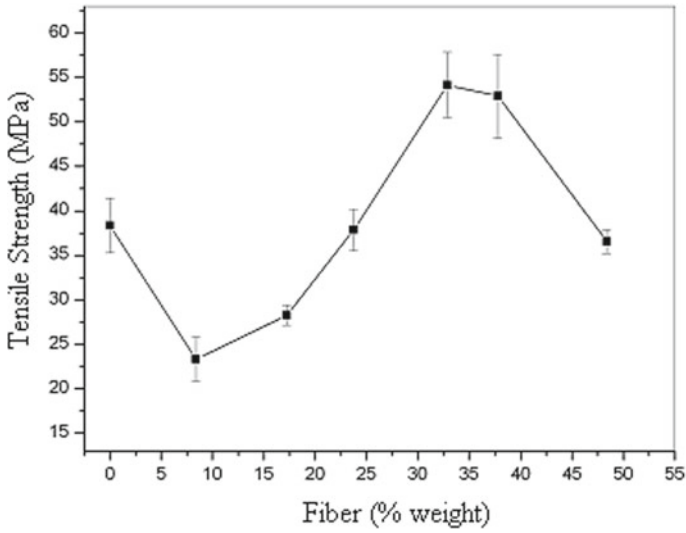
Fig. 3.13 Tensile strength of the caroá fiber-reinforced polymer composite as a function of the fiber content
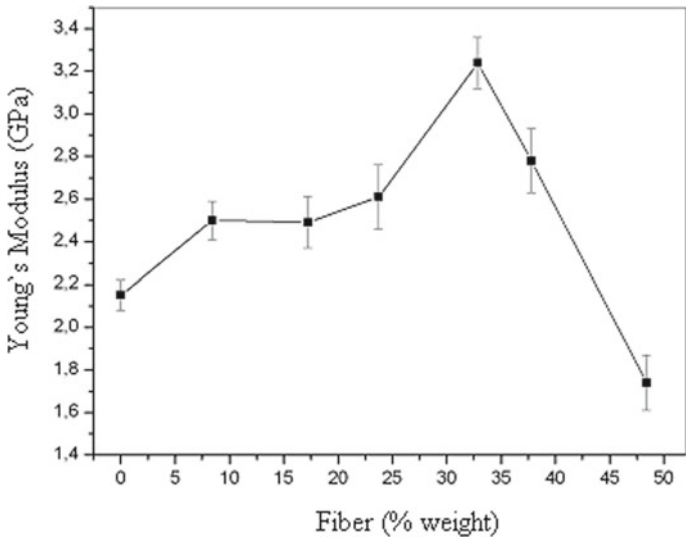
Fig. 3.14 Young's modulus of caroá fiber-reinforced polymer composite as a function of the fiber content

Fig. 3.15   Impact resistance of caroá fiber-reinforced polymer composite as a function of the fiber content
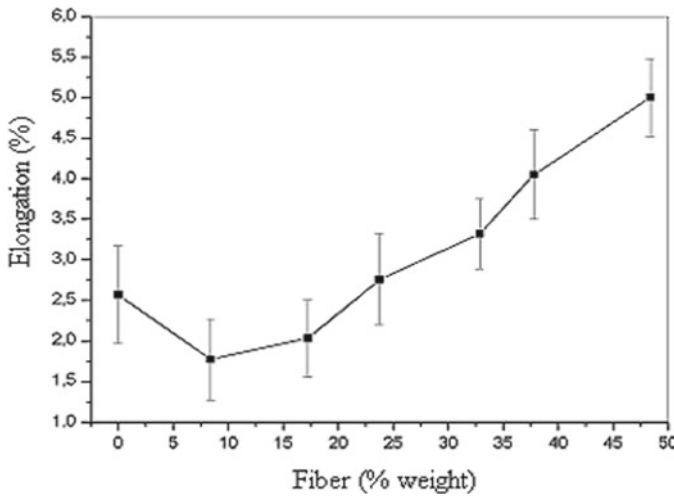
Fig. 3.16   Elongation at break of caroá fiber-reinforced polymer composite as a function of fiber content

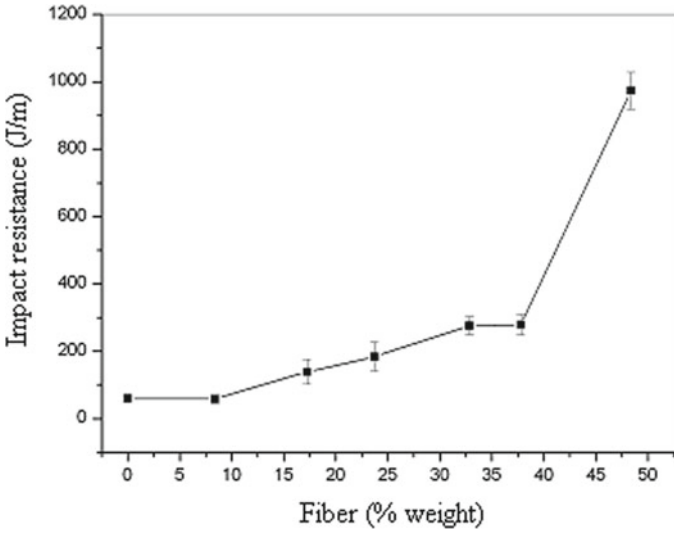Furthermore, it is important to notice that the decrease in mechanical property values of the composite are associated with the poor fiber-matrix interfacial adhesion caused by water absorption as previously discussed [14].
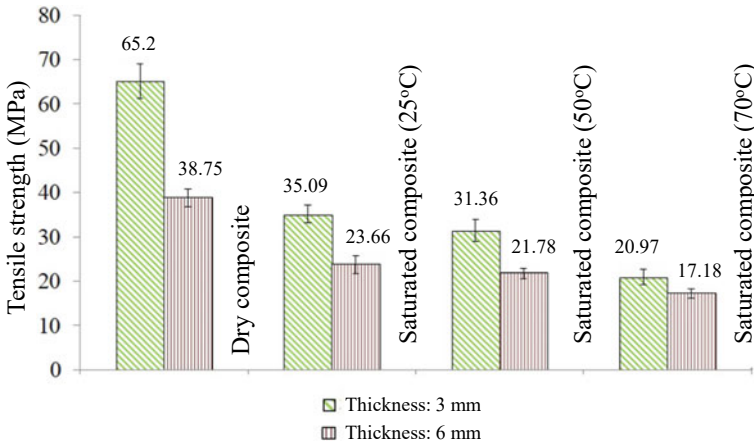
Fig. 3.17   Tensile strength of polyester composite (44.6% sisal fiber)
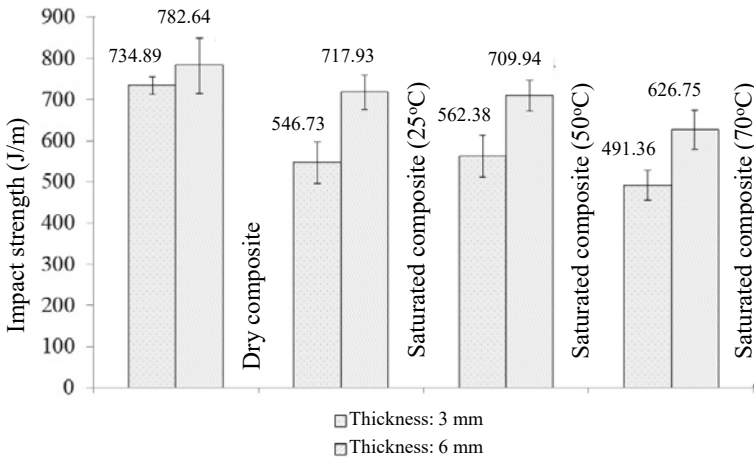
Fig. 3.18   Impact resistance of polyester composite (44.6% sisal fiber)

Different methods to improve fiber/matrix interfacial adhesion have been used in order to minimize this problem. In general, these methods are based on chemical treatment or by addition of coupling agent, as reported by Du et al. [38]. However, drying of vegetable fibers as a pre-treatment has been used as well [39]. Carvalho et al. [39] reported an experimental study about tensile properties of hybrid jute/cotton and sisal/cotton fabrics–polyester matrix composites. According to the authors, the amount of absorbed water on the composites was effectively reduced when the fabrics were pre-dried before their incorporation into the composites. Furthermore, it was verified that composites manufactured with pre-dried fabrics showed smaller strain at break, indicating a better fabric-matrix interaction.
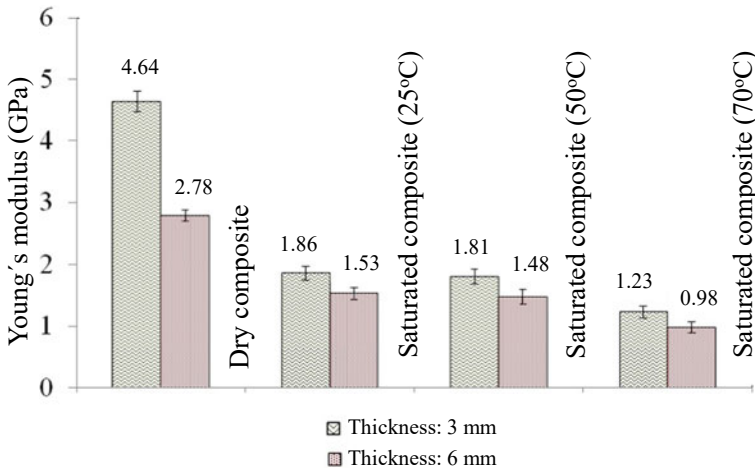
Fig. 3.19 Young's modulus of polyester composite (44.6% sisal fiber)
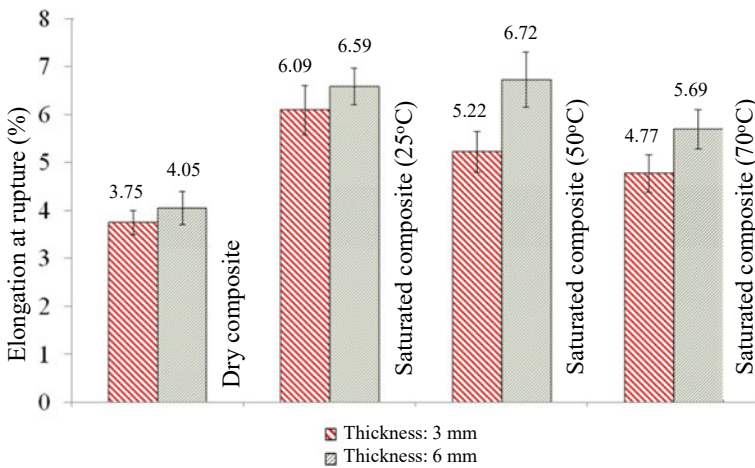
Fig. 3.20 Elongation at break (b) of polyester composite (44.6% sisal fiber)

Figures 3.21 and 3.22 illustrate the polyester-sisal samples with 3 mm and 6 mm thickness in the saturation condition at water bath temperature of 25 °C and 70 °C, respectively [20]. Tese figures show an increase in volume, as well as the deterioration of the composite samples, both due to the thermal effect and the presence of moisture. These effects are most severe at higher water bath temperature.

For composites with 3 mm thickness, there was an increase in volume of 19.77%, 21.77% and 31.34% for temperatures 25 °C, 50 °C and 70 °C, respectively. For composites with a thickness of 6 mm, the increase in volume was 15.95%, 17.25% and 21.32% for the same temperature range. The increase in volume of the samples was

Fig. 3.21 Sisal fiber-reinforced polyester composite (44.6% sisal fiber) at saturation condition (T = 25 °C). **a** 3 mm and **b** 6 mm thickness
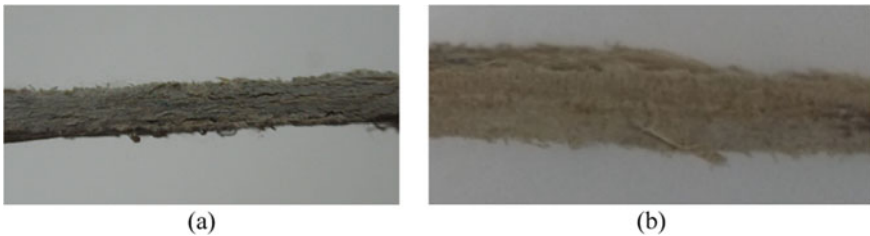
Fig. 3.22 Sisal fiber-reinforced polyester composite (44.6% sisal fiber) at saturation condition (T = 70 °C). **a** 3 mm and **b** 6 mm thickness

greater than the maximum moisture content absorbed, which probably can be associated with the combined effect of the bath temperature and moisture that accelerates the sample deterioration.

With the aim to better identify the interactions between sisal fiber and polyester matrix (compatibility and dispersion), a SEM experimental study was carried out on tensile tested samples. Figures 3.23 and 3.24 illustrate the SEM micrographs of fractured surface of 3 mm and 6 mm thick untreated sisal fiber-reinforced polymer composite samples, respectively, in the saturation condition at water bath temperature 70 °C [20]. It is possible to verify that, due to the random arrangement of the short fibers and severe experimental conditions, a moderate interfacial adhesion was obtained in the composite manufactured. The main failure mechanisms in the composite samples were debonding and fiber breakage, both due to the thermal effect and the presence of moisture, as highlighted in these figures. Other phenomena such as fiber splitting, brittle surface and pull-out were also verified.

Fiber debonding

Rupture of fibers
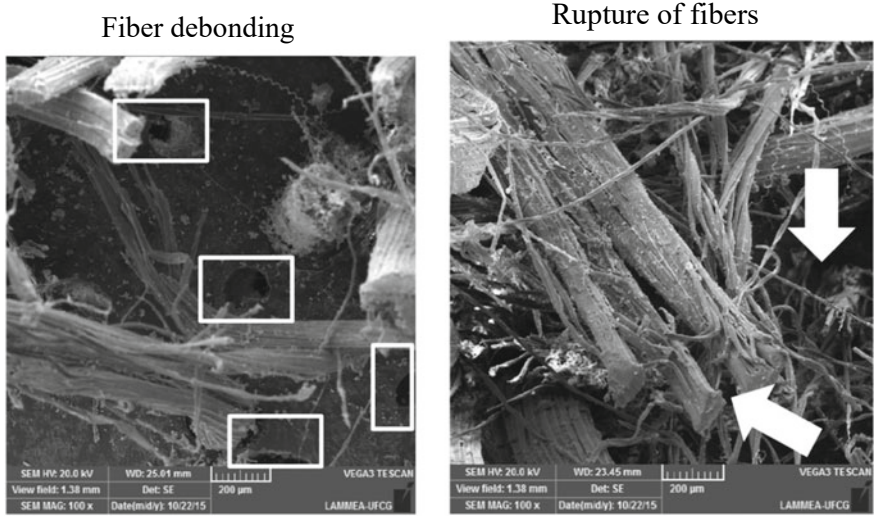
Fig. 3.23 SEM Micrographs (100X) of fractured surface of untreated sisal fiber-reinforced polyester composite (saturation condition at 70 °C and 3 mm thickness)

Fiiber debonding

Rupture of fibers
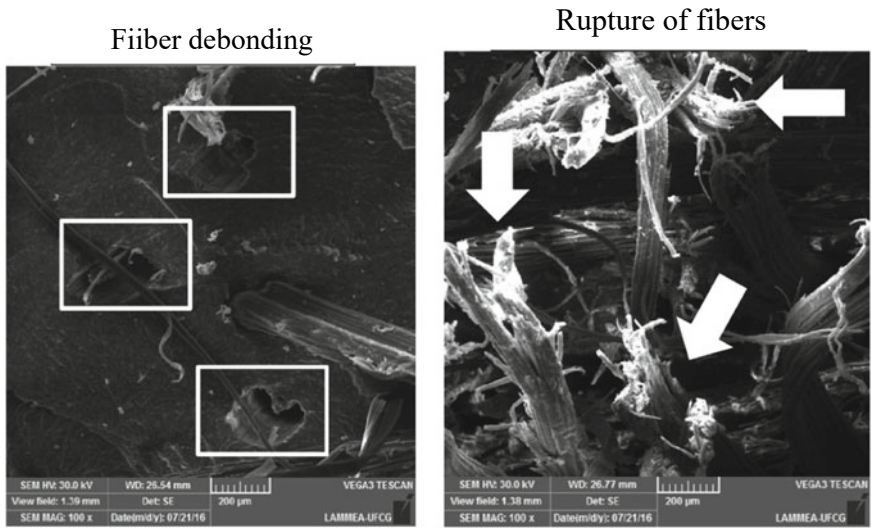
Fig. 3.24 SEM Micrographs (100X) of fractured surface of untreated sisal fiber-reinforced polyester composite (saturation condition at 70 °C and 6 mm thickness)

References

1. Herrera-Franco, P.J., Valadez-Gonzalez, A.: A study of the mechanical properties of short natural-fiber reinforced composites. Compos. Part B Eng. **36**, 597–608 (2005)
2. Chow, C.P.L., Xing, X.S., Li, R.K.Y.: Moisture absorption studies of sisal fibre reinforced polypropylene composites. Compos. Sci. Technol. **67**, 306–313 (2007)
3. Bledzki, A.K., Reihmane, S., Gassan, J.: Properties and modification methods for vegetable fibers for natural fiber composites. J. Appl. Polym. Sci. **59**, 1329–1336 (1996)
4. Clark, R.A., Ansell, M.P.: Jute and glass fibre hybrid laminates. J. Mater. Sci. **21**, 269–276 (1986)
5. Cavalcanti, W.S., Carvalho, L.H., Lima, A.G.B.: Water diffusion in unsaturated polyester composite reinforced by a hybrid jute/glass fabric: modeling and simulation. Revista Matéria **10**(1), 14–23 (2005) (In Portuguese)
6. Bledzki, A.K., Gassan, J.: Composite reinforced with cellulose based fiber. Prog. Polym. Sci. **24**, 221–274 (1999)
7. Andreopoulos, A.G., Tarantili, P.A.: Water sorption characteristics of epoxi resin–UHMPE fibers composites. J. Appl. Polym. Sci. **70**, 747–755 (1998)
8. Nóbrega, M.M.S.: Polyester matrix composite with caroá fibers (Neoglaziovia variegata): Mechanical charcterization and water sorption. Doctorate Thesis, Process Engineering, Federal University of Campina Grande, Paraíba, Brazil (2007) (In Portuguese)
9. Tsai, Y.I., Bosze, E.J., Barjasteh, E., Nutt, S.R.: Influence of hygrothermal environment on thermal and mechanical properties of carbon fiber/fiberglass hybrid composites. Compos. Sci. Technol. **69**(3–4), 432–437 (2009)
10. Marcovich, N.E., Reboredo, M.M., Aranguren, M.I.: Moisture diffusion in polyester-woodflour composites. Polym. **40**, 7313–7320 (1999)
11. Thwe, M.M., Liao, K.: Effects of environmental aging on the mechanical properties of bamboo-glass fiber reinforced polymer matrix hybrid composites. Compos. Part A Appl. Sci Manuf. **33**, 43–52 (2002)
12. Mulinari, D.R.: Thermal, mechanical and morphological behavior of high density polyethylene composites reinforced with sugarcane bagasse cellulose fiber. Thesis in Mechanical Engineering, Paulista State University (2009). Guaratinguetá, Brazil (In Portuguese)
13. Sreekala, M.S., Kumaran, M.G., Thomas, S.: Water sorption in oil palm fiber reinforced phenol formaldeyde composites. Compos. Part A Appl. Sci. Manuf. **33**, 763–777 (2002)
14. Espert, A., Vilaplana, F., Karlsson, S.: Comparison of water absorption in natural cellulosic fibres from wood and one-year crops in polypropylene composites and its influence on their mechanical properties. Compos. Part A **35**, 1267–1276 (2004)
15. Angrizani, C.A.; Vieira, C.A.B.; Zattera, A.J.; Freire, E.; Santana, R.M.C., Amico, S.C.: Influence of sisal fiber length and its chemical treatment on the properties of composites with polyester. In 17th Brazilian Congress of Engineering and Science Materials, Foz do Iguaçu, Paraná, Brazil (2006) (In Portuguese)
16. Fernandes, R.I.M.: Development and characterization of polypropylene/glass fiber/pineapple fiber composites. Ph.D Thesis in Mechanical Engineering, Paulista State University (2010). Guaratinguetá, Brazil (In Portuguese)
17. Vieira, C.A.B.: Evaluation of manufacturing methods of hybrid fabrics of short glass and sisal fibers in polymer composites, Master Dissertation in Engineering and Materials Science, University of Caxias do Sul (2008). Caxias do Sul, Brazil (In Portuguese)
18. Jayamol, G., Bhagawan, S.S., Thomas, S.: Effects of environment on the properties of low-density polyethylene composites reinforced with pineapple-leaf fibre. Compos. Sci. Technol. **58**, 1471–1485 (1998)
19. Cavalcanti, W.S.; Carvalho, L.H.; Alsina, O.L.S.; Lima, A.G.B.: Water sorption from insulated polyester composite reinforced with jute and jute/glass: modeling, simulation and experimentation. Polym. Sci. Technol. **20**, 78–83 (In Portuguese)

20. Santos, D.G.: Thermo-hydric study and mechanical characterization of polymeric matrix composites reinforced with vegetable fiber: 3D simulation and experimentation. Doctoral Thesis in Process Engineering, Federal University of Campina Grande (2017). Campina Grande, Brazil

21. Sanchez, E.M.S., Calvani, C.S., Leal, C.V., Sanchez, C.G.: Unsaturated polyester resin composite reinforced with sugarcane bagasse: influence of the treatment of fibers on properties in the composite. Polym. Sci. Technol. **20**, 194–200 (In Portuguese)

22. Tita, S.P.S., Paiva, J.M.F., Frollini, E.: Impact strength and other properties of lignocellulosic composites: phenolic thermoset matrices reinforced with sugarcane bagasse fibers. Polym. Sci. Technol. **12**:228–239 (In Portuguese)

23. Rao, R.M.V.G.K., Balasubramanian, N., Chanda, M.: Moisture absorption phenomenon in permeable fiber polymer composites. J. Appl. Polym. Sci. **26**, 4069–4079 (1981)

24. Semsarzadeh, M.A., Amiri, D.: Binder for jute-reinforced unsaturated polyester resin. Polym. Eng. Sci. **25**, 618–619 (1985)

25. Idriss Ali, K.M., Uddin, M.K., Bhutyan, M.I.U., Khan, M.A.: Improvement of jute fiber through ultraviolet-cured film of uretane acrylate. J. Appl. Polym. Sci. **54**, 303–308 (1994)

26. Soni, R.P., Soni, M.: Studies on natural fibre reinforced phenolic composites. J. Sci. Ind. Res. **58**, 34–36 (1999)

27. Srihari, S., Revathi, A., Rao, R.M.V.G.K.: Hygrothermal effects on RT-Cured glass-Epoxi composites in immersion environments. Part A: moisture absorption characteritics. J. Reinf. Plast. Compos. **21**, 983–991

28. Pavlidou, S., Papaspyrides, C.D.: The effect of hygrothermal history on water sorption and interlaminar shear strength of glass/polyester composites with different interfacial strength. Compos. Part A Appl. Sci. Manuf. **34**, 1117–1124 (2003)

29. Pegoretti, A., Penati, A.: Effects of hygrothermal aging on the molar mass and thermal properties of recycled Poly(Ethylene Terephathalate) and its short glass fibre composites. Polym. Degrad. Stab. **86**, 233–243 (2004)

30. Kumosa, L., Benedikt, B., Armentrout, D., Kumosa, M.: Moisture absorption properties of unidirectional glass/polymer composites used in composite (non-ceramic) insulators. Compos. Part A **35**, 1049–1063 (2004)

31. Nóbrega, M.M.S., Cavalcanti, W.S., Carvalho, L.H., Lima, A.G.B.: Water absorption in unsaturated polyester composites reinforced with caroá fiber fabrics: modeling and simulation. Mat.-wiss. u.Werkstofftech. **41**(5), 300–305 (2010)

32. Cruz, V.C.A., Nóbrega, M.M.S., Silva, W.P., Carvalho, L.H., Lima, A.G.B.: An experimental study of water absorption in polyester composites reinforced with macambira natural fiber. Mat.-wiss. u.Werkstofftech. **42**(11), 979–984 (2011)

33. Pimentel, J.R.M.: Characterization and properties analysis of the macambira fiber (Bromelia laciniosa). Master Dissertation in Mechanical Engineering, Federal University of Rio Grande do Norte (2012). Natal, Brazil

34. Silva, C.J.: Water absorption in composite materials of vegetal fiber: modeling and simulation via CFX. Master Dissertation in Mechanical Engineering, Federal University of Campina Grande (2014). Campina Grande, Brazil

35. Joseph, P.V., Rabello, M.S., Mattoso, L.H.C., Joseph, K., Thomas, S.: Environmental effects on the degradation behaviour of sisal fibre reinforced polypropylene composites Compos. Sci. Technol. **62**, 1357–1372 (2002)

36. Cavalcanti, W.S.: Polyester/hybrid jute-glass fabric composites: Mechanical characterization and water sorption simulation Doctorate Thesis. Federal University of Campina Grande, Paraíba, Brazil, Process Engineering (2006).(In Portuguese)

37. Santos, D.G., Lima, A.G.B., Pinto, M.V.: Silva mechanical characterization and water sorption in polyester matrix composites reinforced with sisal fiber: an experimental investigation. Defect Diffus. Forum. **369**, 131–134 (2016)
38. Du, Y., Yan, N., Kortschot, M.T.: The use of ramie fibers as reinforcements in composites. In: Faruk , O., Sain, M (Eds.) Biofiber Reinforcement in Composites Materials, Elsevier Ltda., Amsterdam, Chapter 4, pp. 104–137 (2015)
39. Carvalho, L.H., Moraes, G.S., d'Almeida, J.R.M.: Influence of water absorption and pre-drying conditions on the tensile mechanical properties of hybrid lignocellulosic fiber/polyester composites. J. Reinf. Plast. Compos. **28**(16), 1921–1932 (2009)

Chapter 4
Fick's Model Analysis

In this chapter, based on the rigorous theory of pure diffusion through fibrous porous media (Fick's second law), different approaches (analytical, numerical and by CFD) and its limitations for the correct description of water absorption process in vegetable fiber-reinforced polymer composites will be presented. In the macroscopic mathematical modeling both fiber and polymer are considered to be a homogeneous mixture and the effect of swelling was not taken into account. Herein, by using a three-dimensional mathematical treatment, different effects of some process parameters (sample thickness and water bath temperature) in the moisture migration behavior inside the material were analyzed. Applications were perfomed on polyester composites reinforced by caroá and macambira vegetable fibers.

4.1 Transport Phenomena in Porous Media: Foundations

Transport phenomena in porous media represent an important research area related to heat and mass transfer, and fluid flow fields. Heat and mass diffusion/convection through any heterogeneous media, depends on the structure of the matrix and the physical properties of each phase (fluid and solid) involved in the physical problem.

For this class of problem, one of the most difficult aspects of the analysis is structural modeling of the domain. A theoretical treatment based upon the traditional method starts with a potential per unit time balance in a differential control volume with arbitrary shape in a macroscopic scale (i.e. porous material is represented as a fictitious continuum).

By assuming local equilibrium between solid and fluid, the heat and mass transfer phenomena in porous media can be modeled by the macroscopic conservation equation in a short form, as follows:

$$\frac{\partial}{\partial t}(\lambda \Phi) + \nabla.(\lambda \vec{v} \Phi) = \nabla.(\Gamma^{\Phi} \nabla \Phi) + S^{\Phi} \tag{4.1}$$

For mass transfer problems, in the Eq. (4.1), we have $\lambda = \rho$; $\Phi = M$ and $\Gamma^{\Phi} = \rho D$, where ρ, M, and D correspond to density, moisture content, and effective mass diffusivity, respectively, and t is the time. In this same equation, $\vec{v}$ is the velocity vector and S^{Φ} is a mass source term.

Mass diffusion is a phenomenon in which matter is transported from one region in space to another due to random molecular motions [1]. Heat and mass transfer creates temperature and moisture gradients inside the solid, which in general, depends on the internal and external conditions of the porous media. For simplicity, several researchers report a model that assumes that water migrates at very low velocity from the external surrounding medium to the center of the solid only by liquid diffusion (diffusive effects are greater than convective effects). Further, gravity, capillarity, and other effects are neglected.

In practical applications, the diffusion process of water in polymeric composites occurs slowly. Generally, the time until moisture saturation is reached in the composite is a few months. The process depends on fiber content, size and shape of the composite as well as on matrix identity and environmental conditions, especially temperature, as already mentioned. In the case of water vapor absorption from the air, relative humidity also plays an important role. Thus, in order to obtain faster information and with lower process costs, researchers have studied the water absorption process using numerical simulation from developed mathematical models. The main one reported in the literature is the well known as Fick's model.

4.2 Moisture Absorption by Fick's Model

4.2.1 The Physical Problem

For the analysis of the physical problem studied here, consider a dry fiber-reinforced polymer composite of parallelepiped geometry, at a given temperature, which is suddenly immersed in a stationary fluid (water) at a different and higher temperature. As the heated fluid surrounding the dry porous media heats it, heat penetrates into the solid (as the result of a temperature difference) and moisture migrates into the solid by diffusion from the surface (due to a concentration difference). Figure 4.1 sechematically illustrates the problem treated here.

4.2.2 The General Mass Diffusion Equation

In this study, it is assumed that moisture sorption occurs only by diffusion. According to Fick's first law, the diffusive flux (J) is directly proportional to the concentration gradient. Thus, the following equation can be written:

Fig. 4.1 Squematic of a composite sample immersed in a stationary fluid
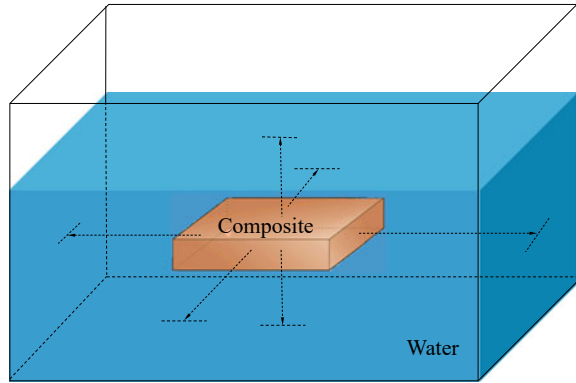
$$J = -D\frac{\partial M}{\partial y} \tag{4.2}$$

In situations where the solid density may be considered constant and without mass generation inside the solid, the partial differential equation that describes the mass diffusion phenomenon (for example, water absorption), well known as Fick's second law of diffusion, can be written as follows:

$$\frac{\partial M}{\partial t} = \nabla \bullet (D\nabla M) \tag{4.3}$$

where D is the effective mass diffusion coefficient and M is the moisture content in a dry basis (mass of absorbed water per mass of the dry solid).

Based in the Fick's model, several works related to moisture absorption in composite systems have presented analytical and/or numerical solutions of the governing equation. However, all these works consider the diffusion through the solid to be one-dimensional [2–9]. Yao and Ziegmann [7] related the water absorption behavior of three types of glass-fiber reinforced plastic (GRP) pipes. A model was developed from Fick's law to predict water diffusion curves of the GRP pipe specimens. It was found that only one of the GPR pipe specimens exhibited near-Fickian behavior and the other two behaved like a two-stage diffusion process because of the abnormal non-Fickian process. Srihari et al. [6] concluded in their studies that the composite (glass/epoxy) and neat resin casting specimens immersed in distilled water and artificial seawater exhibited Fickian behavior. Najafi et al. [8] studied water absorption of wood plastic composites. They concluded that water absorption in these composites follows a Fickian diffusion process. Czél and Czigány [10] in their study of water absorption of glass fiber/polyester composite pipes concluded that the Fickian diffusion model did not fit well the absorption curves, but a special explicit, asymptotically correct function based on the Lucas-Washburn equation was found to be more adequated to describe water uptake process.

In some cases, in order to take into consideration three-dimensional problems, some researchers have used analytical solutions applicable for long times which greatly simplify the problem [11–13]. Chateauminois et al. [11] studied the water diffusion in solids with parallelepiped shape using the short term solution of the one-dimensional Fick's law. For longer times, the water absorption kinetics was computed using the three-dimensional solution of Fick's law. Pavan et al. [12] in their studies on moisture diffusion behavior of glass/epoxy composites found that the diffusion parameters obtained from the experiment conducted up to saturation limits agreed well with the data computed. Bao and Yee [13] showed in their studies of moisture absorption based on longterm absorption data that the fast Fickian diffusion is followed by a slow gradual increase in weight gain. This diffusion behavior can be successfully described by the proposed two-stage diffusion model. In this two-stage model, the first and second stage of diffusion are assumed to be diffusion and relaxation-controlled, respectively.

For a more general formulation, Cavalcanti et al. [14] and Cavalcanti [15] report a three-dimensional mathematical modeling approach to describe moisture absorption in an unsaturated polyester composite reinforced by a hybrid jute/glass fabrics. Predicted results on the average moisture constant inside the material during the whole process were compared with experimental data, in order to validate the model and to obtain the effective diffusion coefficient. According to the authors a good agreement was obtained in all cases evaluated. Also, in complement of those researches, the works of Santos [16], Santos et al. [17], Melo [18], and Carvalho et al. [19] can be cited.

4.2.3   The Mass Diffusion Equation: 3D Approach in Cartesian Coordinates

Based on the hypotheses already reported, the mass transfer in a solid of parallelepiped shape of dimensions $2R_1 \times 2R_2 \times 2R_3$ (Fig. 4.2), the mass conservation equation written in Cartesian coordinates for the three-dimensional case, is given as:

$$\frac{\partial M}{\partial t} = \frac{\partial}{\partial x}\left(D\frac{\partial M}{\partial x}\right) + \frac{\partial}{\partial y}\left(D\frac{\partial M}{\partial y}\right) + \frac{\partial}{\partial z}\left(D\frac{\partial M}{\partial z}\right) \qquad (4.4)$$

For a well-posed mathematical model it is necessary to specify the initial and boundary conditions. Because the symmetry of the problem, we will consider only 1/8 of the volume of the solid. In this chapter, the initial, symmetry and boundary conditions are as follows:
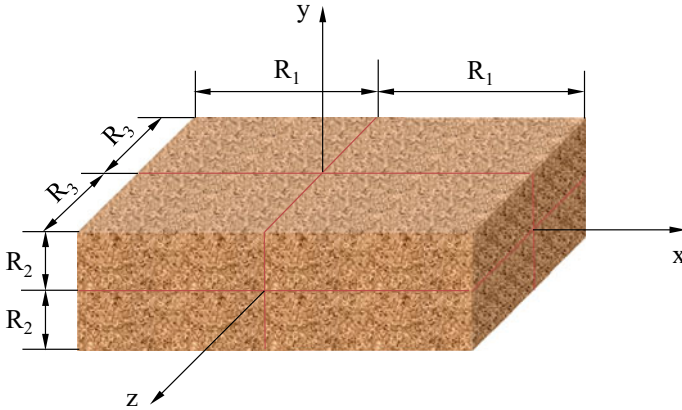
Fig. 4.2 Geometrical configuration of the physical domain

(a) Initial condition:

$$M(x, y, z, t = 0) = M_o, \qquad \begin{cases} 0 < x < R_1 \\ 0 < y < R_2 \\ 0 < z < R_3 \end{cases} \tag{4.5}$$

(b) Symmetry conditions:

$$\frac{\partial M(x = 0, y, z, t)}{\partial x} = \frac{\partial M(x, y = 0, z, t)}{\partial y} = \frac{\partial M(x, y, z = 0, t)}{\partial x} = 0, t > 0 \tag{4.6}$$

(c) Boundary conditions:

$$M(x = R_1, y, z, t) = M(x, y = R_2, z, t) = M(x, y, z = R_3, t) = M_e, t > 0 \tag{4.7}$$

The average moisture content of the solid at any instant of the process is computed as:

$$\overline{M}(t) = \frac{1}{V} \int_V M(x, y, z, t)\, dV \tag{4.8}$$

where V is the volume of the porous solid.

In general, the diffusion coefficient is considered constant or dependent the local moisture content, average moisture content or temperature, or yet as a combination

between of moisture content and temperature. Then, based on these assumptions, the following equations can be used for this purpose:

$$D = D_o \tag{4.9}$$

$$D = D_1 Exp(c_1 M) \tag{4.10}$$

$$D = D_2 Exp(c_2 \overline{M}) \tag{4.11}$$

$$\overline{D} = \frac{1}{(M_e - M_o)} \int_{M_o}^{M} D(\overline{M}) d\overline{M} \tag{4.12}$$

$$D = D_3 Exp\left(\frac{c_3}{T}\right) \tag{4.13}$$

where D_i and c_i are constants, obtained by fitting with experimental data.

4.2.4 Solution Techniques: Three-Dimensional Approach

To solve the diffusion partial differential equation (Eq. 4.4) in conjunction with appropriate initial and boundary conditions, different analytical (for example, separation of variables and Galerkin-based integral method) and numerical (for example, finite-difference, finite-element, boundary-element, and finite-volume) techniques may be used. The choice of a particular technique depends on the easier procedure for a particular physical situation.

4.2.4.1 Analytical Solution

Based on a review of the technical literature, it can be verified that some works analytically solve the diffusion problems with prescribed boundary conditions ($M = Me$) and constant thermo-physical properties ($D = cte$). For this particular situation and using separation of variables technique, the analytical solution of the mass diffusion equation applied to a parallelepiped is given as [20, 21]:

$$\frac{M(x, y, z, t) - M_e}{M_o - M_e} = \sum_{n=1}^{\infty} \sum_{m=1}^{\infty} \sum_{k=1}^{\infty} A_n A_m A_k \times Cos(\beta_n x) \times Cos(\beta_m y) \times$$
$$\times Cos(\beta_k z) \times Exp\left[-\left(\beta_n^2 + \beta_m^2 + \beta_k^2\right) Dt\right] \tag{4.14}$$

where

$$A_n = \frac{2\mathrm{Sen}(\beta_n R_1)}{\beta_n R_1} \tag{4.15}$$

$$A_m = \frac{2\mathrm{Sen}(\beta_m R_2)}{\beta_m R_2} \tag{4.16}$$

$$A_k = \frac{2\mathrm{Sen}(\beta_k R_3)}{\beta_k R_3} \tag{4.17}$$

The moisture content distribution inside the porous media at different times can be obtained using Eq. (4.14). In this equation, the coefficients β_n, β_m and β_k are the so-called eigenvalues. They are obtained using the following equations devived from the boundary conditions previously established:

$$\mathrm{Cos}(\beta_n R_1) = 0 \tag{4.18}$$

$$\mathrm{Cos}(\beta_m R_2) = 0 \tag{4.19}$$

$$\mathrm{Cos}(\beta_k R_3) = 0 \tag{4.20}$$

According to Eq. (4.8), the average moisture content can then be calculated as:

$$\frac{\overline{M}(t) - M_e}{M_o - M_e} = \sum_{n=1}^{\infty}\sum_{m=1}^{\infty}\sum_{k=1}^{\infty} B_n B_m B_k . e^{-[\beta_n^2 + \beta_m^2 + \beta_k^2]Dt} \tag{4.21}$$

where

$$B_n = \frac{2}{(\beta_n R_1)^2} \tag{4.22}$$

$$B_m = \frac{2}{(\beta_m R_2)^2} \tag{4.23}$$

$$B_k = \frac{2}{(\beta_k R_3)^2} \tag{4.24}$$

4.2.4.2 Numerical Solution

It may be difficult to obtain the analytical solution of a partial differential equation with a high level of complexity as, for example, when variable thermo-physical properties are used. In this case a numerical solution may be used as an appropriate

alternative technique. For this purpose, the finite-volume method has been frequently used to discretize the governing equations. In this tecnique, the physical domain is transformed in a discrete domain formed by a finite number of control-volumes. Figure 4.3 shows a structured grid that represents the physical domain in a discretized form. This is only a representative squematics.

Figure 4.4 illustrates the differential volume of the physical and computational domains, Figs. 4.2 and 4.3, respectively, where the nodal points (W, E, N, S, F, T), the dimensions of the control volume (Δx, Δy, Δz) and the distances between nodal points (δx, δy, δz) are presented.

Assuming a fully implicit formulation, where all terms are estimated in $t + \Delta t$, Eq. (4.4) was integrated in the control volume of Fig. 4.4, which corresponds to the
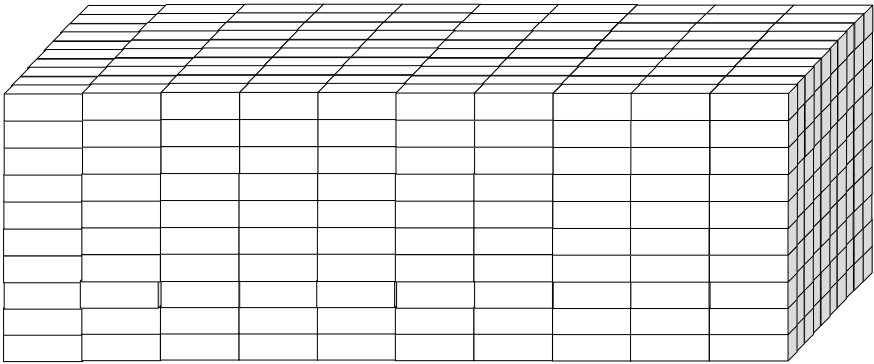

Fig. 4.3 The schematic illustration of a structured numerical grid
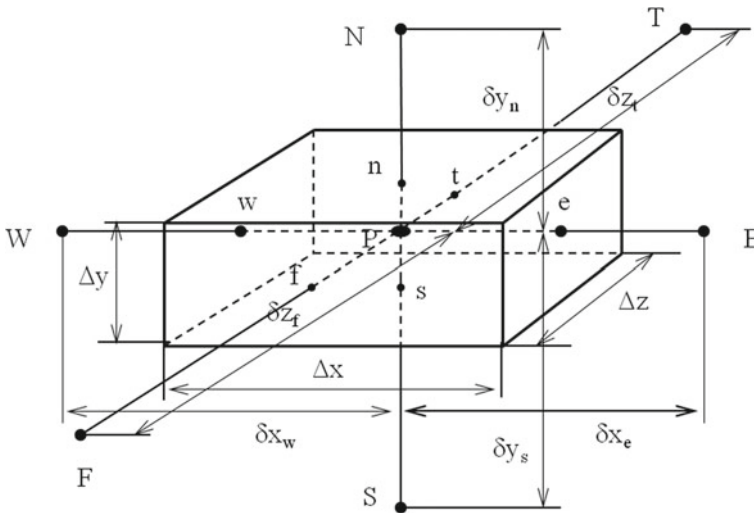
Fig. 4.4 Control volume used in this work

internal points of the domain, and also, in time. As a result, Eq. (4.4) was discretized by using practice B (nodal points in the center of control-volume) [22–24] resulting in a linear algebraic equation as follows:

$$A_P M_P^* = A_E M_E^* + A_W M_W^* + A_N M_N^* + A_S M_S^* + A_T M_T^* + A_F M_F^* + B \quad (4.25)$$

where

$$M^* = \frac{M - M_e}{M_o - M_e} \quad (4.26)$$

$$A_E = \frac{D_e \Delta y \Delta z}{\delta x_e} \quad (4.27)$$

$$A_W = \frac{D_w \Delta y \Delta z}{\delta x_w} \quad (4.28)$$

$$A_N = \frac{D_n \Delta z \Delta x}{\delta y_n} \quad (4.29)$$

$$A_S = \frac{D_s \Delta z \Delta x}{\delta y_s} \quad (4.30)$$

$$A_T = \frac{D_t \Delta x \Delta y}{\delta z_t} \quad (4.31)$$

$$A_F = \frac{D_f \Delta x \Delta y}{\delta z_f} \quad (4.32)$$

$$A_P^o = \frac{\Delta x \Delta y \Delta z}{\Delta t} \quad (4.33)$$

$$B = A_P^o M_p^{*o} \quad (4.34)$$

$$A_P = A_E + A_W + A_N + A_S + A_T + A_F + A_P^o \quad (4.35)$$

In the discretized form, the average moisture contents can be written, as follows:

$$\overline{M} = \frac{1}{V} \sum_{i=2}^{npx-1} \sum_{j=2}^{npy-1} \sum_{k=2}^{npz-1} M_{i,j,k} \Delta V_{i,j,k} \quad (4.36)$$

in which i, j e k represent the position of the nodal point in the x, y, and z directions, respectively, and *npx*, *npy* and *npz* are the nodal point numbers in the x, y, and z directions, respectively.

According to the literature [22], the mass diffusion coefficient at the interface of the control-volume is calculated as:

$$D_i = \frac{2D_P D_E}{D_P + D_E} \tag{4.37}$$

where the subscript $\underline{i}$ refers to the interface, and D_P and D_E are the values of the mass diffusion coefficient in the nodal points P and E, respectively.

The set of algebraic linear equations obtained from Eq. (4.25) (when applied for all internal nodal points) can be solved interactively, for example, using the Gauss–Seidel method. The following convergence criterion is frequently used:

$$\left| M^{*n-1} - M^{*n} \right| \leq 10^{-8} \tag{4.38}$$

where n represents the n-th iteration in each time.

In practical applications, because of the large variety of materials and operating conditions, in general, the diffusion coefficient is unknown. Thus, in general, this process parameter is found by varying it to minimize the sum of the squared deviations between the actual and predicted data (the least square error technique). The relative deviation between the experimental and calculated values (relative residual, ERMQ) and the variance (S^2) are defined as [25]:

$$ERMQ = \sum_{i=1}^{m} \left(\overline{M}^*_{i,\,\text{Numerical}} - \overline{M}^*_{i,\,\text{Numerical}} \right)^2 \tag{4.39}$$

$$S^2 = \frac{ERMQ}{(m-1)} \tag{4.40}$$

where m is the number of experimental points. The smallest values of ERMQ and S^2 are used as criteria to obtain the best value of the diffusion coefficient for each operating condition. This numerical formulation was used to predict the water uptake in caroá and macambira fiber-reinforced polyester composite; the operating conditions and experimental data are reported in Chap. 3, in details.

4.2.4.3 Solution by Commercial Software (Ansys CFX)

In this topic, the software Ansys CFX was used to simulate the water absorption process in caroá fiber-reinforced polyester composites. The study was developed and reported in detail in Silva [26, 27] and Silva et al. [28]. The geometry considered in this research is of a solid parallelepiped with dimensions as illustrated in Fig. 4.2.
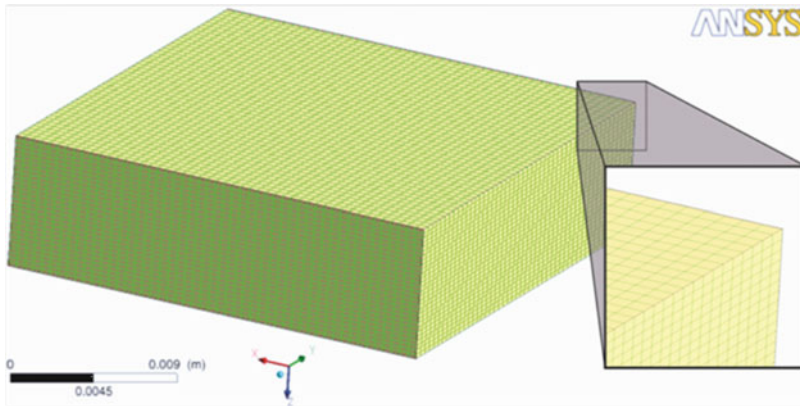
Fig. 4.5 Numerical mesh used in this study

In this work, the mesh built using the ICEM CFD (ANSYS CFX®) software (6 × 20 × 20 mm³), is composed of 75,000 nodal points and 60,623 hexahedral elements. Figure 4.5 illustrates the geometry, the numerical grid and detail of regions close to the surface of the composites. For the transient numerical solution, a time step of 200 s and a 10^{-5} convergence criterion was used. The operating conditions and experimental data were reported in Chap. 3.

4.2.5 Fick's Model Application

4.2.5.1 Analytical Results

(a) Water Sorption Kinetics

Santos [16] and Santos et al. [17] reported an analytical study about water absorption in sisal fiber-reinforced polyester composites using Eq. (4.21). The analytical results of the average moisture content of the composites were compared with the experimental data at different temperatures and sample thicknesses. Figures 4.6, 4.7 and 4.8 illustrate these comparisons. For this comparison, the authors used 30 terms of the infinite series reported in Eq. (4.21). Upon analyzing these figures we can see a good agreement between the results. Variations between the experimental and analytical data can be attributed to several factors such as: the nature of the studied composites, i.e. vegetable fiber has hygroscopic nature, the lack of uniformity in the diameter of sisal fibers, and the small temperature variations during measurements, even if the tests were carried out at controlled bath temperatures. Furthermore, it can be noted that after the samples were immersed in water, the moisture absorption occurs quite rapidly in the first 50 h. These effects were more pronounced at higher water bath temperature.

Fig. 4.6 Dimensionless average moisture content during the water absorption in sisal fiber reinforced unsaturated polyester composites, at 25 °C

Fig. 4.7 Dimensionless average moisture content during the water absorption in sisal fiber reinforced unsaturated polyester composites, at 50 °C

For longer times, the curve gradually changes its slope until levelling off, reaching moisture saturation level. This relief in the absorption rate is attributed to how water molecules moves into the fibers by capillarity which is in its surface or into the lumen. In 6 mm thick samples, maximum saturation times were longer, which may be associated to the way the moisture is transmitted between fibers. Initially moisture
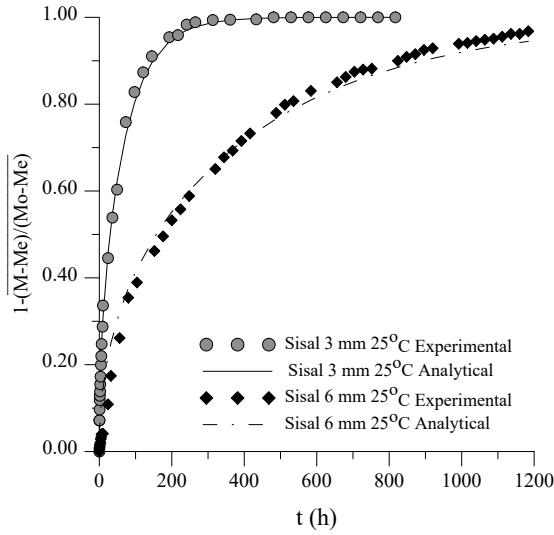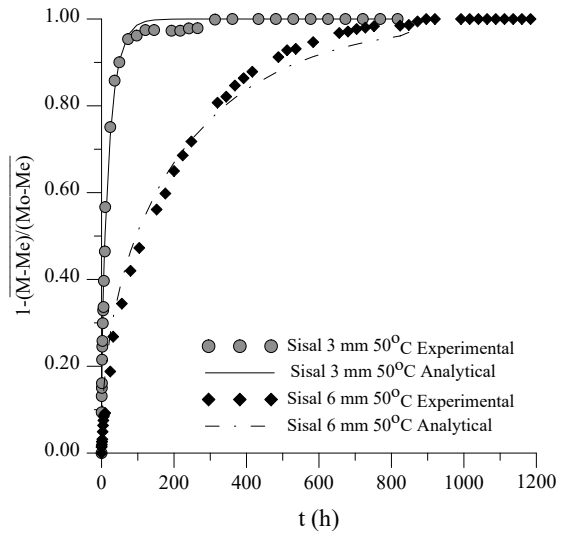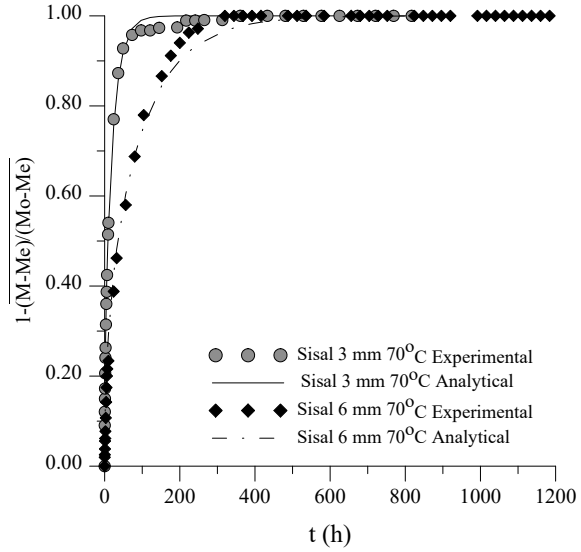
Fig. 4.8 Dimensionless average moisture content during the water absorption in sisal fiber reinforced unsaturated polyester composites, at 70 °C

is absorbed on the fiber surface and then migrates to the lumen where it proceeds by capillary action so that the diffusive process is maintained. Since thicker samples have higher volume, the maximum saturation time is also higher, which justifies the data obtained. Furthermore, it was verified that, for the thinner composites (3 mm thick), water absorption is faster, which is though to be due to the greater area/volume ratio displayed by these samples.

This phenomenon can be attributed to the thermal and geometric expansions of the matrix (variation in the area/volume ratio). As the water bath temperature increases, so does the kinetic energy of the water molecules that, in turn cause, a decrease in water intermolecular forces decreasing its viscosity and thus favoring its migration into the composite.

According to those authors [16, 17], the effect of moisture and temperature has been studied using as reference different parameters such as: tensile and shear strengths, elastic modulus, fatigue behavior, creep, stress rupture, response to dynamic impact, electrical resistance, and dimensions variations (swelling). These studies indicated that composite moisture content and water bath temperature up to about glass-transition temperature have provoked small effects on fiber-dominated composite properties, but significantly reduce matrix-dominated composite properties.

4.2.5.2 Numerical Results

(a) Absorbed Water Kinetics

Numerical results of average moisture content of the composites under investigation were compared with the experimental data as reported in Chap. 3. To obtain the numerical results, a computational code using $20 \times 20 \times 20$ nodal points and a time step of $\Delta t = 1$ s was developed. These parameters were obtained after a time step and mesh refining study [15]. The numerical results obtained from a given mathematical model are strongly dependent on the boundary conditions, thermo-physical properties and geometry. A comparison between the experimental and numerical predicted average moisture content for the investigated caroá/polyester composites, shown in Figs. 4.9, 4.10 and 4.11, and macambira/polyester composites, shown in Figs. 4.12, 4.13, indicates that the model employed here is appropriate. These figures, show that a good agreement was obtained in all cases investigated.

In general, the curves are similar to those of other natural fiber reinforced polymer matrix composites. For all investigated composites the moisture content increases monotonically with water immersion time until it reaches the equilibrium moisture content (saturation condition).

A comparison between Figs. 4.9, 4.10, 4.11, 4.12 and 4.13 indicates that the wetting process in the 3-mm thick composite was faster than in the 6-mm thick composite. This behavior may be attributed to the increase in area/volume ratio and the high water affinity for the cellulosic material. The effect of the thickness sample is more pronounced at lower temperatures. At high temperature the kinetics of water absorption is dominated by thermal effects, and moisture diffusion inside the material is strongly dependent on the temperature.

Fig. 4.9 Dimensionless average moisture content during the water absorption in caroá fiber reinforced unsaturated polyester composites, at 25 °C

Fig. 4.10 Dimensionless mean moisture content during the water absorption in caroá fiber reinforced unsaturated polyester composites, at 50 °C

Furthermore, the results indicate that, the water uptake of the composite sample immersed in a water bath at 70 °C was faster than under the other (25 and 50 °C) experimental conditions adopted. This behavior is attributed to the increased water mobility within the solid at higher temperature due to thermal dilation and increased composite porosity (thermo-activation).

According to the data reported in the literature, it was verified that water absorption for the composites is higher than for the matrix. Neat polyester shows a very low
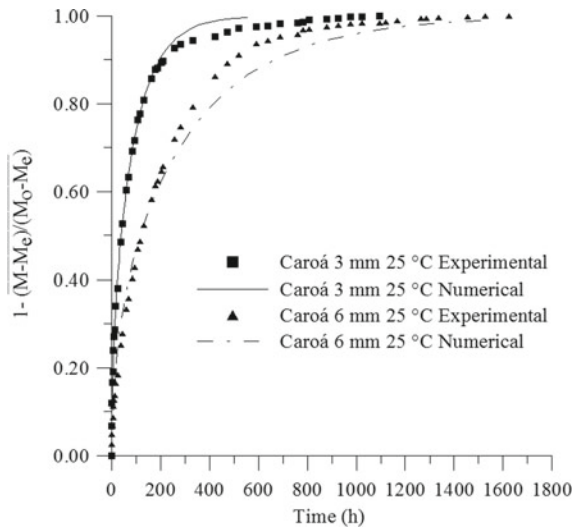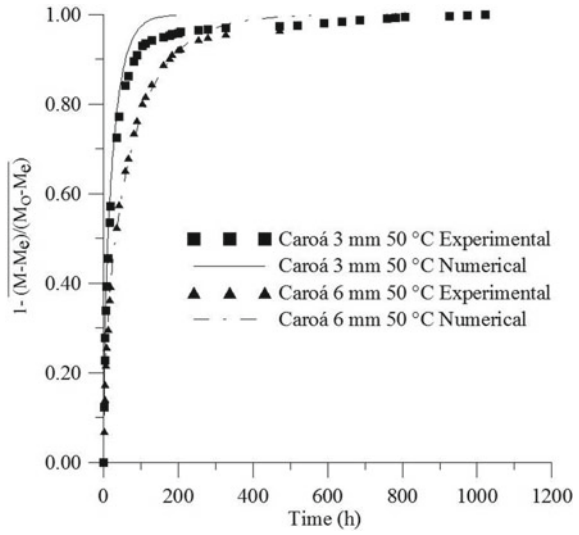

Fig. 4.11 Dimensionless mean moisture content during the water absorption in caroá fiber reinforced unsaturated polyester composites, at 70 °C
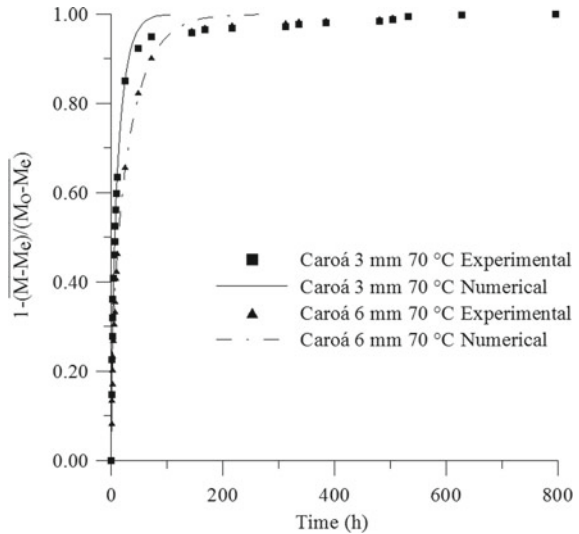
Fig. 4.12 Dimensionless average moisture content during the water absorption in macambira fiber reinforced unsaturated polyester composites, at 25 °C
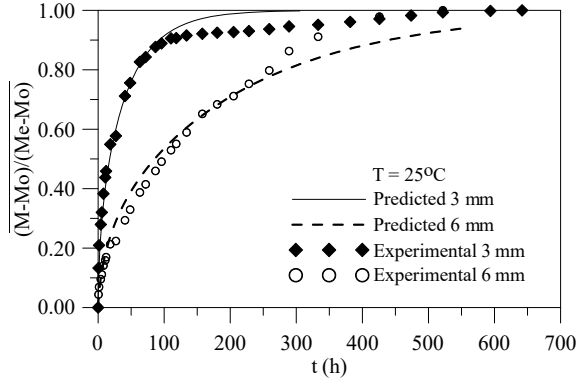
Fig. 4.13 Dimensionless average moisture content during the water absorption in macambira fiber reinforced unsaturated polyester composites, at 70 °C
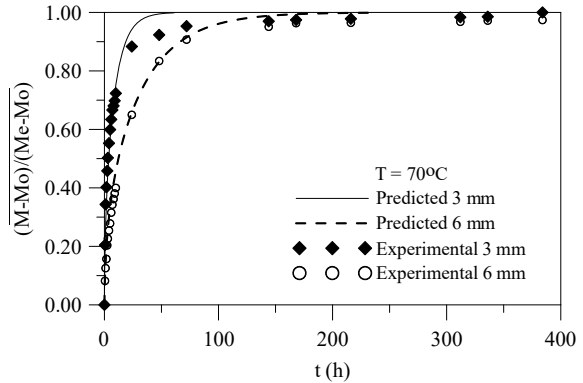
percentage of absorbed water. While the water sorption in equilibrium for the unsaturated polyester is about 1.2%, for the composites it was about 14%. Degradation or delamination was not verified in the composites after each experiment.

These results are consistent with those reported in similar systems for unsaturated polyester/jute composites [14, 15] unsaturated polypropylene/sisal composites [29, 30], and cabonfiber/fiberglass hybrid composites [31].

It is important to notice that moisture degrades natural fiber reinforced composites, but this effect was not measured here. However, weight loss varying with immersion time and fiber content was verified for dried sisal fiber reinforced polypropylene composites [30].

(b) Absorbed Water Distribution

The dimensionless moisture content distribution, $(M - M_e)/(M_o - M_e)$, in the 70% unsaturated polyester/30% caroá fiber composites in the plane x = 5 mm, at elapsed time of 20 h, is presented in Figs. 4.14 and 4.15, for 3 and 6 mm thickness, respectively. Figures 4.16 and 4.17 illustrate the same results for unsaturated polyester composites reinforced with macambira natural fiber. Upon analyzing these

Fig. 4.14 Moisture content distribution inside the composite 30% caroá fiber/70% unsaturated polyester, at 25 °C (**a**), 50 °C (**b**) and 70 °C (**c**) for a thickness of 3 mm, in the plane x = 5 mm, elapsed time 20 h
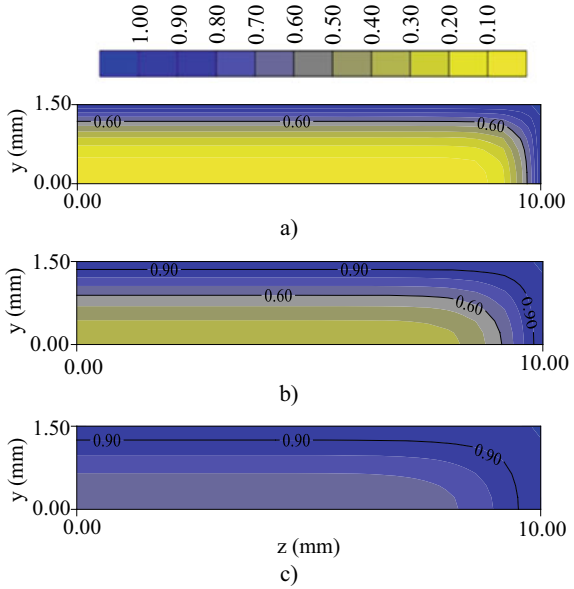
Fig. 4.15 Moisture content distribution inside the composite 30% caroá fiber /70% unsaturated polyester, at 25 °C (**a**), 50 °C (**b**) and 70 °C (**c**) for a thickness of 6 mm, in the plane x = 5 mm, elapsed time 20 h
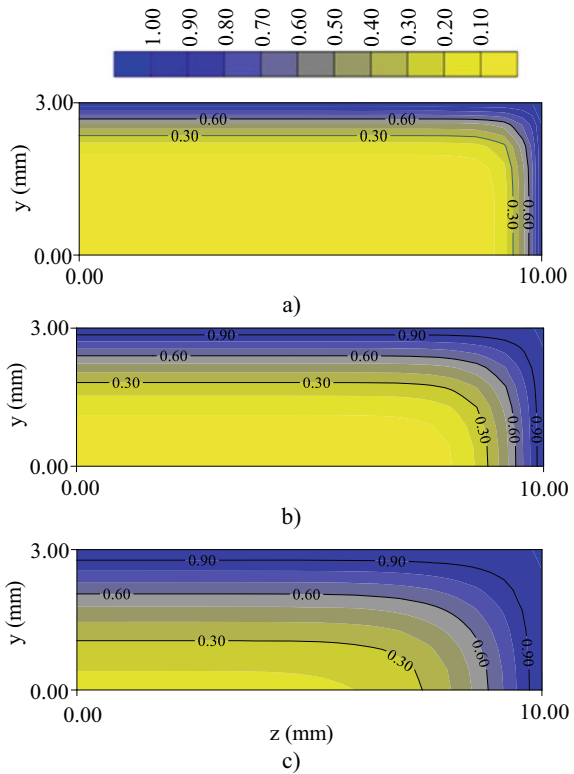
Fig. 4.16 Dimensionless moisture content distribution inside the macambira composite (3 mm thickness, x = 5 mm, elapsed time 20 h). **a** 25 °C, **b** 50 °C and **c** 70 °C
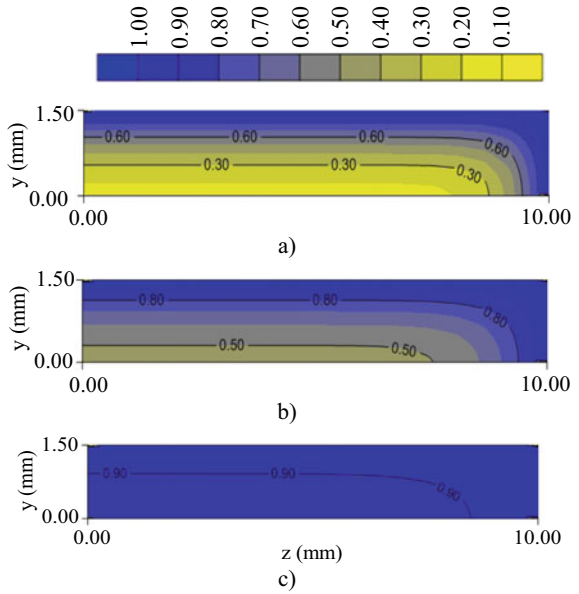
Fig. 4.17 Dimensionless moisture content distribution inside the macambira composite (6 mm thickness, x = 5 mm, elapsed time 20 h). **a** 25 °C, **b** 50 °C and **c** 70 °C
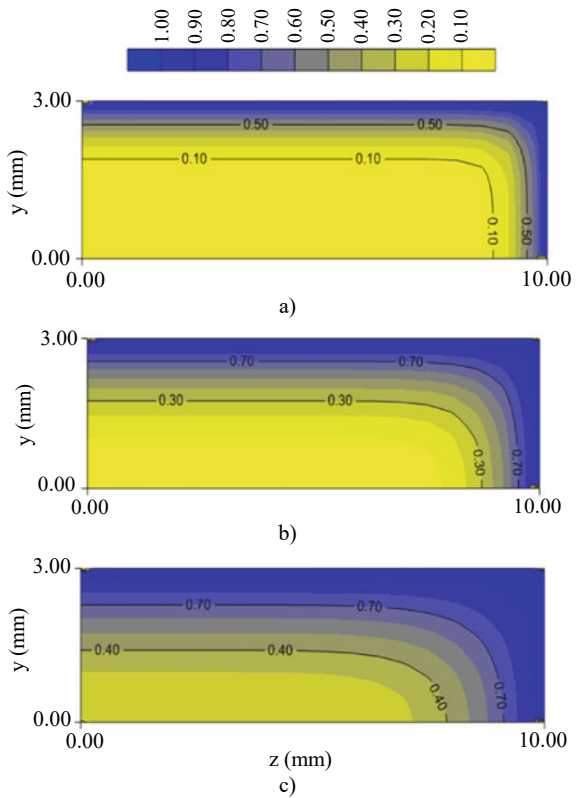
figures, we can see the existence of high moisture gradients closed to the vertices of the composite. These figures also show the influence of temperature on the water absorption rate. It can be observed that 20 h after the test had started, the moisture gradients at higher temperature is significantly higher for both 3 and 6 mm thick composites studied.

Figure 4.18 illustrates the dimensionless moisture content distribution inside the macambira fibe-reinforced polyester composite at different moments of the process. Analysis of this figure indicates that water migrates from the surface to center of the solid until saturation is reached. Absorption rate is higher at the first hour of the process, decreasing for longer times.

In order to predict which areas are more sensitive to thermo-hygro-mechanical stresses, it is important to know the moisture content inside the material as moisture may cause cracks, deformations and delaminations and, consequently, decrease the composites' mechanical properties.

Fig. 4.18 Dimensionless moisture content distribution inside the macambira composite at different elapsed times (3 mm thickness, x = 5 mm, T = 25 °C)
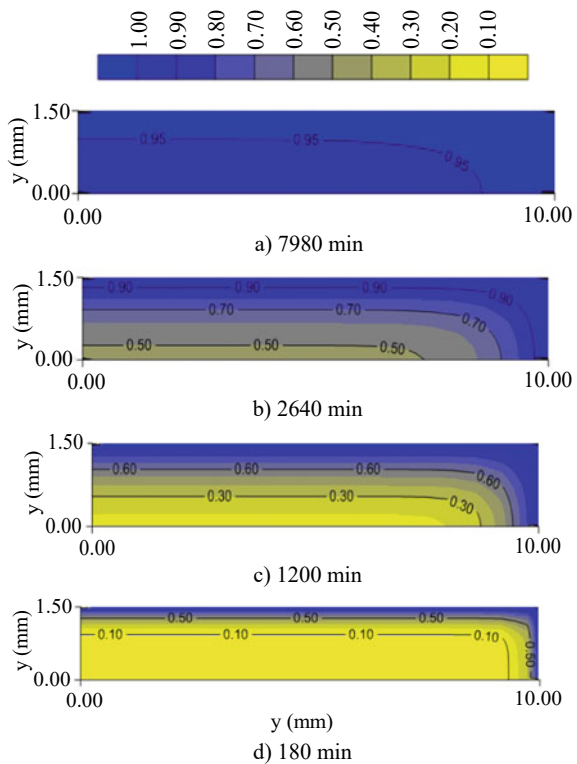
4.2.5.3 CFD Simulation Results

(a) Water Sorption Process

Figure 4.19 illustrates a comparison between the predicted (Ansys CFX® software) and experimental average moisture content of caroá fiber-reinforced unsaturated polyester composite as a function of water exposure time (water absortion kinetics). Details of the experimental procedure are found in Chap. 3. Analyses of these curves show that a good agreement was obtained.

Transient behavior of the average moisture content of the polymer composite at different temperatures is illustrated in Fig. 4.20. Results indicate that, as expected, the water absorption of samples immersed in water at 70 °C is faster than those immersed at 25 and 50 °C. This behavior is attributed to the increased movement of water molecules within the solid due to the high temperature. It is observed that in the initial stages (first 50 h), the water absorption increases quickly and tends to continue increasing slowly until hygroscopic equilibrium is achieved. This effect is more pronounced for higher temperatures (T = 70 °C).

(b) Absorbed Water Distribution

Figures 4.21 and 4.22 show the moisture content spatial distribution inside the unsaturated polyester composites reinforced with caroá fiber at different planes: (x = 0, y, z), (x, y = 0, z), (x, y, z = 0) and elapsed times 4, 20, 44, 133 and 208 h of wetting. The reported results are those for water bath temperatures of 25 and 70 °C, respectively.
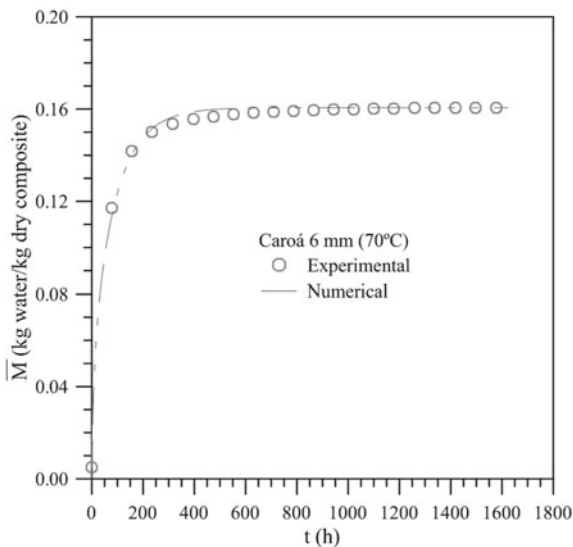
Fig. 4.19 Experimental and theoretical (proposed model) results of the average moisture content during the wetting process of unsaturated polyester composite reinforced with caroá fiber (thickness 6 mm and temperature 70 °C)
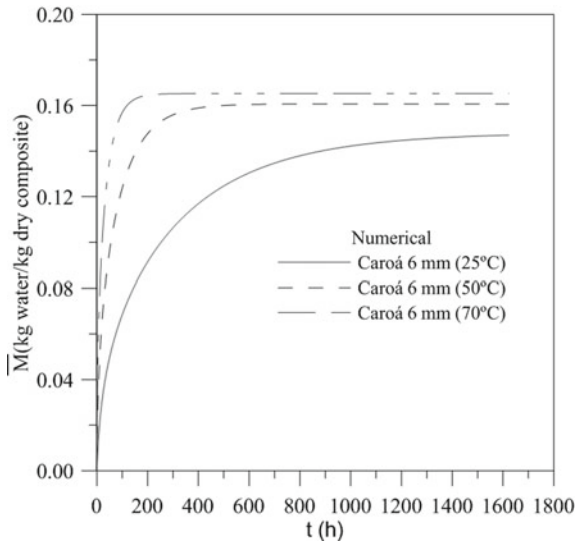
Fig. 4.20 Predicted water sorption kinetics of the polymer composites reinforced with caroá fibers at different water bath temperatures (6 mm thickness)

Analysis of these figures indicate that there is high moisture gradient in the composite near the vertex regions and that distribution of moisture content is not uniform with immersion time. In the areas close to the corners, water absorption is faster because these areas are in direct contact with water for the different sides of the samples. The water enters in the composite and generates higher moisture content gradients within the solid, decreasing as immersion time increases. Thus, at any point within the solid, the moisture content increases with time until the steady state condition (hygroscopic equilibrium condition) is reached.

It can be observed that, 20 h after the wetting process has started, moisture gradients at higher temperature are significantly higher than at lower temperature. This behavior is provoked by an increase in mass diffusion coefficient that is strogly dependent on water bath temperature. Then, the increase in moisture diffusion inside the composite with immersion time and test temperature can be attributed to a reduction in water density and viscosity as well as on the thermal expansion suffered by the matrix, which favors the penetration of water into the composite [32, 33].

4.2.5.4 Mass Diffusion Coefficient Estimation

The mechanism of diffusion and structure/diffusivity relationships, have not been extensively studied. Some authors have suggested that water diffusivity in polymer composites is due to morphology [34], local molecular mobility [35], free volume [36] or fiber distribution in the polymer matrix [37].

Moisture content (T=25°C)
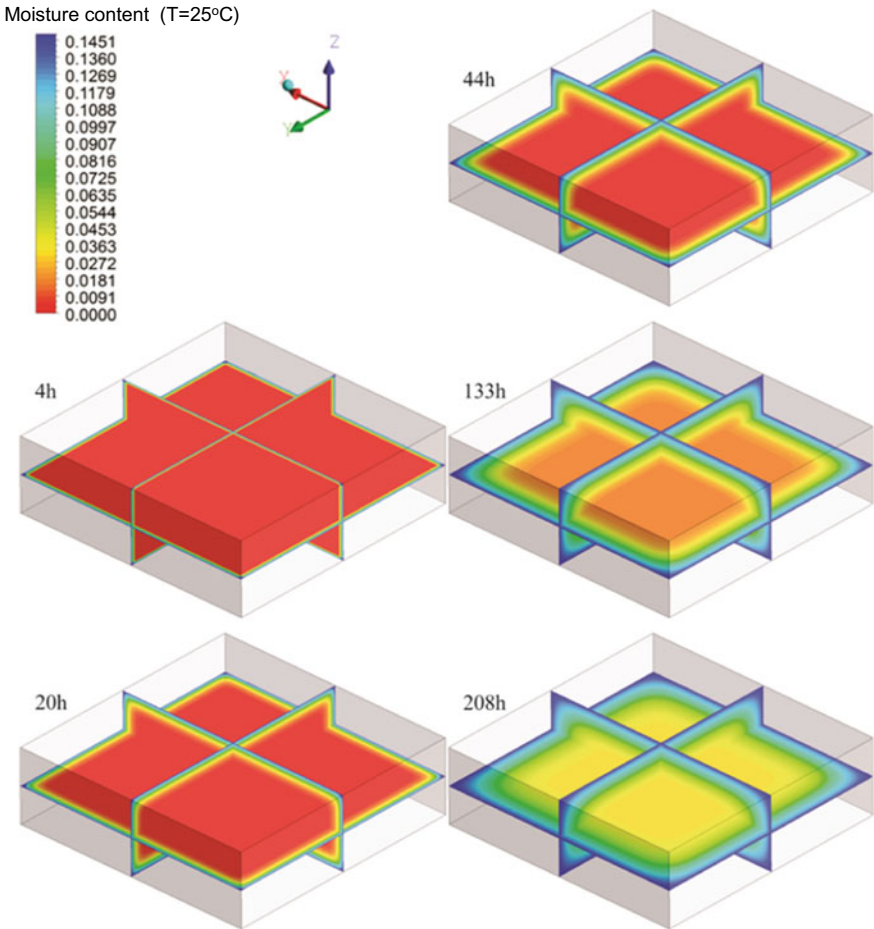
Fig. 4.21 Moisture content distribution inside the polymer composite reinforced with caroá fiber at different planes (x = 0, y, z), (x, y = 0, z) and (x, y, z = 0) and elapsed times (water bath temperature 25 °C)

According to Merdas et al. [38] apparent water diffusivity decreases with increasing hydrophilicity and it increases when temperature increases [31], showing that moisture diffusion rate within the solid is strongly affected by fiber/polymer/water interactions. Therefore, all factors mentioned above, including fiber content, thermal stability and shape of the composite, need to be investigated in order to fully understand moisture absorption mechanisms.

As previously discussed, mass diffusion coefficients were estimated by fitting the predicted values to the experimental data obtained on average moisture content during the process of water absorption in unsaturated polyester/vegetable fiber composites.
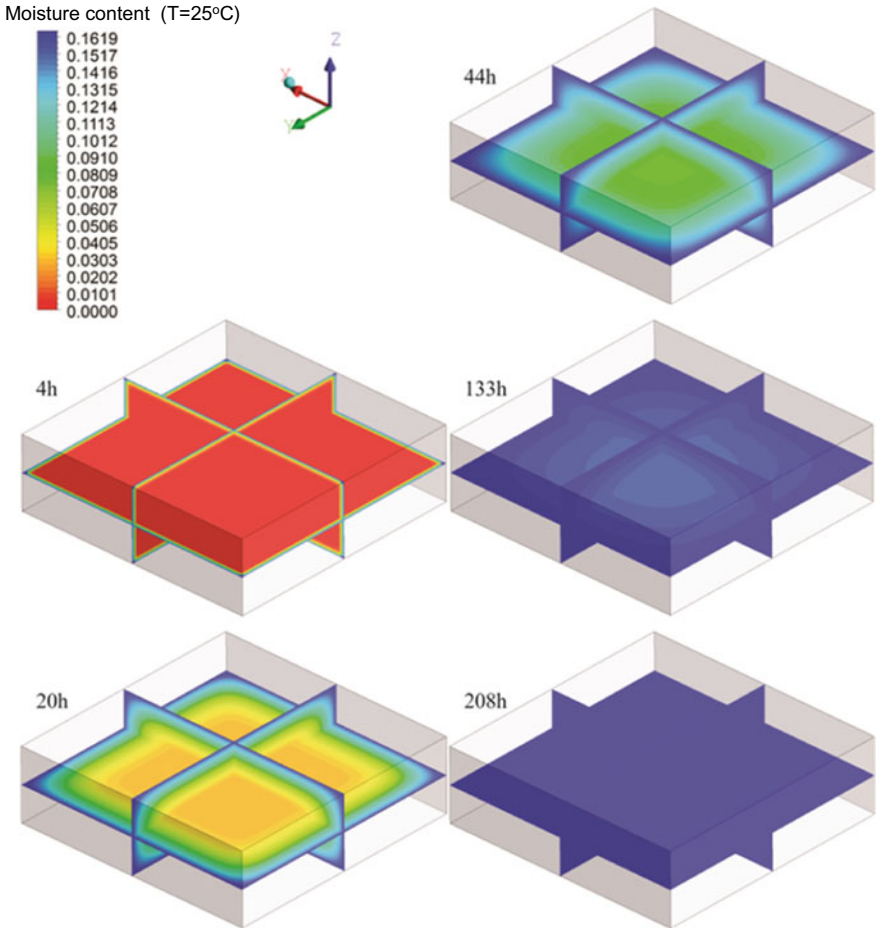
Fig. 4.22 Moisture content distribution inside the polymer composite reinforced with caroá fiber at different planes (x = 0, y, z), (x, y = 0, z) and (x, y, z = 0) and elapsed times (water bath temperature 70 °C)

Tables 4.1 and 4.2 present the value of the mass diffusion coefficient obtained for all experimental conditions presented in Chap. 3.

Analysis of these tables indicate that mass diffusion coefficient changes with moisture content and temperature for all cases investigated. This process parameter tends to decrease with increasing moisture content and to increase with increasing temperature for all samples. The use of moisture content dependent mass diffusivity led to numerical values that adjusted well to the experimental data, with smaller errors than those obtained when constant mass diffusivity was assumed.

The data obtained also showed that the mass diffusion coefficient is higher for thinner samples, which is attributed to the fact that the area to be coverd by the water

Table 4.1 Parameters of the Eq. 4.11 and variance estimated for all wetting experiments with caroá and mamcabira reinforced composites and pure polyester

Sample	$D_2 \times 10^{+12}$ m^2/s	C_2	ERMQ	$S^2 \times 10^{+3}$	Time (h)
Pure polyester 3 mm	2.8	−26.0	0.267	9.54	600
Caroá 3 mm 25 ℃	2.2	−0.4	0.045	1.12	1095
Caroá 6 mm 25 ℃	2.3	−0.1	0.093	1.94	1623
Caroá 3 mm 50 ℃	8.0	−0.4	0.086	2.39	1022
Caroá 6 mm50 ℃	8.5	−0.1	0.022	0.61	1022
Caroá 3 mm 70 ℃	15.0	−0.4	0.035	1.35	796
Caroá 6 mm 70 ℃	21.0	−0.1	0.043	1.65	796
Macambira 3 mm 25 ℃	5.7	−1.32	0.1285	4.43	642
Macambira 6 mm 25 ℃	2.9	2.00	0.1915	7.66	594
Macambira 3 mm 50 ℃	11.2	−0.50	0.1254	4.18	687
Macambira 6 mm 50 ℃	9.3	0.74	0.0513	1.71	687
Macambira 3 mm 70 ℃	25.1	−0.30	0.1291	6.79	384
Macambira 6 mm 70 ℃	21.4	0.58	0.0262	1.24	648
Sisal 3 mm 25 ℃	3.04	0.00	0.0504	1.44	817
Sisal 6 mm 25 ℃	1.68	0.00	0.1692	3.38	1328
Sisal 3 mm 50 ℃	9.34	0.00	0.1073	3.07	817
Sisal 6 mm 50 ℃	2.77	0.00	0.1698	4.72	848
Sisal 3 mm 70 ℃	10.20	0.00	0.0493	1.41	817
Sisal 6 mm 70 ℃	7.54	0.00	0.0529	1.47	848

during the humidifiation of thicker samples is bigger and the area/volume ratio is smaller. The data also showed that, for lower water bath temperatures, water sorption is dominated by water affinity to cellulose and to composite area while for higher water bath temperature, water absorption kinetics is dominated only by thermal effects. This implies that mass diffusion within the material is strongly dependent on temperature.

Based on the lower least square error and variance presented in Table 4.1, we conclude that the proposed model for the diffusion coefficient as a function of the average moisture content (Eq. 4.11) led to moisture content values that are in agreement with the experimental data.

It is well known that diffusion processes in systems with two or more components, such as polymer composites reinforced with vegetable fiber as they absorb water, depend on several factors such as volume fractions, nature, distribution and orientation of the fillers as well as on fiber/matrix interfacial characteristics [13, 39]. In general, the comparison with mass diffusion coefficients reported in the technical literature is very difficult for a number of different reasons that include models and calculation methods adopted, porosity, dimensions, temperature, compositions, and physical and chemical structures of the material [15, 40]. Table 4.3 summarizes some

Table 4.2 Range of the mass diffusion coefficients estimated by Eq. 4.11 and initial and final moisture content for all studied cases

Sample	Fiber total content (%)/T (°C)	$D_{initial} \times 10^{+12}$–$D_{final} \times 10^{+12}$ (m²/s)	Initial and final moisture content (dry basis)
Pure polyester	0/28	2.80–2.31	0–0.01252
Caroá 3 mm	30/25	2.20–2.07	0–0.14488
Caroá 6 mm		2.30–2.26	0–0.14810
Caroá 3 mm	30/50	8.00–7.53	0–0.15162
Caroá 6 mm		8.50–8.36	0–0.16067
Caroá 3 mm	30/70	15.00–14.10	0–0.15609
Caroá 6 mm		21.00–20.65	0–0.16523
Macambira 3 mm	30/25	5.70–4.56	0–0.16810
Macambira 6 mm		2.90–3.84	0–0.14040
Macambira 3 mm	30/50	11.20–10.29	0–0.17020
Macambira 6 mm		9.30–10.46	0–0.15890
Macambira 3 mm	30/70	25.10–23.77	0–0.18090
Macambira 6 mm		21.40–23.51	0–0.16180
Sisal 3 mm	44.6/25	3.04–3.04	0–0.1468
Sisal 6 mm		1.68–1.68	0–0.1227
Sisal 3 mm	44.6/50	9.34–9.34	0–0.1496
Sisal 6 mm		2.77–2.77	0–0.01242
Sisal 3 mm	44.6/70	10.20–10.20	0–0.1504
Sisal 6 mm		7.54–7.54	0–0.1246

mass diffusity values reported in the literature for different materials, sample shape, and experimental conditions.

A reasonable agreement is observed when the mass diffusivity values of different composites obtained in this study are compared with those reported in similar systems. Since the diffusive model was used in all works reported in Table 4.3, the difference between the values may be attributed mainly to composite variety; geometry assumptions; different equilibrium moisture content; composite physical structure and expansion effects caused by water absorption.

As final comment, despite of the extended use of the Fick's second law to study diffusion process, due to several reasons such as experience of the researchers, available equipments, and available exact solutions of the diffusion equation for simple geometries, it fails to address the complex structure of the polymer composite absorption process. The reason for this failure is the different water absorption capacity of the polymer matrix and the natural fiber, and their iteractions inside the composite, especialy in the final stages of the process. Thus, new or improved mathematical modelis to adequately predict water migration in poymer composites when exposed to moist environment for long times have been proposed in the literature. This topic is addressed in detail in the next chapter of this book.

Table 4.3 Moisture diffusivity in polymer composites as reported in the literature

Composite sample (Shape)	Time (h)	Dimension (mm)	T (°C)	D × 10^{+13} (m²/s)	References
Carbon-glass fiber/Epoxy (Rod)	5300	66.5 × 9.53	40	1.42	[31]
Carbon-glass fiber/Epoxy (Rod)	5300	66.5 × 9.53	60	3.84	[31]
Carbon-glass fiber/Epoxy (Rod)	5300	66.5 × 9.53	90	27.00	[31]
Sisal fiber/Polypropylene (Rectangular prism)	166	25 × 10 × 2.50	28	0.36	[29]
Sisal fiber/Polypropylene (Rectangular prism)	166	25 × 10 × 2.50	50	0.56	[29]
Sisal fiber/Polypropylene (Rectangular prism)	166	25 × 10 × 2.50	28	0.69	[29]
Jute-glass fiber/Polyester (Rectangular prism)	1249	20 × 20 × 2.82	28	16.50	[41]
Jute fiber/Polyester (Rectangular prism)	500	20 × 20 × 2.30	28	18.00	[42]
Kenaf fiber/Polyester (Rectangular prism)	911	127 × 12.5 × 3.2	25	25	[43]
Kenaf fiber/Polyester (Rectangular prism)	911	127 × 12.5 × 3.2	50	108	[43]
Sisal-Cotton fiber/Polyester (Infinite plate)	450	20 × 20 × 3.0	30	0.17	[44]
Sisal-Cotton fiber/Polyester (Infinite plate)	450	20 × 20 × 3.0	60	0.67	[44]
Ramie-Cotton fiber/Polyester (Infinite plate)	450	20 × 20 × 3.0	30	0.33	[44]
Ramie-Cotton fiber/Polyester (Infinite plate)	450	20 × 20 × 3.0	60	1.51	[44]
Jute-Cotton fiber/Polyester (Infinite plate)	450	20 × 20 × 3.0	30	0.05	[44]
Jute-Cotton fiber/Polyester (Infinite plate)	450	20 × 20 × 3.0	30	0.55	[44]

References

1. Farias, V.S.O., Silva, W.P., Silva, C.M.D.P.S., Delgado, J.M.P.Q., Farias Neto, S.R., Lima, A.G.B.: Transient diffusion in arbitrary shape porous bodies: Numerical analysis using boundary-fitted coordinates. In: Delgado, J.M.P.Q., de Lima, A.G.B, Silva, M.V. (eds.) Numerical Analysis of Heat and Mass Transfer in Porous Media, vol. 27, pp. 85–119. Springer, Heidelberg (2012)
2. Ellis, B.E., Found, M.S.: The effects of water absorption on a polyester/chopped strand mat laminate. Compos. **14**(3), 237–243 (1983)
3. Han, K.S., Koutsky, J.: Effect of water on the interlaminar fracture behaviour of glass fibre-reinforced polyester composites. Compos. **14**, 67–70 (1983)
4. Camino, G., Luda, M.P., Polishchuk, A.Y., Revellino, M., Blancon, R., Merle, G., Martinez-Veja, J.J.: Kinetic aspects of water sorption in polyester resin/glass-fibre composites. Compos. Sci. Technol. **57**, 1469–1482 (1997)
5. Choi, H.S., Ahn, K.J., Nan, J.-D., Chun, H.J.: Hygroscopic aspects of epoxy/carbon fiber composite laminates in aircraft environments. Compos. Part A: Appl. Sci. Manuf. **32**, 709–720 (2001)
6. Srihari, S., Revathi, A., Rao, R.M.V.G.K.: Hygrothermal effects on RT-cured glass-epoxi composites in immersion environments. Part A: Moisture absorption characteritics. J. Reinf. Plast. Compos. **21**, 11, 983–991 (2002)
7. Yao, J., Ziegmann, G.: Water absorption behavior and its influence on properties of GRP pipe. J. Compos. Mater. **41**(8), 993–1008 (2007)
8. Najafi, K.S., Kiaefar, A., Hamidinia, E., Tajvidi, M.: Water absorption behavior of composites from sawdust and recycled plastics. J. Reinf. Plast. Compos. **26**(3), 341–348 (2007)
9. Katzman, H.A., Castaneda, R.M., Lee, H.S.: Moisture diffusion in composite sandwich structures. Compos. Part A: App. Sci. Manuf. **39**(5), 887–892 (2008)
10. Czél, G., Czigány, T.: A study of water absorption and mechanical properties of glass fiber/polyester composite pipes — Effects of specimen geometry and preparation. J. Compos. Mater. **42**(26), 2815–2827 (2008)
11. Chateauminois, A., Vicent, L., Chabert, B.E., Soulier, J.P.: Study of the interfacial degradation of a glass-epoxi composite during hygrothermal ageig using water diffusion measurements and dynamic mechanical thermal analysis Polym. **35**(22), 4766–4774 (1994)
12. Pavan, R.M.V., Saravanan, V., Dinesh, A.R., Rao, Y.J., Srihari, S., Revathi, A.: Hygrothermal effects on painted and unpaited glass/epoxy composites- part a: moisture absorption characteristics. J. Reinf. Plast. Compos. **20**(12), 1036–1046 (2001)
13. Bao, L.R., Yee, A.F.: Moisture diffusion and hygrothermal aging in bismaleimide matrix carbon fiber composites-part I: uni-weave composites. Compos. Sci. Technol. **62**, 2099–2110 (2002)
14. Cavalcanti, W.S., Carvalho, L.H., Lima, A.G.B.: Water diffusion in unsaturated polyester composite reinforced by a hybrid jute/glass fabric: modeling and simulation. Rev. Matér. **10**(1), 14–23 (2005) (In Portuguese)
15. Cavalcanti, W.S.: Polyester/hybrid jute-glass fabric composites: mechanical characterization and water sorption simulation Doctorate Thesis. Federal University of Campina Grande, Paraíba, Brazil, Process Engineering (2006).(In Portuguese)
16. Santos, D.G.: Thermo-hydric study and mechanical characterization of polymeric matrix composites reinforced with vegetable fiber: 3D simulation and experimentation. Doctoral Thesis in Process Engineering, Federal University of Campina Grande, Campina Grande, Brazil (2017)
17. Santos, D.G., Lima, A.G.B., Costa, P.S., Lima, E.S., Moreira, G., Nascimento, J.J.S.: Water absorption in sisal fiber reinforced-polymeric matrix composites: three-dimensional simulations and experiments. Diffus. Found. **20**, 143–154 (2018)
18. Melo, J.B.C.A.: Water absorption in fiber reinforced polymer composites of pineapple leaf: modeling and simulation. Doctorate Thesis in Process Engineering. Federal University of Campina Grande, Campina Grande, Brazil (2014) (In Portuguese)

19. Carvalho, L.H., Canedo, E.L., Neto, S.F., Lima, A.G.B.: Moisture transport process in vegetable fiber composites: theory and analysis for technological applications. In: Delgado, J.M.P.Q. (ed.) Industrial and Technological Applications of Transport in Porous Materials, pp. 37–62. Springer, Berlin (2013)
20. Luikov, A.V.: Analytical Heat Diffusion Theory. Academic, London (1968)
21. Gebhart, B.: Heat Conduction and Mass Diffusion. McGraw-Hill Inc., New York (1993)
22. Patankar, S.V.: Numerical Heat Transfer and Fluid Flow. Hemisphere Publishing Corporation, New York (1980)
23. Maliska, C.R.: Computational Heat Transfer and Fluid Mechanics. LTC, Rio de Janeiro (2004).(In Portuguese)
24. Versteeg, H.K.; Malalasekera, W.: An Introduction to Computational Fluid Dynamics: the finite volume method. Pearson Education Limited, Harlow, England (1995)
25. Figliola, R.S., Beasley, D.E.: Theory and Design for Mechanical Measurements. Wiley, New York (1995)
26. Silva, C.J.: Water Absorption in Composite Materials of Vegetal Fiber: Modeling and Simulation via CFX. Master Dissertation in Mechanical Engineering, Federal University of Campina Grande, Campina Grande, Brazil (2014)
27. Silva, C.J., Barbosa de Lima, A.G., Silva, E.G, Andrade, T.H.F., MELO, R.Q.C.: Water Absorption in Caroá-Fiber Reinforced Polymer Composite at Different Temperatures: A Theoretical Investigation. Diffusion Foundations, vol. 10, pp. 16–27 (2017)
28. Silva, C.J., Andrade, T.H.F., Silva, E.G., Lima, A.G.B.: Water absorption in composites reinforced with Caroa- fiber fabrics: modeling and simulation via ANSYS CFX®. Defect Diffus. Forum. 353, 84–89 (2014)
29. Joseph, P.V., Rabello, M.S., Mattoso, L.H.C., Joseph, K., Thomas, S.: Environmental effects on the degradation behaviour of sisal fibre reinforced polypropylene composites. Compos. Sci. Technol. 62, 1357–1372 (2002)
30. Chow, C.P.L., Xing, X.S., Li, R.K.Y.: Moisture absorption studies of sisal fibre reinforced polypropylene composites compos. Sci. Technol. 67, 306–313 (2007)
31. Tsai, Y.I., Bosze, E.J., Barjasteh, E., Nutt, S.R.: Influence of hygrothermal environment on thermal and mechanical properties of carbon fiber/fiberglass hybrid composites. Compos. Sci. Technol. 69, 432–437 (2009)
32. Nóbrega, M.M.S.: Polyester matrix composite with caroá fibers (Neoglaziovia variegata): Mechanical charcterization and water sorption, Doctorate Thesis, Process Engineering, Federal University of Campina Grande, Paraíba, Brazil (2007), (In Portuguese)
33. Nóbrega, M.M.S., Cavalcanti, W.S., Carvalho, L.H., Lima, A.G.B.: Water absorption in unsaturated polyester composites reinforced with caroá fiber fabrics: modeling and simulation. Mat.-wiss. u.Werkstofftech. 41, 300–305 (2010)
34. Gupta, V.B., Drzal, J.L., Rich, M.J.: The physical basis of moisture transport in a cured epoxy resin system. J. Appl. Polym. Sci. 30(11), 4467–4493 (1985)
35. Lagouvardos, P.E., Pissis, P., Kyritsis, A., Daoukaki, D.: Water sorption and water-induced molecular mobility in dental composite resins. J. Mater. Sci. Mater. Med. 14(9), 753–759 (2003)
36. Duda, J.L., Vrentas, J.S., Ju, S.T., Liu, H.T.: Prediction of diffusion coefficients for polymer-solvent systems. AIChE J. 28, 279–285 (1982)
37. Wang, W., Sain, M., Cooper, P.A.: Study of moisture absorption in natural fiber plastic composites. Compos. Sci. Technol. 66, 379–386 (2006)
38. Merdas, I., Thominette, F., Tcharkhtchi, A., Verdu, J.: Factors governing water absorption by composite matrices. Compos. Sci. Technol. 62, 487–492 (2002)
39. Marcovich, N.E., Reboredo, M.M., Aranguren, M.I.: Moisture diffusion in polyester - woodflour composites. Polym. 40(26), 7313–7320 (1999)
40. Lima, A. G. B.: Diffusion phenomena in prolate spheroidal solids: Studied case: Drying of banana. Doctorate Thesis, Mechanical Engineering, State University of Campinas, Campinas, Brazil (1999) (In Portuguese)

41. Silva, W. P., Silva C. M. D. P. S., Farias, V. S. O., Lima A. G. B.: Effect of the geometry on the description of the water absorption by composite materials using diffusion models. Mat.-wiss. u.Werkstofftech. 42, 8, 747–752 (2011)
42. Cavalcanti, W. S., de Lima, A. G. B., Carvalho, L. H.: Water sorption in unsaturated polyester composites reinforced with jute and jute/glass fiber fabrics: Modeling, simulation and experimentation. Polímeros: Ciência e Tecnologia 20, 1, 78–83 (2010) (In Portuguese)
43. Osman, E., Vakhguelt, E., Sbarski, I., Mutasher, S.: Water absorption behavior and its effect on the mechanical properties of kenaf natural fiber unsaturated polyester composites. In: Proceedings of the 18th International Conference on Composite Materials, Edinburgh, Scotland (2009)
44. Alsina, O.L.S.; Carvalho, L.H.; Ramos Filho, F.G.; d'Almeida, J.R.M.: Immersion temperature effects on the water absorption behavior of hybrid lignocellulosic fiber reinforced-polyester matrix composites. Polym. – Plast. Technol. Eng. **46**(5), 515–520 (2007)

Chapter 5
Langmuir-Type Model Analysis

In this chapter, based on the rigorous theory of anomalous diffusion through fibrous porous media (Langmuir-type model), its advantagens, limitations, and different approaches (analytical and numerical), we present the correct prediction for the water absorption process in vegetable fiber-reinforced polymer composites. In the macroscopic and advanced mathematical modeling, both fiber and polymer are considered a homogeneous mixture having water molecules in the free and entrapped states inside the material, and the effect of swelling is neglected. Herein, different 1D and 3D simulation results of the average moisture content, moisture content as well as free and entrapped water molecules concentration distribution at different times are presented and analyzed. Applications have been focused to caroá fiber- reinforced polyester composites and other arbitrary cases.

5.1 Fundamentals

The effects of moisture absorption on the physical and chemical properties of polymer composite materials have received wide attention, not only due to the durability of these materials in operation but also because of their wide field of application.

As already mentioned, the properties of composite materials depend on the behavior of the matrix, the reinforcement and the fiber/matrix interface. Absorption of water molecules in materials leads to degradation of the interface and swelling of the matrix, generating internal stresses and decreasing mechanical properties. Decreasing properties are intrinsically associated to the moisture diffusion process in composite materials and therefore, in order to predict long-term behavior, in-service failure and useful life estimation [1], it is essential to know the water absorption rate.

Diffusion models must reflect the moisture sorption process in different ways, considering certain additional phenomena that can occur inside the material. Thus,

each specific case must be analyzed not only based on the results of a good approximation between the experimental data and those predicted by the equations, but also by the physical interpretation of the water sorption process included in the models.

In some cases, the water absorption kinetics is described assuming that water absorption follows the classical treatment given by Fick's second law of diffusion, that is, that the diffusion process is driven by the water concentration gradient between the medium and the material and continues until hygroscopic equilibrium is reached. In others, this model is not well suited [2, 3], because the material presents an anomalous water diffusion behavior, which implies in the existence of different stages of sorption until the final mass balance is reached (hygroscopic equilibrium condition). In this case, single-phase models cannot easily describe this kind of diffusion, and one needs other more sophisticated models to describe the behavior of the material under these physical conditions [4]. The Langmuir-type model is appropriate to predict the non-Fickian diffusion process in this situation [5].

The Langmuir-type model explains moisture sorption by assuming that water exists simultaneously in two phases: free (unbound) and entrapped (bound), during the process. In this model, water molecules in the free phase are adsorbed (bound) with a probability α per unit time, and the entrapped water molecules can leave the connected state with a probability β per unit time. Thus, the diffusion process is described by the classical diffusion equation, which is modified to take into account the two phases of the moisture inside the material.

Figure 5.1 illustrates the moisture content transient behavior predicted by Fick's model and Langmuir-type model. According to the Langmuir-type model, during the water absortion process, moisture migration is controlled by two phenomena: dispersion of free water molecules due to random molecular motion and trapping of water molecules due to interaction between the free water molecules and porous within the polymer composite.

In Fig. 5.1, the pseudo-equilibrium point represents the point at which the moisture migration rate drops dramatically.

The Langmuir-type model is well described in Glaskova et al. [6], Carter and Kilber [5], Bonniau and Bunsell [1], Grace and Altan [2], Cotinaud et al. [7] and Apicella et al. [8].

According to Carter and Kilber [5], the diffusive characteristics of the Langmuir-type model are correlated to the simplest form of neutron transport theory, while that the characteristics associated to free and entrapped water molecules are related to the classical Langmuir's adsorption isotherms theory.

According to these authors, composite anisotropy (structural heterogeneity), swelling, size and distribution of micropores (microvoids), mechanical loading, rearrangement of the polymer network (long-term relaxation), or some other phenomenon not yet fully understood are responsible for the intensity of the physical or chemical interactions at the microscopic level between polar water molecules and molecular groups of the polymer chains (molecular binding). A detailed discussion on the applications of this model are presented in the next section.

Fig. 5.1 Typical moisture
absorption kinetics predicted
by Langmuir-type model and
Fick´s model

 Polymer chain

 Water molecule

 Entrapped water molecules

 Free water molecules

—— Langmuir-type model

–·–· Fick´s model
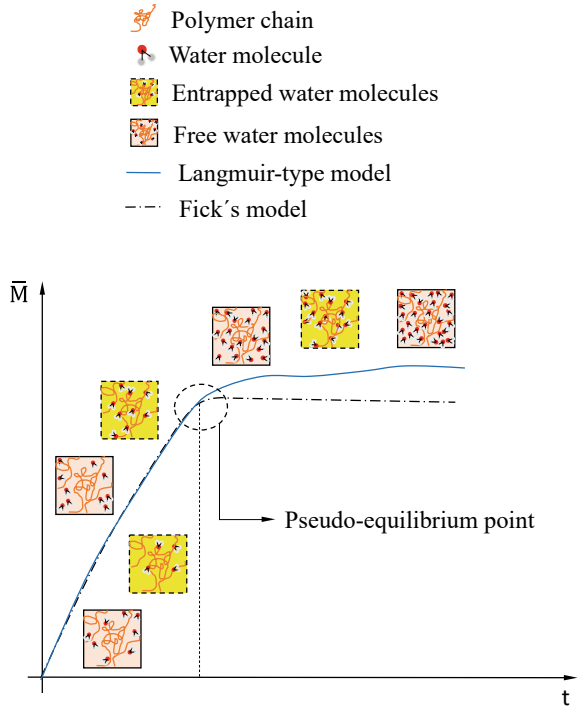
5.2   Moisture Absorption by Langmuir-Type Model

5.2.1   The Physical Problem

For the analysis of the physical problem studied here, consider a dry polymer
composite of parallelepiped geometry, at low temperature, suddenly immersed in
a stationary, heated, saturated fluid (water). As the surrounding fluid heats the dry
porous media, heat penetrates into the solid (as the result of a temperature differ-
ence) and moisture migrates into the solid by diffusion from the surface. Figure 5.2
illustrates the problem treated here. In this figure Lx, Ly, and Lz are the distances
from the composite surface to the maximum level of water in the container.

5.2.2   The General Mass Diffusion Equation

In the Langmuir-type model, the non-Fickian moisture absorption behavior can be
explained quantitatively by assuming that moisture absorption occurs in the pres-
ence of two simultaneous stages, one being the free water stage and the another
the entrapped water stage [5]. The following mass transfer equations describe this
model:

Fig. 5.2 Squematic of the composite immersed in a stationary fluid and the distance of the material to borders of the fluid domain
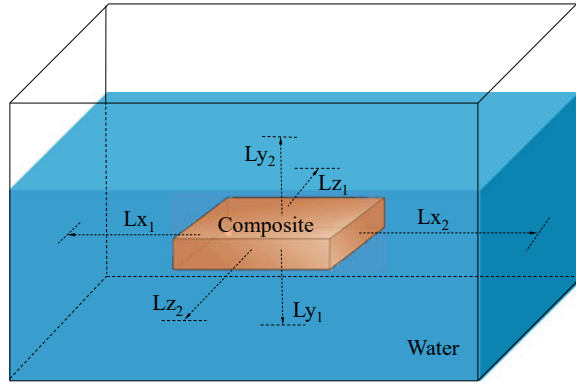
$$\frac{\partial C}{\partial t} = \nabla \cdot (D\nabla C) - \frac{\partial S}{\partial t} \qquad (5.1)$$

$$\frac{\partial S}{\partial t} = \lambda C - \mu S \qquad (5.2)$$

where: C is the concentration of the free solute diffusing into the material; S is the concentration of the entrapped solute; D is the mass diffusion coefficient (free solute molecules); t is the time; λ is the probability of a free solute molecule is entrapped inside the solid and μ is the probability that an entrapped solute molecule becomes free.

Careful analysis of Eq. (5.1), indicates that if $\lambda = 0$ or $\mu \gg \lambda$, it is reduced to the simple diffusion theory (Fick´s second law of diffusion).

5.2.3   The Mass Diffusion Equation: 3D Approach in Cartesian Coordinates

For a three-dimensional and transient approach, based on the considerations adopted, the Langmuir model, in Cartesian Coordinates, can be written as:

$$\frac{\partial C}{\partial t} = \frac{\partial}{\partial x}\left(D\frac{\partial C}{\partial x}\right) + \frac{\partial}{\partial y}\left(D\frac{\partial C}{\partial y}\right) + \frac{\partial}{\partial z}\left(D\frac{\partial C}{\partial z}\right) - \frac{\partial S}{\partial t} \qquad (5.3)$$

$$\frac{\partial S}{\partial t} = \lambda C - \mu S \qquad (5.4)$$

In order to solve Eqs. 5.3 and 5.4, the following initial and boundary conditions were used:

(a) **_Initial conditions_**: if the solid is completely dry at the beginning of the process,
then one can write:

$$C = S = 0; \begin{cases} -R_1 < x < R_1 \\ -R_2 < y < R_2 \\ -R_3 < z < R_3 \end{cases} \tag{5.5}$$

(b) **_Boundary conditions:_** the variation in the concentration of the solute in the
fluid medium on the surface of the solid is equal to the diffusive flux of solute
into the material. Then, one can write:

$$Lx_1 \frac{\partial C}{\partial t} = -D\frac{\partial C}{\partial x}; \begin{cases} x = -R_1 \\ t > 0 \end{cases} \tag{5.6}$$

$$Lx_2 \frac{\partial C}{\partial t} = -D\frac{\partial C}{\partial x}; \begin{cases} x = +R_1 \\ t > 0 \end{cases} \tag{5.7}$$

$$Ly_1 \frac{\partial C}{\partial t} = -D\frac{\partial C}{\partial y}; \begin{cases} x = -R_2 \\ t > 0 \end{cases} \tag{5.8}$$

$$Ly_2 \frac{\partial C}{\partial t} = -D\frac{\partial C}{\partial y}; \begin{cases} x = +R_2 \\ t > 0 \end{cases} \tag{5.9}$$

$$Lz_1 \frac{\partial C}{\partial t} = -D\frac{\partial C}{\partial z}; \begin{cases} x = -R_3 \\ t > 0 \end{cases} \tag{5.10}$$

$$Lz_2 \frac{\partial C}{\partial t} = -D\frac{\partial C}{\partial z}; \begin{cases} x = +R_3 \\ t > 0 \end{cases} \tag{5.11}$$

Once C and S are determined at any point inside the material, it is possible to calculate
the total moisture content present in the material at any position and instant of time.
Therefore, the total moisture content is given by the sum of the concentrations of C
and S, as follows:

$$M(x,y,z,t) = C(x,y,z,t) + S(x,y,z,t) \tag{5.12}$$

It follows from Eq. 5.12 that the average moisture content of the solid at any time of
the process is given by:

$$\overline{M} = \frac{1}{V} \int_V M(x,y,z,t)dV \tag{5.13}$$

Fig. 5.3 Geometrical
representation of the
one-dimensional physical
problem
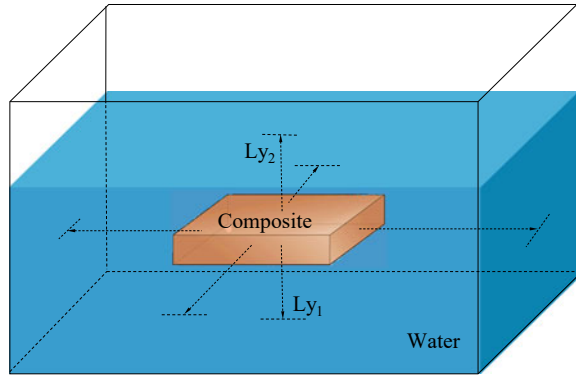
in which V is the total volume of the solid and dV = dxdydz is the volume of an
infinitesimal sample of the porous solid.

5.2.4 The Water Absorption Process: 1D Approach in Cartesian Coordinates

5.2.4.1 The Physical Problem

For the physical model, a porous plate with thickness $2R_2 = 2a$, immersed in a fluid
solution (water) of height $(Ly_1 + 2a + Ly_2)$, as illustrated in Fig. 5.3 was considered.

Considering that $R_1 = R_3 >> R_2$, water absorption can be analysed just in the y
direction and the following assumptions were made: the material is homogeneous
and isotropic; the mass diffusion coefficient is constant; the solid is axisymmetric;
the process is transient; the dimensions of the material during the diffusion process
do not change; the capillary transport through the solid is negligible; mass generation
inside the solid is neglected; the solid is totally dry at the beginning of the process and
the solid is in equilibrium with the surrounding medium at the surface (equilibrium
boundary condition).

5.2.4.2 The Mass Diffusion Equation

In the Langmuir-Type model, the anomalous moisture absorption can be quantita-
tively determined by assuming that absorbed moisture consists of a mobile phase
and a bound phase. The model considers the interaction between the polar water
molecules and the resin molecular groups, predicting the existence of free and
bound molecules within the polymer network. This can be taken into account by
adding a new parameter to the classical Fick's equation [9]. Considering the assump-
tions already cited, the Langmuir equation, written in Cartesian coordinates in a
one-dimensional approach, is described as follows:

$$\frac{\partial C}{\partial t} = D\frac{\partial^2 C}{\partial y^2} - \frac{\partial S}{\partial t} \tag{5.14}$$

where,

$$\frac{\partial S}{\partial t} = \lambda C - \mu S \tag{5.15}$$

For the proposed problem the following initial and boundary conditions were considered:

- Initial condition:

$$S = C = 0, -a < y < a, \ t = 0 \tag{5.16}$$

- Boundary condition:

$$Ly_1\frac{\partial C}{\partial t} = -D\frac{\partial C}{\partial y} \ \ y = -a, t > 0 \tag{5.17}$$

$$Ly_2\frac{\partial C}{\partial t} = -D\frac{\partial C}{\partial y} \ \ y = +a, \ t > 0 \tag{5.18}$$

where Ly_1 and Ly_2 represent the distance between the solid surface and the bottom and top of the water tank, respectively. According to Eqs. (5.17) and (5.18), it is assumed that the rate of solute that leaves the solution is equal to the diffusive flux of solute at the surface of the plane sheet (see Fig. 5.3).

5.2.4.3 Solution Techniques: 1D Approach

Analytical Solution

Based on the works of Carter and Kibler [5] and Crank [10], Santos et al. [3] present the exact solution for the Eqs. (5.14) and (5.15) using the method of Laplace Transform. The application of the Laplace Transform consists in converting a partial differential equation in an ordinary differential equation which can be solved more easily. After this procedure, the inverse Laplace transform is calculated to get the original function of the problem that represent the solution of the governing equations [11, 12].

In order to obtain the exact solution of the physical problem, the model was simplified considering a porous plate with thickness $2R_2 = 2a$, immersed in a fluid (water) of height $(2L + 2a)$, where $Ly_2 = Ly_1 = L$ (Fig. 5.3).

The final equation for the concentration of free solute inside the solid during the water absorption process is obtained by considering the boundary conditions, the domain of the functions and with the use of necessary simplifications. This equation can be written as:

$$C(y,t) = \frac{LC_e}{L + (R + 1)a}$$
$$+ \sum_{n=1}^{\infty} \frac{C_e \cos(k_n y) \mathrm{Exp}(p_n t)}{\cos(k_n a)\left\{1 + \left[1 + \frac{\mu\lambda}{(p_n + \mu)^2}\right]\left[\frac{Lp_n^2 a}{2D^2 k_n^2} + \frac{p_n}{2Dk_n^2} + \frac{a}{2L}\right]\right\}} \tag{5.19}$$

where p_n and k_n are eigenvalues and C_0 represent the initial solute concentration.

The final equation for the concentration of solute entrapped on the solid is written as:

$$S(y,t) = \left(\frac{\lambda}{\mu}\right)\frac{LC_e}{L + (R + 1)a}$$
$$+ \sum_{n=1}^{\infty} \left(\frac{\lambda}{p_n + \mu}\right)\frac{C_e \cos(k_n y)\mathrm{Exp}(p_n t)}{\cos(k_n a)\left\{1 + \left[1 + \frac{\mu\lambda}{(p_n + \mu)^2}\right]\left[\frac{Lp_n^2 a}{2D^2 k_n^2} + \frac{p_n}{2Dk_n^2} + \frac{a}{2L}\right]\right\}} \tag{5.20}$$

The total moisture content inside the material in a specific position x and instant t is obtained from the sum of the amount of free solute and the amount of solute entrapped according with the following equation:

$$M = S + C \tag{5.21}$$

Based on Eq. (5.21), the average moisture content of the solid at different moments of the water uptake can be computed as follows:

$$\overline{M} = \frac{1}{V} \int_V M dV \tag{5.22}$$

or yet,

$$\overline{M} = \frac{1}{2a} \int_{-a}^{a} M(y,t)dy \tag{5.23}$$

where V is the volume of the solid.

From Eq. (5.23), the average moisture content of the solid at different water uptake times can be computed as follows:

$$\frac{\overline{M}}{M_e} = 1 - \sum_{n=1}^{\infty} \frac{(1 + \alpha)e^{p_n t}}{1 + \left[1 + \frac{\mu\lambda}{(p_n + \mu)^2}\right]\left[\frac{Lp_n^2 a}{2D^2 k_n^2} + \frac{p_n}{2k_n^2 D} + \frac{a}{2L}\right]} \tag{5.24}$$

where:

$$\alpha = \frac{L}{(R+1)a} \tag{5.25}$$

$$M_e = \frac{LC_e}{(1+\alpha)a} \tag{5.26}$$

In Eq. (5.24), $\overline{M}$ corresponds to the total amount of solute, both free and immobilized to diffusion at a given time t, M_e corresponds to the amount of moisture at equilibrium, obtained after an infinite time, and $R = \lambda/\mu$. The terms p_n and k_n together form pairs of eigenvalues and aim to refine the approximate calculation and the results. Thus, the higher the number of eigenvalues, the more accurate the analytical results obtained. They correspond to non-zero roots of the Eq. (5.27) that are originated from applying Eqs. (5.19) in (5.18).

$$\frac{Lp}{D} = k \tan(k \times a) \tag{5.27}$$

In Eq. (5.27), the values of k are given by:

$$k^2 = -\frac{p}{D}\left(\frac{p+\mu+\lambda}{p+\mu}\right) \tag{5.28}$$

For a 3D physical situation, the analytical solution can be obtained as the product of the analytical solution for three infinite plates. In this case, each of the plates must have thickness equal to $2R_1$, $2R_2$ and $2R_3$. Special care must be given in the determination of the eigenvalues p and k, which are different for each of the x, y and z diretions [2, 13–15].

Numerical Solution

The numerical solution of a partial differential equation basically consists of two steps: (a) discretizing the physical domain under study in several sub domains and (b) transforming the governing equation into a linear algebraic equation in the discretized form applied to each sub domain contained in the solid under investigation. After these procedures, the result is a set of linear algebraic equations whose solution provides the distribution of the potential unknown inside the domain and in time.

Herein, the finite-volume method for numerical solution of the governing equation [16–18] was used. For the discretization of Eqs. (5.14) and (5.15), the continuous solid of a thickness 2a was subdivided in (np-2) control volumes, as shown in Fig. 5.4.

In Fig. 5.4 each control volume has thickness Δx; S, P and N represent nodal points, while s and n represent the left and right faces of the control volume P,
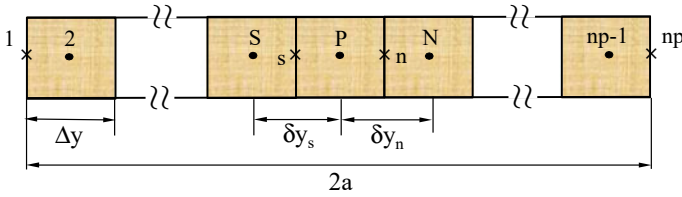
Fig. 5.4 Representation of the one-dimensional simulation domain with (np-2) control volumes

respectively; δy_s and δy_n represent the distance between nodal point P and nodal points S and N, respectively.

(a) **Solution for the concentration of free solute**

- *Internal points*

In the finite volume method, discretization is done by integrating all terms of Eq. (5.14) in volume and time. Thus, after integration and using a fully implicit formulation, rearranging the terms in the linearized discrete algebraic form at P, leads to:

$$A_P C_P = A_N C_N + A_S C_S + A_P^o C_P^o + B_P^C \tag{5.29}$$

where,

$$A_P = \left(\frac{\Delta x}{\Delta t} + \frac{D_n}{\delta x_n} + \frac{D_s}{\delta x_s} + \lambda \Delta x \right) \tag{5.30}$$

$$A_N = \frac{D_n}{\delta y_n} \tag{5.31}$$

$$A_S = \frac{D_s}{\delta y_s} \tag{5.32}$$

$$A_P^o = \frac{\Delta y}{\Delta t} \tag{5.33}$$

$$B_P^C = \mu \Delta y S_P^o \tag{5.34}$$

where the coefficients A_P, A_N, and A_S are the conductance between the nodal points P and their corresponding neighbors. The term A_P^o represents the influence of the value of C on the value of C at t prior to that at the current time t. Equation (5.29) is valid for all internal points of the domain except for the boundary and symmetry points.

- **Bottom boundary points**

In this case, the boundary flux is replaced by the existing boundary condition (Eq. 5.17). By doing this, the linear discretized equation for the bottom boundary points is:

$$A_P C_P = A_N C_N + A_s^o C_s^o + A_P^o C_P^o + B_P^C \tag{5.35}$$

where,

$$A_P = \frac{\Delta y}{\Delta t} + \frac{D_n}{\delta\, y_n} + \frac{1}{\left(\frac{\delta y_s}{D_s} + \frac{\Delta t}{Ly_1}\right)} \tag{5.36}$$

$$A_N = \frac{D_n}{\delta y_n} \tag{5.37}$$

$$A_s^o = \frac{1}{\left(\frac{\delta y_s}{D_s} + \frac{\Delta t}{Ly_1}\right)} \tag{5.38}$$

$$A_P^o = \frac{\Delta y}{\Delta t} \tag{5.39}$$

$$B_P^C = \mu \Delta y S_P^o \tag{5.40}$$

- **Upper boundary points**

In this case, the boundary flux that must be replaced by the existing boundary condition (Eq. 5.18) and the linear discretized equation for the boundary points is given by:

$$A_P C_P = A_S C_S + A_n^o C_n^o + A_P^o C_P^o + B_P^C \tag{5.41}$$

where,

$$A_P = \frac{\Delta y}{\Delta t} + \frac{D_s}{\delta\, y_s} + \frac{1}{\left(\frac{\delta y_n}{D_n} + \frac{\Delta t}{Ly_2}\right)} \tag{5.42}$$

$$A_S = \frac{D_s}{\delta y_s} \tag{5.43}$$

$$A_n^o = \frac{1}{\left(\frac{\delta y_n}{D_n} + \frac{\Delta t}{Ly_2}\right)} \tag{5.44}$$

$$A_P^o = \frac{\Delta y}{\Delta t} \tag{5.45}$$

$$B_P^C = \mu \Delta y S_P^o \tag{5.46}$$

Equations 5.29, 5.35 and 5.41 when applied at each of the control volumes form a system of algebraic linear equations whose solution indicates the concentration of free solute within the solid during the water absorption process.

(b)   **Solution for the concentration of entrapped solute**

In order to obtain the equations associated to the concentration of entrapped solute in the solid, Eq. (5.15) is integrated in volume and time. Reorganizing the terms, we obtain the following linear algebraic equation, valid for all control volume of the domain:

$$A_P S_P = A_P^o S_P^o + B_P^S \tag{5.47}$$

where,

$$A_P = \frac{\Delta y}{\Delta t} + \mu \Delta y \tag{5.48}$$

$$A_P^o = \frac{\Delta y}{\Delta t} \tag{5.49}$$

$$B_P^S = \lambda \Delta y C_P \tag{5.50}$$

It is important to notice that the Eq. (5.47) is an explicit equation, depending only of the values of the free solute concentration at each nodal point and time.

The total moisture inside the material in a specific position x and instant t is given by summing the amounts of free and entrapped solute as follows:

$$M = S + C \tag{5.51}$$

Equation (5.23) yields the average moisture content of the solid at any time. This equation in the discretized form is written as:

$$\overline{M} = \frac{1}{2a} \sum_{i=2}^{np-1} M_i \Delta y_i \tag{5.52}$$

where np represents the total number of nodal points considered.

The linear algebraic equation system can be solved iteratively using the Gauss–Seidel method, where is assumed that the numerical solution converges when, from the initial condition, the following criterion is satisfied at each nodal point of the domain, at a given time:

$$\left|C_P^{n+1} - C_P^n\right| \leq 10^{-10} \tag{5.53}$$

where n represents the nth iteration at each instant. To obtain the predicted results, a time step and mesh refinement study was performed. After this process a grid with $np = 20$ nodal points and a time step $\Delta t = 20$ s was chosen.

(c)   **Estimation of the model parameters**

For the computer simulation of the water absorption process using the Langmuir-type modl, it is necessary to use D, λ and μ values consistent with the experimental data. This procedure is described in detail below.

• *Initial estimate of the probabilities λ and μ*

Considering a one-dimensional approach, $\kappa = \pi^2 D/(2R_2)^2$ and satisfying $2\lambda <<$ κ and $2\mu << \kappa$, the following approximate solution for determining the average moisture content (Eq. 5.24) is valid [5]:

$$\frac{\overline{M}}{M_e} = \frac{\mu}{\lambda + \mu} e^{-\lambda t} \left[1 - \frac{8}{\pi^2} \sum_{n=1}^{\infty} \frac{e^{-\kappa(2n+1)^2 t}}{(2n+1)^2} \right]$$
$$+ \frac{\mu}{\lambda + \mu} \left(e^{-\mu t} - e^{-\lambda t} \right) + \left(1 - e^{-\mu t} \right) \tag{5.54}$$

For long times, when $\kappa \times t >> 1$, Eq. (5.54) is reduced to:

$$\frac{\overline{M}}{M_e} = 1 - \frac{\lambda}{\lambda + \mu} \mathrm{Exp}(-\mu \times t) \tag{5.55}$$

which can be written, as follows:

$$\frac{\overline{M}}{M_e} = 1 - A\mathrm{Exp}(-B \times t) \tag{5.56}$$

where

$$A = \frac{\lambda}{\lambda + \mu} \tag{5.57}$$

$$B = \mu \tag{5.58}$$

With the values of the average moisture content over time obtained experimentally, it is possible to perform a nonlinear regression of Eq. (5.56), to obtain the values of A and B statistical parameters and, with those, determine the values of λ and μ parameters using Eqs. (5.57) and (5.58).

- *Initial estimate of the probabilities λ and μ*

In this case, considering a one-dimensional approach, for short times ($t \leq 0.7/\kappa$), the following approximate solution for determining the average moisture content (Eq. 5.59) is valid [5]:

$$\overline{M} = \frac{4}{\pi^{3/2}} \left(\frac{\mu}{\lambda + \mu} M_e \right) \sqrt{\kappa \times t} \tag{5.59}$$

or yet,

$$\overline{M} = \frac{4}{\pi^{3/2}} \left(\frac{\mu}{\lambda + \mu} M_e \right) \sqrt{\kappa} \times \sqrt{t} \tag{5.60}$$

Thus, substituting $\kappa = \pi^2 D/(2R_2)^2$ in Eq. (5.60) we get:

$$\overline{M} = \frac{4}{\pi^{3/2}} \left(\frac{\mu}{\lambda + \mu} M_e \right) \sqrt{\frac{\pi^2 D}{(2R_2)^2}} \times \sqrt{t} \tag{5.61}$$

Calculating the derivative of Eq. (5.61) with respect to time and since, for initial times, the behavior of the average moisture content is approximately linear with time, we can write:

$$\frac{d\overline{M}}{d\sqrt{t}} \approx \frac{\overline{M}_2 - \overline{M}_1}{\sqrt{t_2} - \sqrt{t_1}} = \left(\frac{4}{\pi^{3/2}} \right) \left(\frac{\mu}{\lambda + \mu} M_e \right) \left(\frac{\pi}{2R_2} \right) \times \sqrt{D} \tag{5.62}$$

which leads to:

$$D = \pi \times \left(\frac{R_2}{2M_e} \right)^2 \left(\frac{\lambda + \mu}{\mu} \right)^2 \left(\frac{\overline{M}_2 - \overline{M}_1}{\sqrt{t_2} - \sqrt{t_1}} \right)^2 \tag{5.63}$$

where $\overline{M}_1$ and $\overline{M}_2$ are values of the average moisture content obtained experimentally, at times t_1 and t_2, respectively, and M_e is the equilibrium moisture content.

An alternative method to estimate the mass diffusion coefficient is to consider $\lambda = 0$ (Langmuir-type model tending to the Fick´s model) and determine D using the least square error technique to minimize the error between theoretical and experimental data (Eq. 5.64).

It is important to notice that the model parameters D, μ, and λ determined as already mentioned are only an initial estimate and that the mathematical procedures reported above can also be used for a three-dimensional analysis.

Table 5.1 Geometrical parameters used in the simulation

Parameter	Value
L (m)	0.3
a (m)	1.5×10^{-3}

- *Actual estimate of the parameters D, μ, and λ*

Once the initial estimate of parameters D, μ and λ was made, the real estimate of these parameters can be performed, comparing the least square error between the predicted and experimental data of the average moisture content, and varying these parameters until a minimum error is reached, according to Eq. (5.64).

$$ERQM = \sum_{i=1}^{n} \left[\overline{M}_{predict} - \overline{M}_{experimental} \right]^2 \qquad (5.64)$$

where n is the number of experimental points.

5.2.4.4   Langmuir-Type Model Application: 1D Approach

Analytical and Numerical Results

- *Absorbed Water Kinetics*

The exact and numerical solutions of the governing equations were applied to predict moisture diffusion in polymer composites reinforced with caroá fibers. As already mentioned, the composites studied have width and length greater that its thickness. The results that presented here refer to the case where $Ly_{2} = Ly_{1} = L$ and $R_2 = a$. It is assumed that water penetrates only in the thickness. direction. Table 5.1 presents the geometric parameters used in the simulation.

For the validation of the model, the predicted result of the average moisture content was compared with analytical results reported by Santos et al. [3] and the experimental data reported by Silva [19] and Nóbrega et al. [20] for polymer composite materials reinforced with Caroá fiber (T = 25 °C). From this comparison, the mass diffusion coefficient and the probabilities μ and λ, of the model were estimated using the least squares error technique, given by the following equation:

$$ERQM = \sum_{i=1}^{n} \left[\overline{M}_{predicted} - \overline{M}_{experimental} \right]^2 \qquad (5.54)$$

where n is the number of experimental points. According to Santos et al. [3], an average quadratic error of 0.047467 $kg_{water}/kg_{dry\ solid}$) was obtained. Table 5.2 shows the estimated data.

**Table 5.2** Physical parameters used in the simulation

Parameter	Value
D (m^2s^{-1})	7.020×10^{-12}
μ (s^{-1})	1.697×10^{-6}
λ (s^{-1})	0.836×10^{-6}

Table 5.3 Some values of the p and k eigenvalues

n	k_n (m^{-1})	P_n (m^{-1})
1	1049.07	-7.5768×10^{-6}
2	1058.21	-1.29658×10^{-6}
3	3142.29	-6.06761×10^{-6}
4	3171.09	-1.44941×10^{-6}
5	5236.41	-1.67169×10^{-6}

Fig. 5.5 Numerical, analytical and experimental dimensionless average moisture content of polymer composites reinforced with caroá fiber during the water absorption process (T = 25 °C, $Ly_2 = Ly_1 = 0.3$ m)
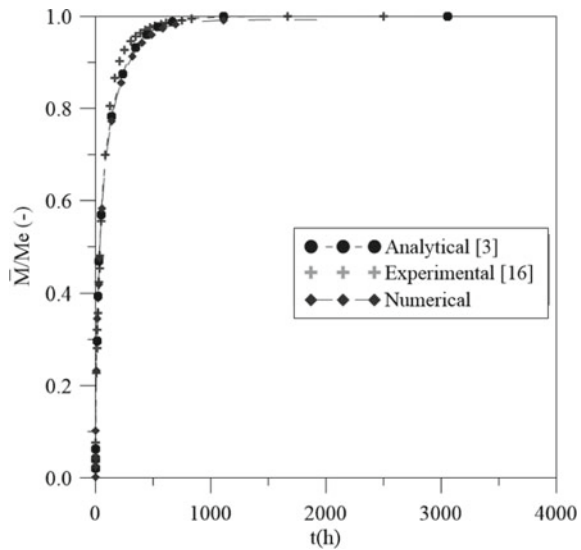

These values led to 30 pairs of eigenvalues and one pair of imaginary root which were used to obtain the exact solution of Eqs. (5.19), (5.20) and (5.24). Table 5.3 presents five values of p_n and k_n engeinvalues determined by Santos et al. [3].

Figure 5.5 illustrates the comparison between numerical, analytical and experimental data of the average moisture content obtained during water absorption in caroá fiber-reinforced polymer composites immersed in water at 25 °C.

Figure 5.5 shows some discrepancies between experimental and numerical data, which can be attributed to the lack of suitable boundary conditions for the model and the assumption of constant properties. The numerical results, however, showed good

Fig. 5.6 Dimensionless average moisture content of the caroá fiber reinforced polymer composite as a function of modified Fourier number of mass transfer during the water absorption process (T = 25 °C, $Ly_2 = Ly_1 = 0.3$ m)
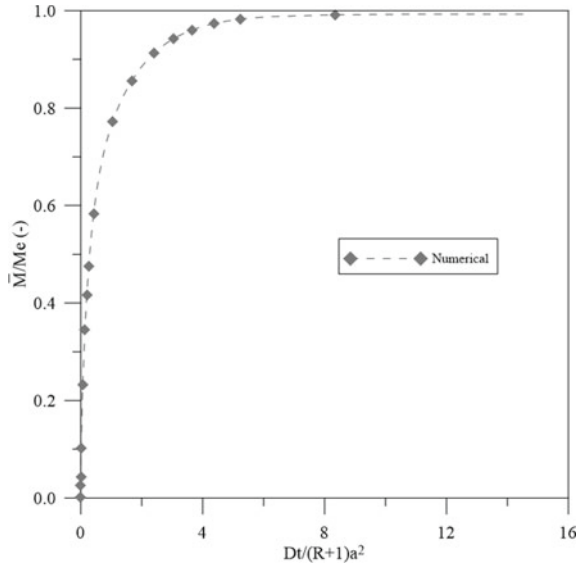
agreement with analytical results, indicating that the proposed mathematical model properly describes the water diffusion process inside the material.

A more general mathematical analysis was obtained by plotting the dimesionless average moisture content as a function of another dimensioless parameter Fo = $Dt/[(R + 1)a^2]$ namely modified Fourier number for mass transfer. These results are shown in Fig. 5.6. This procedure allows for results to be independent of mass diffusivity, λ and μ probabilities, composite thickness and time. Analysis of this figure indicates that water sorption is very quick in the early stages up to a modified Fourier number of mass transfer of approximately 2.0, and tends to decline for long exposure times until equilibrium is achieved (saturation condition, $M_e = 14.488\%$), where the dimensionless average moisture content tends to a maximum value. The time to achieve the hygroscopic equilibrium was estimated to Fo $\cong 10F_o \approx 12$.

- *Absorbed Free and Entrapped Water Molecules Distribution*

Figure 5.7 shows the variation of dimensionless free solute concentration (analytical and numerical) along the thickness of the solid, given by C/Ce, where Ce (estimated by Eq. 5.22 as Ce = 0.09778 kg/kg) represents the equilibrium concentration of the solute in the fluid medium. Since the solid in question is symmetrical with respect to its center, results are ploted only from the center (y = 0 m) to the composite surface (y = 0.0015 m). This figure shows that, for shorter times, moisture concentration variation is higher close to the surface of the material, that is, there is a high concentration gradient of free water, in these regions. With increasing time, this relationship tends to approach 1.0, as the hygroscopic equilibrium condition (saturation) is reached. Besides, at any point within the solid, the moisture content increases with time until it reaches equilibrium.
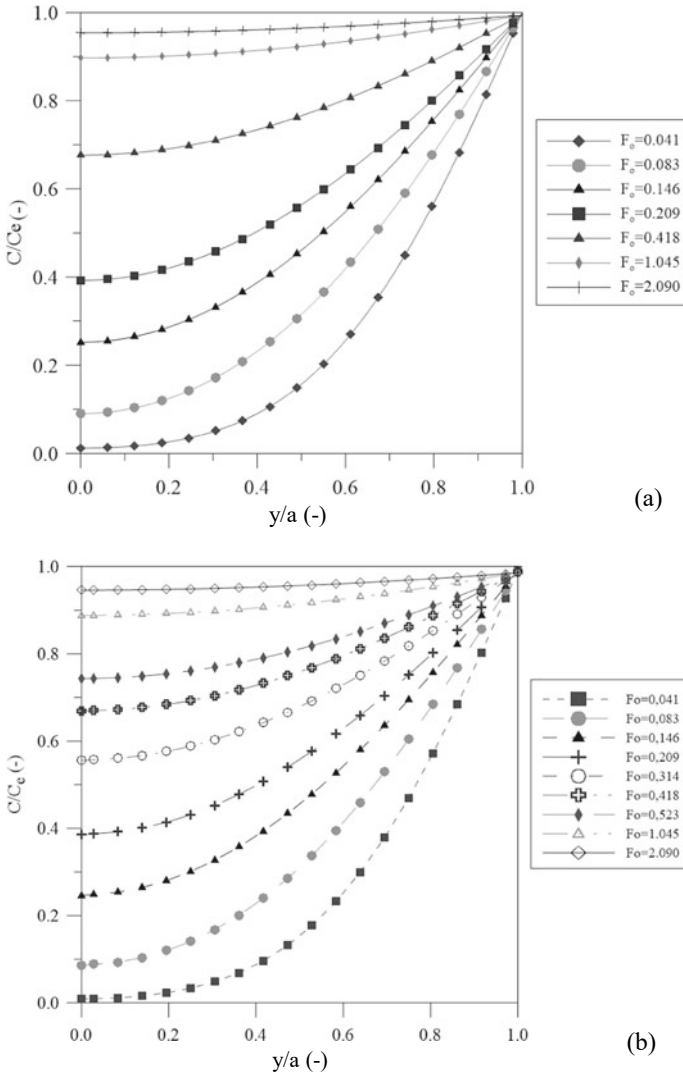
Fig. 5.7 Dimensionless free solute concentration distribution inside the caroá fiber reinforced plymer composite for different modified Fourier number of mass transfer. **a** Analytical and **b** Numerical results (T = 25 °C, Ly2 = Ly1 = 0.3 m)

Figure 5.8 illustrates the distribution of the dimensionless bound (entrapped) water molecules (numerical) along the thickness of the caroá fiber-reinforced polymer composite. Analysis of this figure shows that an increase in the content of bound water molecules depends on the increase in the concentration of free water molecules into the material. The major bound water concentration gradients are found near the solid surface. For longer times, or when there is a greater amount of free water molecules
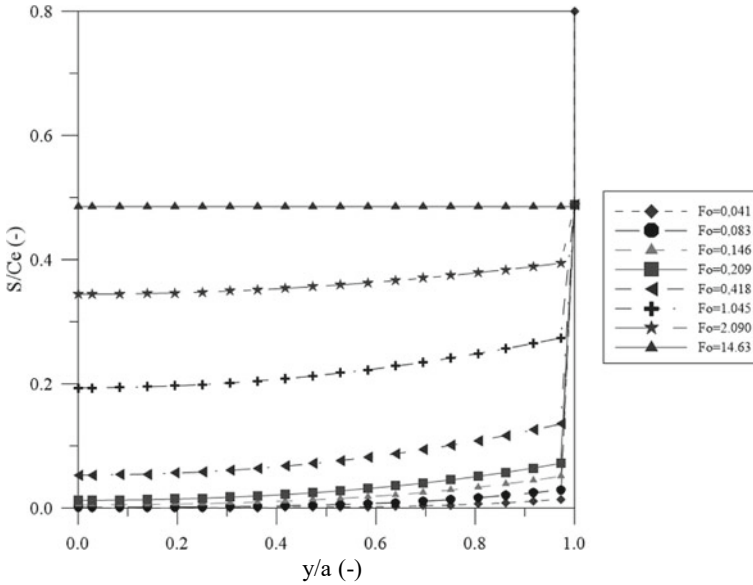
Fig. 5.8 Predicted dimensionless entrapped solute concentration inside the caroá fiber reinforced plymer composite for different modified Fourier number of mass transfer (T = 25 °C, Ly2 = Ly1 = 0.3 m)

within the material, there is a higher number of entrapped water molecules, and this condition occurs until that equilibrium is reached. This occurs as $\partial S/\partial t = 0$, or yet, $\lambda C = \mu S$, which implies that $S/C_e = \lambda/\mu = 0.493$, for $t \rightarrow \infty$.

At the beginning, the observed behaviour for water absorption is Fickian, that is, there is moisture migration of water molecules in "free" state. However, as time goes by and as more moisture is absorbed, the water diffusion rate decreases. This behaviour is explained by two phenomena: (a) as water absorbed more molecules are linked to the polymer chains, thus reducing the amount of water that can be absorbed, and (b) the relaxation rate becomes larger than the diffusion rate, controlling the final stages of the process.

Figure 5.9 shows the dimensionless moisture content absorbed into the material, obtained by the sum of the free water molecules concentration and the entrapped water molecules concentration. In regions near the surface, water absorption is faster, because there is a larger area in direct contact with water bath. The water penetrates the interior of the material generating a higher moisture content gradient along the thickness, which decreases with increasing immersion time. Thus, at any point inside the solid, the moisture content increases with time until it reaches equilibrium, i.e., its saturation point. It is intuitive to say that at longer immersion times there is an increase in the amount of molecules entrapped within the material while the amount of free molecules to diffuse decreases.
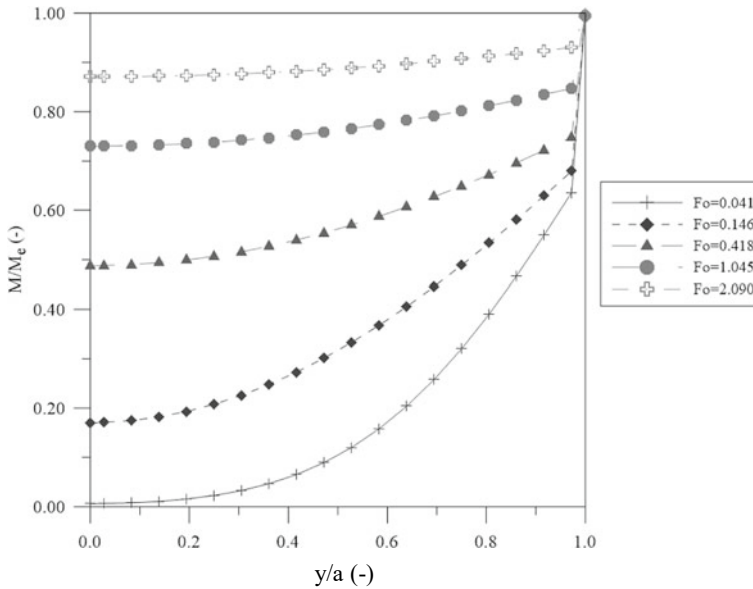
Fig. 5.9 Predicted dimensionless misture content inside the caroá fiber reinforced plymer composite for different modified Fourier number of mass transfer (T = 25 °C, $Ly_2 = Ly_1 = 0.3$ m)

For a more complex physical situation, for example, where $Ly_2 \neq Ly_1$, Melo et al. [21] reported a theoretical analysis aiming to evaluate the effect of the water layer thickness (upper and bottom) on the water absorption behavior inside the material. In that research, the authors considered equilibrium moisture content Me = 0.14488 kg/kg, water bath temperature 25 °C, and total process time 2250 h. Table 1 summarizes the data used in the simulations.

Figure 5.10 illustrates the average moisture content in the material along the process for different arbitrary cases, as reported in Table 5.4. Figure 5.11 shows the local moisture contents obtained from the sum of the free and bound water molecule concentrations along the thickness of the material for different elapsed times and distances from the composite surface to maximum water level in the container. Figure 5.12 shows the behavior of the variation rate of the local moisture content as a function of time in the center of the composite.

According to Melo et al. [21], water absorption kinetics is strongly affected by the water layer thickness, the moisture content gradient, and the equilibrium moisture content inside the material. These authors verified that the higher gradients are found in the regions where Ly_1 or Ly_2 have higher value. Furthermore, the largest concentration gradients of free and entrapped water molecules are at the composite surface, and an asymmetric behavior of the process variables is obtained when the geometric parameters Ly_2 and Ly_1 are different.
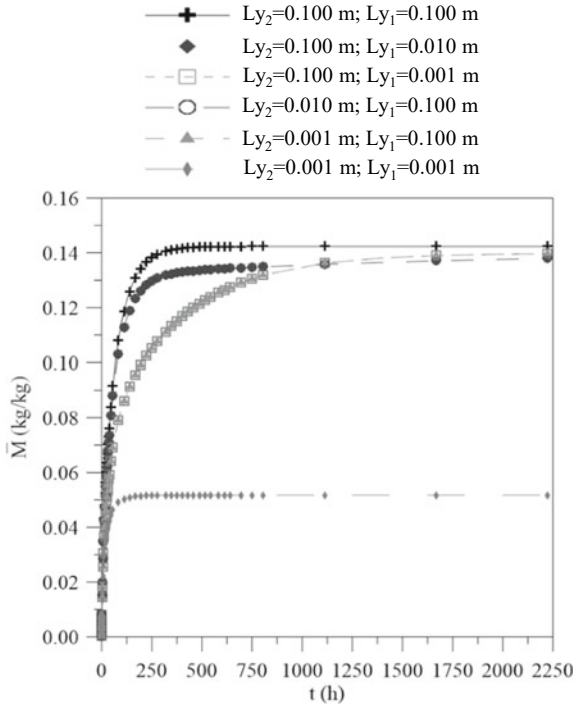
Fig. 5.10 **a** Average moisture content as a function of the process time for different physical saturations. **b** Detailed view of **a**

Table 5.4 Process parameters values of the polymer composite used in the simulations

To (°C)	2a (m)	Ly₂ (m)	Ly₁ (m)	μ (10^{-6} s^{-1})	λ (10^{-6} s^{-1})	D (10^{-12} m²s^{-1})
25	0.003	0.100	0.100	5	1	5
25	0.003	0.100	0.010	5	1	5
25	0.003	0.100	0.001	5	1	5
25	0.003	0.010	0.100	5	1	5
25	0.003	0.001	0.100	5	1	5
25	0.003	0.001	0.001	5	1	5

Fig. 5.11 Local moisture
content as function of the
position inside the material
at different process times

(a) 56 h

(b) 195 h
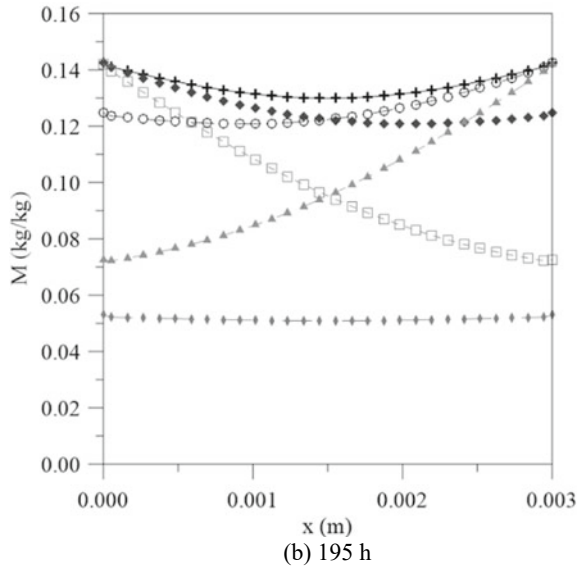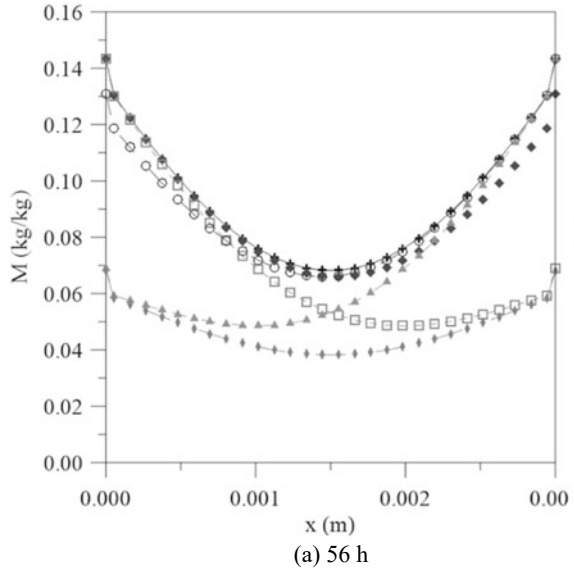
5.2.5 The Water Absorption Process: 3D Approach

5.2.5.1 Solution Techniques: 3D Approach

Numerical Solution

The finite volume method was used for the three-dimensional numerical solution
of the governing equations applied to moisture absorption in polymer composites
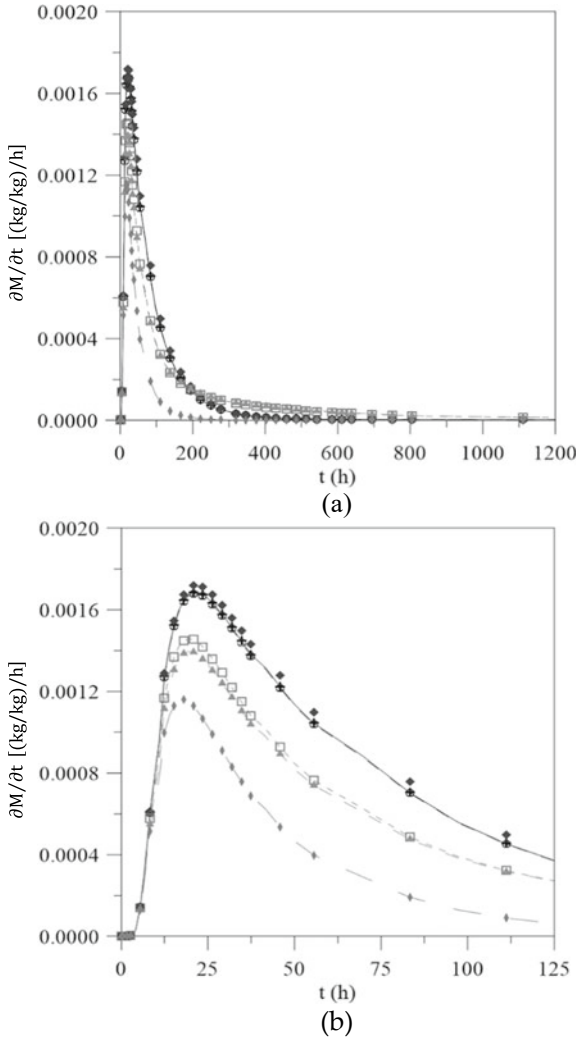
Fig. 5.12 Temporal variation rate of the local moisture content in the center of the polymer composite **a** and detail of the figure **b**

with parallelepipedic form, as reported by Santos et al. [22, 23], Brito et al. [24] and Santos [25]. In this solution, a fully implicit formulation for the concentration of free solute and explicit formulation for the concentration of trapped solute were used. Figure 5.13 illustrates a control volume (sub domain) used for discretization of the governing equations. The nodal point P (in the center of the control volume), its adjacent neighbors W, E, S, N, T, and F, the distances between these nodal points, and the dimensions Δx, Δy, and Δz, of the control volume are also shown in this Figure.
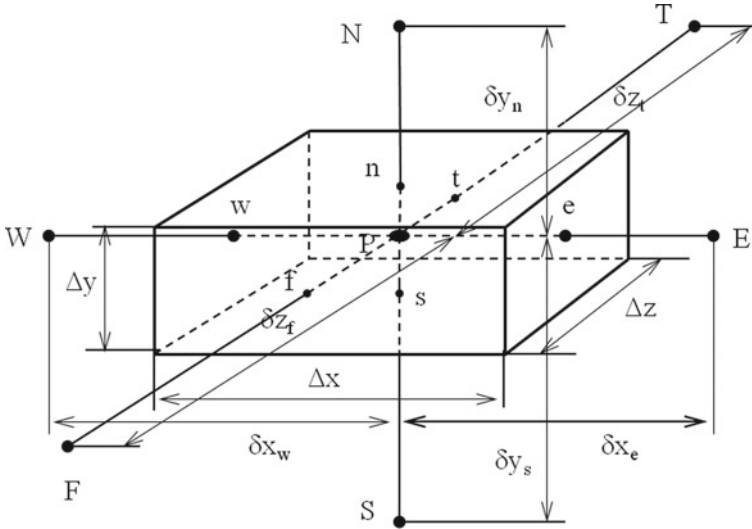
Fig. 5.13 Three-dimensional control volume used in this work

Complete detailing of the numerical procedure used for the solution of the governing equations is given below.

(a) **Solution for the Free Water Molecules Concentration**

- *Internal points*

The numerical solution of Eq. (5.3) is obtained by integrating it in volume and time. Assuming a fully implicit formulation, one can write the Eq. (5.3) in its discretized linear form as follows:

$$A_P C_P = A_E C_E + A_W C_W + A_N C_N + A_S C_S + A_F C_F + A_T C_T$$

$$+ A_P^o C_P^o + B_P^C \tag{5.66}$$

where:

$$A_E = \frac{D_e}{\delta x_e} \Delta y \Delta z \tag{5.67}$$

$$A_W = \frac{D_w}{\delta x_w} \Delta y \Delta z \tag{5.68}$$

$$A_N = \frac{D_n}{\delta y_n} \Delta x \Delta z \tag{5.69}$$

Fig. 5.14 Numerical grid showing the internal and surface control-volumes

$$A_S = \frac{D_s}{\delta y_s} \Delta x \Delta z \tag{5.70}$$

$$A_F = \frac{D_f}{\delta z_f} \Delta y \Delta x \tag{5.71}$$

$$A_T = \frac{D_t}{\delta z_t} \Delta y \Delta x \tag{5.72}$$

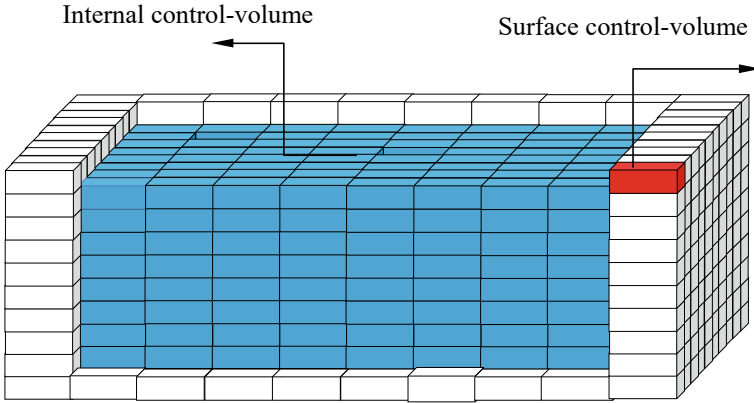$$A_P^o = \frac{\Delta x \Delta y \Delta z}{\Delta t} \tag{5.73}$$

$$A_P = \frac{\Delta x \Delta y \Delta z}{\Delta t} + \frac{D_e}{\delta x_e} \Delta y \Delta z + \frac{D_w}{\delta x_w} \Delta y \Delta z + \frac{D_n}{\delta y_n} \Delta x \Delta z + \frac{D_s}{\delta y_s} \Delta x \Delta z$$

$$+ \frac{D_f}{\delta z_f} \Delta y \Delta x + \frac{D_t}{\delta z_t} \Delta y \Delta x \tag{5.74}$$

$$B_P^C = -\left(S_P - S_P^o\right) \frac{\Delta x \Delta y \Delta z}{\Delta t} \tag{5.75}$$

- *Boundary points*

It should be noted that Eq. (5.66) is only applied to the internal control volumes of the computational domain (Fig. 5.14). For the other control volumes (symmetry and border), a mass balance in each one of them is performed. In total, there are 27 different types of control volumes. As an example, the result of Eq. 5.3 applied to the control volume of the right upper corner of the computational domain, as shown in Fig. 5.14, is given by the following equation:

$$A_P C_P = A_W C_W + A_S C_S + A_T C_T + A_P^o C_P^o + B_P^C \tag{5.76}$$

where:

$$A_W = \frac{D_w^C}{\delta x_w} \Delta y \Delta z \tag{5.77}$$

$$A_S = \frac{D_s}{\delta y_s} \Delta x \Delta z \tag{5.78}$$

$$A_T = \frac{D_t}{\delta z_t} \Delta y \Delta x \tag{5.79}$$

$$A_P^o = \frac{\Delta x \Delta y \Delta z}{\Delta t} \tag{5.80}$$

$$
A_P = \frac{\Delta x \Delta y \Delta z}{\Delta t} + \frac{D_w}{\delta x_w} \Delta y \Delta z + \frac{D_s}{\delta y_s} \Delta x \Delta z + \frac{D_t}{\delta z_t} \Delta y \Delta x + \frac{\Delta y \Delta x}{\left(\frac{\delta z_f}{D_f} + \frac{\Delta t}{l_z} \right)}
$$
$$
+ \frac{\Delta z \Delta x}{\left(\frac{\delta y_n}{D_n} + \frac{\Delta t}{l_y} \right)} + \frac{\Delta y \Delta z}{\left(\frac{\delta x_e}{D_e} + \frac{\Delta t}{l_x} \right)} \tag{5.81}
$$

$$
B_P^C = \frac{C_f^o \Delta x \Delta y}{\left(\frac{\delta z_f}{D_f} + \frac{\Delta t}{l_z} \right)} + \frac{C_e^o \Delta y \Delta z}{\left(\frac{\delta x_e}{D_e} + \frac{\Delta t}{l_x} \right)} + \frac{C_n^o \Delta x \Delta z}{\left(\frac{\delta y_n}{D_n} + \frac{\Delta t}{l_y} \right)} - \left(S_P - S_P^o \right) \frac{\Delta x \Delta y \Delta z}{\Delta t} \tag{5.82}
$$

(b) Solution for the entrapped water molecules concentration

The numerical solution of Eq. (5.4) is obtained by integrating it in volume and time. Assuming an explicit formulation, one can write the Eq. 5.4, in its discretized linear form, as follows:

$$A_P S_P = A_P^o S_P^o + B_P^S \tag{5.83}$$

where:

$$A_P^o = \frac{\Delta x \Delta y \Delta z}{\Delta t} \tag{5.84}$$

$$A_P = \frac{\Delta x \Delta y \Delta z}{\Delta t} + \mu \Delta x \Delta y \Delta z \tag{5.85}$$

$$B_P^S = \lambda C_P \Delta x \Delta y \Delta z \tag{5.86}$$

In the discretized form, the local and average moisture contents can be written, respectively, as follows:

$$M_{i,j,k} = C_{i,j,k} + S_{i,j,k} \tag{5.87}$$

$$\overline{M} = \frac{1}{V} \sum_{i=2}^{npx-1} \sum_{j=2}^{npy-1} \sum_{k=2}^{npz-1} M_{i,j,k} \Delta V_{i,j,k} \tag{5.88}$$

in which i, j e k represent the position of the nodal point in the x, y, and z directions, respectively, and npx, npy and npz are the nodal point numbers in the x, y, and z directions respectively.

From the discretization of the governing equations, a system of liear algebraic equations is generated that must be solved to obtain the values of C, S and M within the material throughout the process. The Gauss–Seidel iterative method can be used for solving this system of algebraic equations. In order to obtain the numerical results, simulations were performed using a grid with $20 \times 20 \times 20$ nodal points and time step $\Delta t = 20$ s. Other details about this numerical procedure can found in the references already cited in this chapter.

5.2.5.2 Langmuir-Type Model Application: Three-Dimensional Approach

Numerical Results

Based on the references already mentioned, the influence of the geometrical parameter L_y (see Fig. 5.2), in the process of water absorption in fiber-reinforced polymer composites was evaluated. For this analysis, the authors considered $\mu = \lambda = 1.0 \times 10^{-6}$ s^{-1}, D $= 1 \times 10^{-12}$ m^2/s, R$_1$ = R$_3$ = 0.0100 m, R$_2$ = 0.0015 m, R$_3$ = 0.000 m, Lx$_1$ = Lx$_2$ = 0.1000 m, Lz$_1$ = Lz$_2$ = 0.1000 m and Ly$_1$ = Ly$_2$ = 0.0010 m, 0.0100 m and 01,000 m,

The obtained results indicated that variations in L_y values strongly affect the average moisture content, and also average free and entrapped water molecules concentrations. The higher the L_y value, the higher the water layer close to the composite wall and the faster the water absorption rate. For initial times of the process, the differences among the predicted results are not significant, however, in the course of the process a different behavior of the water absorption kinetics can be clearly observed.

Upon analyzing the free water molecules concentration distribution was verified that, for small value of L_y, there is essentially no free water flux in the y-direction but, in the opposite directions, the water flux is more intense and free water molecules move horizontally (x—and z—directions) with nearly equal velocities.

A similar behavior for the distribution of entrapped water molecules concentration to that presented by free solute concentration was observed. In general, the geometric parameter L_y affects both the distribution of free and entrapped solute concentration and, as a result, the total moisture content of the composite immersed in water.

Besides, it was observed small values of the bound water molecules concentration when compared to unbound water molecules concentration. Furthermore, a transient analysis of the predicted results showed that the free water molecules concentration is increasing from the composite surface to its center with a horizontal flux of moisture. Compared with the y-direction, the greatest moisture fluxes occur in x and z- direction. The same behavior is observed when the entrapped water molecules concentration is considered. Nevertheless, entrapped water concentration increases more slowly than free water molecules concentration, mainly at the initial process times.

As final comment, we notice that water absorption is facilitated when polymer molecules have clusters capable of forming hydrogen bonds. Plant fibers are rich in cellulose, hemicellulose and lignin which have hydroxyl groups, i.e., have high affinity for water. The absorption of water by the resin, in turn, can be considered practically null, since it has a considerable hydrophobic character [26]. Addition of the plant fibers to hydrophobic resins leads to an increase in the water absorption levels, so an important parameter to be analyzed is how much water is absorbed by the material over time.

The effects caused by long time exposure to moisture may be irreversible due to the water molecules affinity with specific functional groups of the polymeric matrices. Destructive changes usually occur due to degradation of existing physical–chemical interactions between the resin and fiber and, as a consequence, there are changes in the fiber, causing delamination and reduction in the composite material properties. Thus, understanding of the water absorption process is crucial to predict the quality of the material e wet environments.

From the physical and mathematical point of views is important to analyse quantitatively what happens with the general solution for the extreme values of the probability μ which correspond to very fast or very slow process. When μ is very large as compared to λ, the process is very rapid compared with diffusion. In this situation, the immobilized component is in equilibrium with the component free to diffuse into the composite, or yet, the number of free molecules that become entrapped and remain entrapped by a time long enough to hinder diffusion is very small, and process is controlled by diffusion. However, if $\mu \to 0$, the process is infinitely slow, the composite is occuped, by simple diffusion, and only a fraction of solute (moisture) can be accommodated in the freely diffusing state and none in the immobilized state. On the other hand, when λ increases sufficiently, moisture absorption is hindered due to the higher probability that a free water molecule will become entrapped instead of freely diffusing into the composite [10, 13]. Further, for the case where D is very large, the diffusion is so rapid that the concentration of free and immobilized solute (water) are almost uniform through the composite during the water uptake process.

From the explanation above it is possible to conclude that variations in the mass diffusion coefficient and the probabilities that water molecules are free or entrapped, deeply modifies the water absorption process, which proves the great potential of the Langmuir-type model and its ability of adequately describing moisture migration behaviour inside the polymer composite.

References

1. Bonniau, P., Bunsell, A.R.: A comparative study of water absorption theories applied to glass epoxy composites. J. Compos. Mater. **15**(3), 272–293 (1981)
2. Grace, L.R., Altan, M.C.: Characterization of anisotropic moisture absorption in polymeric composites using hindered diffusion model. Compos. A Appl. Sci. Manuf. **43**(8), 1187–1196 (2012)
3. Santos, W.R.G., Melo, R.Q.C., Lima, A.G.B.: Water absorption in polymer composites reinforced with vegetable fiber using Langmuir-type model: An exact mathematical treatment. Defect Diffus. For. **371**, 102–110 (2016)
4. Perreux, D., Suri, C.: A study of the coupling between the phenomena of water absorption and damage in glass/epoxy composite pipes. Compos. Sci. Technol. **57**(9–10), 1403–1413 (1997)
5. Carter, H.G., Kibler, K.G.: Langmuir-type model for anomalous moisture diffusion in composite resins. J. Compos. Mater. **12**(2), 118–131 (1978)
6. Glaskova, T.I., Guedes, R.M., Morais, J.J., Aniskevich, A.N.: A comparative analysis of moisture transport models as applied to an epoxy binder. Mech. Compos. Mater. **43**(4), 377–388 (2007)
7. Cotinaud, M., Bonniau, P., Bunsell, A.R.: The effect of water absorption on the electrical properties of glass-fibre reinforced epoxy composites. J. Mater. Sci. **17**(3), 867–877 (1982)
8. Apicella, A., Estiziano, L., Nicolais, L., Tucci, V.: Environmental degradation of the electrical and thermal properties of organic insulating materials. J. Mater. Sci. **23**(2), 729–735 (1988)
9. Popineau, S., Rondeau-Mouro, C., Sulpice-Gaillet, C., Shanahan, M.E.: Free/bound water absorption in an epoxy adhesive. Polymer **46**(24), 10733–10740 (2005)
10. Crank, J.: The mathematics of diffusion, 2nd edn. Oxford University Press, Oxford (1975)
11. Fu, Z., Chen, W., Yang, H.: Boundary particle method for laplace transformed time fractional diffusion equations. J. Comput. Phys. **235**, 52–66 (2013)
12. Zhu, S., Satravaha, P., Lu, X.: Solving linear diffusion equations with the dual reciprocity method in Laplace space. Eng. Anal. Bound. Elem. **13**(1), 1–10 (1994)
13. Grace, L.: Non-Fickian three-dimensional moisture absorption in polymeric composites: development and validation of hindered diffusion model. Ph.D Thesis, University of Oklahoma, Norman, USA, (2012)
14. Luikov, A.V.: Analytical heat diffusion theory, p. 684. Academic Press, Inc. Ltd., London (1968)
15. Carslaw, H.S., Jaeger, J.C.: Conduction of heat in solids. 2nd edn, p. 510. University Press, Oxford, New York (1959)
16. Melo, R.Q.C., Santos, W.R.G., Lima, A.G.B.: Applying the Lagmuir-type model on the water absorption in vegetable fiber reinforced polymer composites: A finite-volume approach. In: XXXVIII Iberian Latin-American Congress on Computational Methods in Engineering, Florianópolis, Brazil. (2017)
17. Patankar, S.V.: Numerical heat transfer and fluid flow. Hemisphere Publishing Corporation, New York (1980)
18. Maliska, C.R.: Computational heat transfer and fluid mechanics. LTC, Rio de Janeiro (2004).(In Portuguese)
19. Silva, C.J.: Water absorption in composite materials of vegetal fiber: modeling and simulation via CFX. Master Dissertation in Mechanical Engineering, Federal University of Campina Grande, Brazil (2014) (In Portuguese)
20. Nóbrega, M.M.S., Cavalcanti, W.S., Carvalho, L.H., Lima, A.G.B.: Water absorption in unsaturated polyester composites reinforced with caroá fiber fabrics: modeling and simulation. Mat.-wiss. u.Werkstofftech. 41(5), 300–305 (2010)
21. Melo, R.Q.C., Fook, M.V.L., Lima, A.G.B.: Non-fickian moisture transport in vegetable-fiber-reinforced polymer composites using a Langmuir-type model. Polymers 12, 2503 (2020)
22. Santos, W.R.G., Melo, R.Q.C., Correia, B.R.B., Magalhães, H.L.F., Cabral, E.M., Figueiredo, M.J., Lima, A.G.B.: Water absorption in vegetable fiber-reinforced polymer composites: A

three-dimensional investigation using the Langmuir-type model. Defect Diffus For **399**, 164–170 (2020)

23. Santos, W.R.G., Brito, M.K.T., Lima, A.G.B.: Study of the moisture absorption in polymer composites reinforced with vegetal fiber using Langmuir's model. Mater. Res. 22, e20180848 (2019)

24. Brito, M.K.T., Santos, W.R.G., Correia, B.R.B., Queiroz, R.A., Tavares, F.V.S., Oliveira Neto, G.L., Lima, A.G.B.: Moisture absorption in polymer composites reinforced with vegetable fiber: a three-dimensional investigation via Langmuir model. Polymers 11, 1847 (2019)

25. Santos, W.R.G.: Heat and mass transfer in polymeric composites reinforced by vegetable fibers: advanced modeling and simulation. Campina Grande: Doctoral Thesis in Process Engineering, Federal University of Campina Grande, Campina Grande, Brazil, (2019)

26. Sanchez, E.M., Cavani, C.S., Leal, C.V., Sanchez, C.G.: Composites of unsaturated polyester resin with sugarcane bagasse: influence of fiber treatment on properties. Polymer **20**(3), 194–200 (2010)

Chapter 6
Conclusions

This book is entirely dedicated to diffusion processes in polymer composites, with particular reference to moisture absorption in vegetable fiber-reinforced polymer composites. An overview of basic issues related to this class of physical problem including fundamentals, experiments, advanced mathematical modeling, and engineering applications are shown in detail. Special attention is given to unsaturated polyester composites reinforced by caroá and macambira vegetable fibers.

Composite is a multiphase material consisting of a continuous phase (matrix) and one or more dispersed phases (reinforcement). The majority of the composites use thermoset matrices, with particular attention to epoxies and polyesters. Vegetable fibers may be used reinforment in polymer composites.

The use of raw materials from renewable sources, such as, vegetable fibers have been the subject of several sudies for many years due to different reasons such as high potential for diverse industrial and technological applications especially those related to socio-economic and environmental benefits.

Despite of their importance, environmental factors such as, moisture and temperature, strongly affect the durability, mechanical properties and many other characteristics of vegetable fiber-reinforced polymer composites. The hydrophilic nature of the vegetable fibers leads to weak interfacial adhesion which causes a reduction in the mechanical properties of the composite. Thus, it can be stated that these materials are very sensitive to water and heat and, to address new researches related to water absorption process in vegetable fiber-reinforced polymer composites, it is crucial to control the process in order to obtain good quality composites when in operation.

The contents of this book evince that the mechanisms governing water absorption in polymer composite are very different from those which are encountered in traditional materials, and requires a full understanding of their constituents (reinforcing and matrix) and their interaction at the fiber-matrix interface (adhesion) or interphase. The adhesion quality is vital to obtain high mechanical performance of the composite, avoiding failure and premature damage in the composite (matrix cracking, local deterioration, delamination, fiber debonding, and pull-out). Thus, the present book deals specifically with water absorption in vegetable fiber-reinforced

unsaturated polyester composites. Emphasis is given to unsaturated polyester matrix composites reinforced with caroá, macambira and sisal natural fibers by theoretical (analytical and numerical) and experimental techniques.

Herein, based on the Fick´s second law and non-Fickian diffusion model (Langmuir´s model) different transient macroscopic models were proposed, and the mathematical formalism based on the finite-volume method (numerical solution), Laplace transform and Separation of variables (exact solution) were used to solve the governing equations. Experimental tests for water absorption were performed by immersing the composite samples in a bath of distilled water at different temperatures, and the water uptake was measured gravimetrically along the process. The unsaturated polyester composites reinforced by caroá, macambira and sisal fibers were manufactured by hand lay-up. For both, the theoretical and experimental analyses, the effect of the composite dimensions, water bath temperature, and water layer thickness above the composite surface were evaluated. Microscopic images on the vegetable fibers were also analyzed.

The content of this book has demonstrated that the water uptake process and its effects in fiber-reinforced polymer composites is now a well-understood topic.

From the experimental and theoretical results of apparent weight gain of the polymer composites associated with water absorption, it can be concluded that mechanical properties (Tensile strength, Young's modulus, impact resistance, and elongation at break) of these materials effectively are affected by moisture content and temperature. The proposed mathematical models adequately describe the process of water diffusion inside the fiber-reinforced polymer composites and simulations proved to be an essential tool in understanding the process. The Langmuir-type model proved to be able to predict both Fickian and non-Fickian moisture absorption with equal ease. For this purpose, it is only necessary to change the problabilities parameters intrinsic to the model to make it truly comprehensive.

It was verified that water absorption by composites increases with fiber loading and is higher than for the polymer matrix alone. Temperature strongly influences the kinetics of water absorption and the absorption rate is higher at higher temperatures. Also, the highest rates of water diffusion were obtained in the first stages of sorption, and the sorption rate decreases at longer water immersion times. At lower temperatures, sample thickness affects water absorption more than temperature, but, at higher temperatures, the opposite occurs, i.e., the temperature in the water absorption were more relevant than that due to changes in the sample´s area/volume ratio.

The knowledge of moisture distribution inside the polymer composite is very important and allows identification of more propicious areas for delamination problems (moisture induced degradation) due to the weakness of the fiber-matrix interface and, consequently, reduction in the composites mechanical properties. The data presented demonstrates that the regions in the neighborhood of the vertices (corners) of the polymer composite (rectangular prism) had the highest mass transfer rates, being more susceptible to crack and deformation.

The demands of vegetable fibers has effectively increased in the composite industry. Reasons for this increased demands include their ecofriendly nature, light weight, good set of mechanical properties, worldwide abundance and availability and

low cost which effectively reduce the cost of composite materials and increase their sustainability. Vegetable fiber reinforced polymer composites have some disadvantages already mentioned in this book, particularly their sensitivity to moisture and temperature, which limit their widespread applications and affect service life. Future trends in polymer composite materials reinforced by vegetable fibers must focus on guaranteeing property control, so that there are minimum variations in these properties. There is a need to investigate ways to increase their mechanical propertries, thermal stability and decrease their moisture sensitivity through processing, drying and/or chemical modifications. Studies to define universal testing standards and establish a worldwide database directed to numerical and experimental investigation of continuous intrinsic problems are needed. These must include shape, dimension, manufacturing technique, composition, and microstructure of the samples, moisture absorption and other related effects, thermal degradation, inadequate toughness, and reduced long-term stability for outdoor application that require high load or yet high working temperatures. Therefore, research to improve the performance of vegetable fiber reinforced polymer composites such as thermal and chemical treatments, use of compatibilizer, addition of other fillers, polymer coating, and filler hybridization are strongly recommended. As for the matrix, the development of biodegradable polymers and blends, and optimization in the use of recyclable polymers are in demand. Under the mathematical point of view, the development of robust mathematical modelis to predict mechanical behavior of these polymer composites and related effects, especially in moist, corrosive, saline and heated environments, are also recommended.

Finally, the expectation of the authors is that the information outlined in this book may help researchers, designers, engineers and academics in their studies and making design decisions on the use of complex systems such as polymer composites, especially those reinforced with vegetable fiber, in technological applications.